A cancer immunotherapy approach

targeting mutant isocitrate dehydrogenase 1

Theresa Schumacher

2014

DISSERTATION

submitted to the

Combined Faculties for the Natural Sciences and for Mathematics

of the Ruperto-Carola University of Heidelberg, Germany

for the degree of

Doctor of Natural Sciences

presented by

Theresa Schumacher, M. Sc. Molecular Biomedicine

born in Frechen

Oral Examination: 14.04.2014

A cancer immunotherapy approach

targeting mutant isocitrate dehydrogenase 1

Referees: PD Dr. Anne Régnier-Vigouroux

Prof. Dr. Michael Platten

ACKNOWLEDGEMENTS

I wish to express my deepest gratitude to my thesis supervisor Prof. Dr. Michael Platten for his continuous support and his comprehensive encouragement and guidance, his unbowed confidence and his ability to focus on the essential. I want to particularly thank him for this translational project and his clever ideas to pursue it to its maximum.

I want to sincerely thank PD Dr. Anne Régnier-Vigouroux for examination of my thesis and for being such a kind member of my thesis advisory committee. I am grateful to Prof. Dr. Ralf Bartenschlager and Prof. Dr. Viktor Umansky for examination and Prof. Dr. Andreas von Deimling for being a member of my thesis advisory committee.
My candid thanks go to Prof. Dr. Wolfgang Wick for his interest and fruitful input.

I am thankful to all our collaboration partners at the German Cancer Research Center, especially Stefan Pusch, Jörg Balß, and Felix Sahm for their constant support and expertise, and also Dr. Wolfram Osen and Prof. Dr. Stefan Eichmüller for their friendly help. Furthermore, I thank Isabel Vogler and Jan Diekmann from Ribological GmbH and Translational Oncology for their scientific contribution and Prof. Dr. Ugur Sahin for his "hard-core" immunological analysis.

I would like to thank all present and former lab members of the "CCU Neuroimmunology and Brain Tumor Immunology" and the "CCU Neurooncology" for their contribution to a familiar working atmosphere and support. My special thanks go to Melanie Keil for her sunny disposition, for being such a pleasant and helpful not only office mate, but friend, and for her willingness to share her expertise in all mouse work; and to Iris Oezen for her unbroken helpfulness, for sharing her experience, and having a good heart, in the lab and as a friend. Thank you to Jonas Blaes for scientific help and evening chats.

I also thank Anne Hertenstein for her faithful friendship throughout the years. Even more, I want to cordially thank Adriane Gardyan for her friendship, for scientific and non-scientific discussions and for being the reliable constant during my time in Heidelberg in the last years.

My truthful gratefulness goes to my parents and my brother for their continuous and loving support and encouragement.

Most importantly, I am most deeply grateful to my boyfriend Lukas Bunse, who came into the lab and into my life, and who had an essential part in the success of this thesis in all possible ways. I want to thank you for pushing me forward, reminding me to relax, for lifting me up and keeping me on the ground. Without you, life would be less wonderful.

ABSTRACT

Point mutations in the *isocitrate dehydrogenase (IDH)* genes are an early, if not the earliest event during the development of gliomas and other tumors, such as acute myeloid leukemia (AML). Among grade II and grade III gliomas, more than 80 % carry an IDH mutation. In these entities, mutations almost exclusively affect the catalytically critical arginine residue of the cytoplasmic IDH1, leading to the amino acid exchange to histidine (R132H). This and other IDH mutations result in a neomorphic enzyme function and the production of the oncometabolite 2-hydroxyglutarate (2-HG) and thus genome-wide hypermethylation and malignant transformation.

The work at hand demonstrates the suitability of IDH1R132H as a target for immunotherapy in an MHC-humanized mouse model, A2.DR1. Peptides encompassing the mutated region bound MHC class II *in vitro* and induced a mutation-specific CD4+ T helper (Th) response *in vivo*, whose antigen-specificity persisted in a specific T cell line and clone and which was accompanied by IDH1R132H-specific antibody production. To detect IDH1R132H-specific IgG in mouse and human serum, a peptide-coated ELISA was established. Several tested patients with IDH1R132H+ gliomas showed spontaneous IDH1R132H-specific antibody and CD4+ Th1 cell responses. Preventive and therapeutic IDH1R132H peptide vaccination of A2.DR1 mice bearing syngeneic IDH1R132H+ sarcomas resulted in an effective mutation-specific antitumor immune response capable of controlling tumor growth in a CD4+ T and B cell-dependent manner. Functionality of the vaccine was evidenced by loss of IDH1R132H expression in IDH1-transduced sarcomas and infiltration of IDH1R132H-specific CD4+ T cells into the tumor bulk. Compared to therapeutic MHC II-mediated peptide vaccination against the well-established cancer testis antigen 1 (CTAG1B, NY-ESO-1), IDH1R132H is a relevant neoantigen of comparable efficacy.

Given the IDH1R132H-mediated accumulation of 2-HG, the effect of this metabolite on human T cells is of potential relevance during IDH1R132H-targeted immunotherapy. However, neither human peripheral CD4+ nor CD8+ T cell functions from healthy subjects were affected by 2-HG.

In conclusion, IDH1R132H represents a potentially clinically meaningful tumor-specific neoantigen. Conceptually, patients with low-grade and anaplastic gliomas with a high

prevalence of the IDH1R132H mutation represent a patient population, which may particularly benefit from a tumor vaccine, as there is currently no therapy preventing recurrence in this relatively young and immunologically competent patient population. Moreover, patient groups with other IDH1R132H-mutated tumors might potentially also benefit from such a vaccine.

ZUSAMMENFASSUNG

Während der Entwicklung von Gliomen und anderer Tumore, wie z. B. akuter myeloischer Leukämie (AML), sind Punktmutationen in den *Isozitrat-Dehydrogenase (IDH)* Genen ein frühes, wenn nicht das früheste Ereignis. Mehr als 80 % der Grad II und Grad III Gliome tragen eine IDH Mutation. In diesen Entitäten betreffen Mutationen fast ausschließlich den katalytisch kritischen Argininrest des zytoplasmatischen IDH1 und führen zum Aminosäureaustausch zu Histidin (R132H). Diese und andere IDH Mutationen resultieren in einer neomorphen enzymatischen Funktion und der Produktion des Onkometaboliten 2-Hydroxyglutarat (2-HG). Die Akkumulation von 2-HG führt zu genomweiter Hypermethylierung und maligner Transformation.

Die vorliegende Arbeit befasst sich mit der Eignung der IDH1R132H Mutation als Zielstruktur für Immuntherapien in einem MHC-humanisierten Mausmodell, in A2.DR1-Mäusen. Peptide, die die Mutationsregion enthalten, banden an MHC Klasse II *in vitro* und induzierten eine mutationsspezifische CD4+ T Helfer (Th) Antwort *in vivo*, deren Antigenspezifität auch in einer spefischen T-Zelllinie und einem Klon persistierte und die von IDH1R132H-spezifischer Antikörperproduktion begleitet war. Um IDH1R132H-spezifische IgG in murinem und humanem Serum zu detektieren, wurde ein Peptid-beschichteter ELISA etabliert. Ein Teil der untersuchten Patienten mit IDH1R132H+ Gliomen wurde positive auf spontane IDH1R132H spezifische Antikörper und CD4+ Th1 Zellen getestet. Präventive und therapeutische Peptidvakzinierung mit IDH1R132H von A2.DR1 Mäusen, die syngene IDH1R132H+ Sarkome trugen, resultierte in einer effektiven mutationsspezifischen anti-Tumor Immunantwort. Abhängig von CD4+ T-Zellen und B-Zellen konnte das Tumorwachstum durch die induzierte Immunantwort kontrolliert werden. Die Funktionalität der Vakzine wurde durch den Verlust der IDH1R132H Expression in transduzierten Tumoren und der Infiltration IDH1R132H-spezifischer CD4+ T-Zellen in die Tumormasse gezeigt. Verglichen mit therapeutischer MHC II vermittelter Peptidvakzinierung gegen das etablierte Tumor-Hoden-Antigen CTAG1B (NY-ESO-1), ist IDH1R132H ein relevantes Neoantigen vergleichbarer Wirksamkeit.

Aufgrund der IDH1R132H-vermittelten Akkumulation von 2-HG ist der Effekt dieses Metaboliten auf humane T-Zellen von potenzieller Relevanz für eine IDH1R132H-gerichtete

Immuntherapie. Jedoch waren weder periphere CD4+ noch CD8+ T-Zellfunktionen von Probanden durch 2-HG beeinträchtigt.

Schlussfolgernd lässt sich sagen, dass die IDH1R132H Mutation ein potentziell bedeutungsvolles, tumorspezifisches Neoantigen ist. Konzeptuell repräsentieren Patienten mit niedriggradigen und anaplastischen Gliomen mit einer hohen Prävalenz der IDH1R132H Mutation eine Patientenpopulation, die besonders von einer Tumorvakzine profitieren kann, da es derzeit keine Therapie gibt, die ein Rezidiv in dieser relativ jungen, immunologisch kompetenten Patientenpopulation verhindert. Darüber hinaus könnten Patientengruppen mit anderen IDH1R132H-mutierten Tumoren möglicherweise von solch einer Vakzine profitieren.

LIST OF PUBLICATIONS

Schumacher T*, Bunse L*, Pusch S, Sahm F, Wiestler B, Quandt J, Menn O, Osswald M, Oezen I, Ott M, Keil M, Balß J, Grabowska AK, Vogler I, Diekmann J, Trautwein N, Eichmüller SB, Okun J, Stevanović S, Riemer AB, Sahin U, Friese MA, Beckhove P, von Deimling A, Wick W, Platten M. A vaccine targeting mutant IDH1 induces antitumor immunity. Revision under review at **Nature**. * Authors contributed equally.

Publications not related to the thesis

Hertenstein A, **Schumacher T**, Litzenburger U, Opitz CA, Falk CS, Serafini T, Wick W, Platten M. Suppression of human CD4+ T cell activation by 3,4-dimethoxycinnamonyl-anthranilic acid (tranilast) is mediated by CXCL9 and CXCL10. **Biochem Pharmacol**. 15;82(6):632-41. (2011).

Opitz CA*, Litzenburger UM*, Sahm F, Ott M, Tritschler I, Trump S, **Schumacher T**, Jestaedt L, Schrenk D, Weller M, Jugold M, Guillemin GJ, Miller CL, Lutz C, Radlwimmer B, Lehman I, von Deimling A, Wick W, Platten M. An endogenous ligand of the human aryl hydrocarbon receptor. **Nature**. 5;478(7368):197-203. (2011). * Authors contributed equally.

TABLE OF CONTENTS

1 INTRODUCTION

1.1 Cancer Immunotherapy

Since the first description of cancer as a disease some thousands of years ago, in 3000 BC [1], and despite of considerable progress in development of treatment and therapy, in most solid tumor entities consisting of surgery, radiotherapy, and chemotherapy, cancer remains the second-leading cause of death in the industrialized world (*World Health Organization. The Global Burden of Disease: 2004 Update. Geneva: World Health Organization; 2008. www.who.int*). The idea of harnessing the immune system to target tumor cells dates back to over a century ago when bacterial toxins were injected into cancer patients for treatment [2, 3]. Since then, the reasons why cancer therapy by employment of the immune system has gained so much interest and raised hope have become more profound. The concept of cancer immunotherapy relies on immunosurveillance mechanisms, which are hypothesized to naturally prevent development of a tumor from transformed cells, and immune escape by transformed cells that are able to evade the surveillance by the immune system, thereby being able to form a tumor. Hence, immunotherapy aims at manipulating the immune system to enhance anti-tumor immunity and at preventing immune escape by the tumor.

Hints for natural tumor immunity comes from observations that after transplantation, which goes along with therapeutic immunosuppression, patients have a higher risk for developing tumors [4, 5]. In addition, it has been shown that in many tumor entities, infiltration of lymphocytes into the tumor is associated with a better prognosis [6-12]. Direct evidence for the role of the immune system in controlling tumor growth came from experiments with immunodeficient mice, which developed tumors faster and at a higher frequency than immunocompetent mice after chemical induction [13]. Furthermore, when tumors from immunodeficient mice were implanted into immunocompetent wildtype (wt) mice, they were completely rejected, suggesting that the immune system is not only capable of preventing tumor development, but also to eliminate established tumors that have not grown under immunosurveillance.

However, in the patient, tumor immunoediting eventually leads to immune escape. When transformation of cells first occurs and a tumor forms, cells of both the innate immune

system, such as dendritic cells (DC) and natural killer (NK) cells, and adaptive immune system, such as T cells, are activated and eliminate tumor cells [14, 15]. Yet, because of genetic instability and heterogeneity of tumor cells, immune selection leads to equilibrium between anti-tumor immunity and immunosuppressive mechanisms and eventually to immune escape and tumor progression. Under immune selection, tumors regulate a variety of pathways to evade immunosurveillance. These include inhibition of DC maturation and functions, leading to inhibited immune response or T cell tolerance [16], downregulation of receptors that are required for targeted NK cell functions [17], downregulation of MHC receptors that are essential for antigen presentation and therefore recognition by cytotoxic T cells (CTL) [15], recruitment of immunosuppressive components of the immune system such as regulatory T cells (T_{reg}) [18] and myeloid-derived suppressor cells (MDSC) [19], and induction of an immunosuppressive microenvironment, e. g. by secretion of transforming growth factor β (TGF-β) and interleukin (IL)-10 [20].

Cancer Immunotherapy follows two distinct strategies to exploit the immune system for targeted cancer treatment. Passive immunotherapies target tumor cells specifically and exert immunological anti-tumor effects by themselves. These include tumor-specific monoclonal antibodies or administration of specific T cells by adoptive T cell transfer. Tumor cell killing mechanisms range from direct action over immune-mediated killing to payload delivery [21]. Prominent examples for passive immunotherapy targets that are involved in immune responses are cytotoxic T lymphocyte-associated antigen 4 (CTLA-4) and programmed cell death protein 1 (PD1). Both are proteins involved in immune checkpoint mechanisms that diminish T cell activation or lead to tolerance induction and are expressed on activated T cells [22, 23]. Both can be inhibited with monoclonal antibodies. Ipilimumab, which is specific for CTLA-4, has proved to strengthen cellular immune responses and anti-tumor activity [24], and has therefore been approved by the U.S. Food and Drug Administration (FDA) for melanoma. In patients with advanced melanoma, ipilimumab enhances overall survival compared to standard care with long-term effects [25, 26], suggesting the generation of an immunological memory as a major advantage of immunotherapy. Likewise, an inhibitory antibody targeting PD1 amplified T cell function, thereby reducing tumor growth in mouse models for melanoma and colon carcinoma [27]. Moreover, in a Phase I clinical trial, blockade of PD1 showed promising results [28].

Adoptive T cell transfer is the re-infusion of autologous or allogeneic tumor antigen-specific T cells into the patient. These T cells can be genetically engineered e.g. to express chimeric antigen receptors (CARs) serving as artificial T cell receptors, or expanded *ex vivo* from the patient (reviewed by [29]). In clinical trials, adoptive transfer of CD8+ as well as CD4+ T cells specific for NY-ESO-1 (see below) into melanoma patients has proven to be effective [30, 31].
Active immunotherapy intends to tip the balance between immunosurveillance and immune escape towards successful eradication of the tumor by stimulation of the host's immune system to generate a tumor antigen-specific cellular and humoral response. Strategies to achieve an antigen-specific T cell-mediated anti-tumor immune response involve cDNA or peptide vaccination and dendritic cell vaccination using whole tumor lysates or specific antigenic proteins. For all approaches, the presentation of a tumor-specific or tumor-associated antigen as target, leading to the induction of antigen-specific and tumor-reactive T cell responses, is required in order to achieve specificity for tumor cells. Typically, targeted antigens can be unaltered tissue differentiation antigens that are overexpressed in corresponding tumor entities, such as gp100, melanoma antigen recognized by T cells 1 (MART1), and tyrosinase-related protein 1 and 2 (TYRP1/2), which are overexpressed in melanoma [32-34], tumor stroma and vasculature antigens, viral antigens e.g. from human papillomavirus (HPV), gene mutation products such as epidermal growth factor receptor variant III (EGFRvIII), which has been targeted in phase II clinical trials [35], and antigens that are derived from epigenetic changes which trigger the expression of so-called cancer-testis antigens that are usually only expressed in the germline, including cancer testis antigen 1 (CTAG1, or New York esophageal squamous cell carcinoma (NY-ESO-1) (reviewed by [29]). In contrast to overexpressed antigens, gene mutation products may induce reactive T cells that have not been subjected to tolerance during thymic development hence may induce stronger responses. The advantage of cancer testis antigens is that they are expressed in many tumor entities but not in normal non-germline tissue. Specific T cells do not recognize the antigen on male germline cells because these lack expression of major histocompatibility complexes (MHC) and therefore do not present the antigen [36].
The most prominent and very potent cancer testis antigen NY-ESO-1 has been identified in esophageal squamous cell carcinoma and is expressed in a variety of cancers such as melanoma, breast, bladder and prostate cancer, and hepatocellular carcinoma [37] and is one of the most immunogenic tumor antigens, inducing both spontaneous humoral and

cellular immune responses in mice and patients. T cell responses to NY-ESO-1 are not restricted to CTL, but NY-ESO-1 also elicits CD4+ T cell reactivity and humoral responses [38-43]. In clinical trials, NY-ESO-1-specific immunotherapy has led to profound immune responses even in NY-ESO-1-negative patients, with a benefit for NY-ESO-1-positive patients [31, 44, 45].

For an efficient anti-tumor immunity against a particular antigen, antigen-presenting cells (APC), mostly DC, need to take up tumor antigens, process them and present them on MHC molecules to CD4+ or CD8+ T cells. Antigen-specific T cells need to differentiate into effector T cells by engagement of peptide-MHC complexes by the T cell receptor (TCR), by co-stimulatory signals delivered to CD28, and by stimulatory cytokines. In Immunotherapy, antigen presentation can be achieved by protein or mostly peptide vaccination using an effective epitope, during which DC take up the antigenic peptide inside the patient. This type of vaccination is the easiest and most cost-effective vaccination. Several studies have targeted NY-ESO-1 by vaccination with protein [44] or peptide [45]. For peptide vaccination, the use of an immune-stimulatory adjuvant is required in order to establish innate immune responses. This is usually achieved by administration of pattern recognition receptor ligands, mostly for toll-like receptors (TLRs) (reviewed in [46]). The TLR-7 agonist imiquimod has proven a potent adjuvant, which enhanced immune responses in a clinical trial in prostate cancer patients [47]. Another example are synthetic oligodeoxynucleotides containing unmethylated CG dinucleotides (CpG), which bind TLR-9 and have proven efficacious against melanoma, renal cell carcinoma [48], and cutaneous T cell lymphoma [49] in clinical studies. Alternatively to peptide, autologous DC from the patient can be isolated and loaded *ex vivo* with defined antigen or autologous tumor lysate to allow optimal DC priming and patient-specific immunity. During DC vaccination, these primed DC are infused back into the patient. As an example, the DC vaccine sipuleucel-T stimulates T cells specific for the overexpressed prostate carcinoma antigen prostatic acid phosphatase (PAP) and has been approved by the FDA for prostate cancer patients [50], significantly increasing overall survival by four months. Since most tumors are strongly immunosuppressive, it is acknowledged that overcoming these conditions at the tumor site and breaking immune tolerance mostly in combination with vaccination are required for induction of potent anti-tumor immunity. Strategies for immunomodulation include the inhibition of immunosuppressive cell populations such as T_{reg}. In colorectal cancer patients, T_{reg} depletion led to elevated antigen-specific T helper cell

responses [51]; however, inhibition of T_{reg} bears the risk of autoimmune induction [52, 53]. Immunomodulatory antibodies for passive immunotherapy as discussed above are also used in combination with active vaccination.

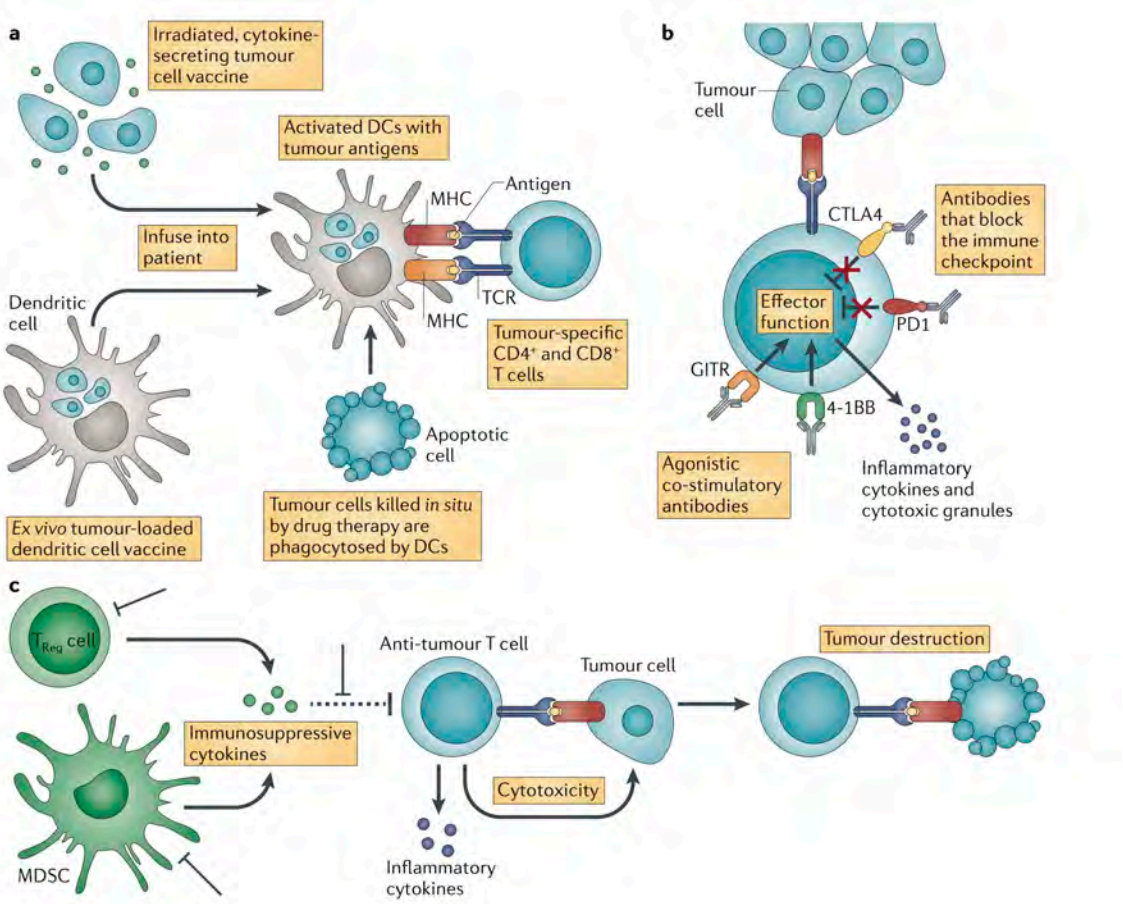

Fig. 1.1. Generation of effective tumor-specific immune responses depends on antigen presentation to and stimulation of T cells, enhancement of T cell functions, and inhibition of immunosuppression. a, DC priming of tumor antigen-specific T cells can be accomplished by injection of irradiated whole tumor cells, which are phagocytosed by DC. DC present tumor antigens to T cells. Alternatively, DC are isolated from the patient, loaded with autologous tumor lysate or specific antigen, matured *ex vivo* and re-implanted into the patient. Besides, chemotherapy or targeted therapy leads to apoptotic tumor cells that can be phagocytosed by DC. **b**, Passive immunotherapy can enhance T cell function through co-stimulation or block of inhibitory signals by agonistic or antagonistic antibodies, respectively. **c**, Immunosuppressive T_{reg} and MDSC inhibit immune responses by release of cytokines IL-10 and TGF-β. Inhibition of cytokine secretion or depletion of these cell populations can boost anti-tumor effective T cell responses. [54]

Taken together, cancer immunotherapy aims at the generation of a potent anti-tumor immune response. This includes (a) DC priming for an efficient antigen-presentation to T cells, (b) enhancement of T cell function, and (c) inhibition of immunosuppression (Fig. 1.1).

1.2 Classification, clinical and molecular characteristics, and standard therapy of glioma

Gliomas belong to the two most abundant types of tumors of the central nervous system (CNS), constituting 29 % of primary CNS tumors, the other group being meningiomas with 35.5 %. Notably, gliomas account for 80 % of malignant primary CNS tumors [55]. CNS tumors are among the rather rare tumor entities with an incident rate of 20.6 cases per 100.000 people in the U.S. in 2012, but belong to the most malignant tumors with low median survival rates [56].

Gliomas were named according to histopathological similarities of tumor cells with glial cells, which are non-neuronal cells of the central and peripheral nervous systems (CNS, PNS, respectively) that support and protect neurons by physical support, nutritient and oxygen supply, myelin formation, immune functions, and homeostasis. Glial cells are classified into macroglia and microglia. In the CNS, macroglia consist of astrocytes, oligodendrocytes, ependymal cells, and radial glia. The most common macroglial cell types in the CNS are astrocytes, which are mainly involved in regulation of blood flow and the formation of the blood-brain-barrier (BBB), and oligodendrocytes, which form myelin sheaths to coat the neuronal axons, allowing efficient propagation of electrical signals along the axons. Ependymal cells line the ventricle walls and secrete the cerebrospinal fluid (CSF), whereas radial glia are the glia cells of the retina. As opposed to macroglia, microglia during development originate in the embryonic yolk sac and arise from the hematopoietic system in the bone marrow during inflammation [57, 58]. They function as brain resident macrophages as they fulfill phagocytotic functions as part of the innate immune system in the brain. Since glial cells are most abundant in the brain, this is the most common site where gliomas occur. In fact, gliomas are the most common brain tumors in adults, constituting 12-15 % of all intracranial neoplasms, 30 % of all CNS and brain tumors, and even 80 % of all primary brain tumors [55].

Gliomas can be classified according to the histologically corresponding normal cell type, malignancy, or location. In accordance with glial cell types, gliomas are grouped into astrocytomas, oligodendrogliomas, ependymomas, mixed gliomas such as oligoastrocytomas, and neuroepithelial tumors. Whether gliomas indeed arise from glial cells remains a matter of debate. Recent *in vivo* studies suggest that the cell of origin can be a committed glial cell like an astrocyte and oligodendrocyte, a more immature precursor cell or a neural stem cell

[59]. According to malignancy, gliomas are classified into World Health Organization (WHO) grades I to IV, whereas grade I tumors are slowly proliferating tumors with a high probability of cure by surgical resection. Low-grade gliomas (WHO °II) are well-differentiated, also slowly proliferating but infiltrate the brain parenchyma, which impairs resection [60]. Diffuse astrocytoma, oligodendroglioma and the mixed subtype oligoastrocytoma belong to low-grade gliomas and patients suffering from these subtypes have a median survival of 7-10 years. However, despite resection and several years of tumor-free survival, these glioma types are prone to recurrence and malignant progression to a higher grade and thus eventually also lethal [60, 61]. High-grade glioma grades III and IV are anaplastic, i.e. de-differentiated, and more malignant, requiring aggressive adjuvant therapies after resection [62]. Grade III gliomas are histologically characterized by nuclear atypia and enhanced proliferation [60]. The median survival for patients with grade III gliomas like anaplastic astrocytoma is highly variable between 2 and 5 years [62]. Glioblastoma multiforme (GBM) is the most malignant glioma (WHO grade IV), highly proliferative with presence of necrotic areas, and accounts for about 50 % of brain tumor cases. Maximal median survival for GBM in study cohorts receiving therapy is only 14-17 months [63, 64].

Glioma patients initially present in the clinic with symptoms like seizures, headaches caused by increased intracranial pressure, and focal neurologic deficits or altered mental status because of mass effect, infiltration or destruction of the affected part of the brain. Primarily, diagnosis is done by magnetic resonance imaging (MRI), which demonstrates tumor lesions. However, a conclusive and differential diagnosis depends on histological analysis of tumor tissue obtained from biopsy or resection [56].

Surgery with maximal possible resection is, if feasible, the first therapeutic intervention for glioma. Standard of care subsequent to surgery depends on tumor type and grade of resection. Adjuvant therapy mostly consists of radiotherapy, frequently accompanied or followed by chemotherapy using the alkylating agent temozolomide (TMZ) [61, 65, 66]. However, with respect to low-grade gliomas, wait-and-watch after surgery might be the best strategy for some patients.

Especially high-grade gliomas are characterized by areas of necrosis and hypoxia and are therefore highly angiogenic tumors that are heavily vascularized. In addition, they are infiltrative tumors with distinct single cells that can be found apart from the tumor bulk, making a complete resection difficult. However, gliomas are not mitogenic, although high-

grade gliomas are associated with a breakdown of the blood-brain barrier (BBB). Gliomas are generally immunosuppressive, especially due to the secretion of immunosuppressive factors such as TGF-β (see 1.4).

On a molecular level, gliomas are hallmarked by a variety of genetic and epigenetic alterations, and the mutational signature of a tumor has been identified to distinguish glioma subtypes and to shed light on the development and progression of the tumor (Fig. 1.2). Astrocytomas in general mostly carry a mutation in the tumor suppressor gene p53 (*TP53*, 65 %) whereas oligodendrogliomas frequently show co-deletion of chromosomes 1p/19q (>75 %). With respect to glioblastoma, different genetic and epigenetic profiles distinguish primary and secondary glioblastoma. The most common genetic alteration in all glioblastomas is the loss of heterozygosity (LOH) on chromosome 10 found in primary and secondary glioblastomas [67]. The majority of glioblastomas (>90 %) develops *de novo* and is named primary glioblastomas. Typical for these tumors are *epidermal growth factor receptor (EGFR)* amplification (35 %) [68] or overexpression (63 %) and loss or mutations of *phosphatase and tensin homologue* (*PTEN*, 25 %). On the other hand, secondary glioblastomas progress from diffuse or anaplastic astrocytoma and therefore show astrocytoma-specific mutations including the TP53 mutation. In addition, they have acquired accessory alterations, including LOH of 19q. An important hallmark that distinguishes primary glioblastoma from other gliomas including astrocytoma, oligodendroglioma, and secondary glioblastoma, is the mutation of the *isocitrate dehydrogenase 1 (IDH1)* [69-71] in 88 % of gliomas except primary gliobastomas (see 1.3). [67]

Based on their molecular and genetic alterations, gliomas have been classified into four main subgroups by integrated genomic analysis, explicitly proneural, neural, classical, and mesenchymal classes [72]. Proneural class gliomas are characterized by two major but mutually almost exclusive alterations, first concomitant focal amplifications with high gene expression levels of *platelet-derived growth factor receptor alpha* (PDGFRA), and second point mutations in the *IDH1* gene (see 1.3). Moreover, TP53 alterations are frequent in this group. Most of secondary GBM are classified into the proneural class. The neural subtype is classified by neuronal marker gene expression, such as *neurofilament light polypeptide* (NEFL), and *gamma-aminobutyric acid (GABA) A receptor, alpha 1* (GABRA1). The classical class exhibits a significant increase in *EGFR* expression accompanied by frequent mutations in this gene. Mesenchymal gliomas are identified by *neurofibromin 1* (NF1) mutations or

deletions and mesenchmymal and astrocytic marker expression such as *CD44* and *c-mer proto-oncogene tyrosine kinase* (MERTK). [72]

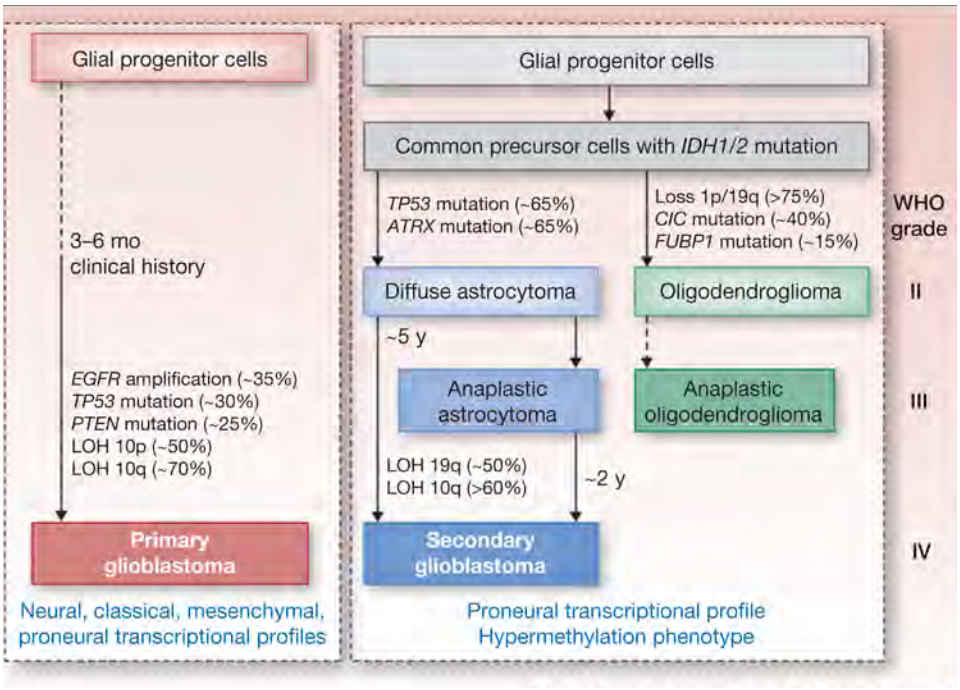

Fig. 1.2 Genetic pathways to primary and secondary glioblastomas. [67]

Epigenetically, gliomas can be catagorized according to promotor methylation patterns since the discovery of the glioma CpG island methylator phenotype (G-CIMP), which is defined by hypermethylated regions (CpG islands) throughout a large number of loci [73]. G-CIMP gliomas belong to the proneural class and are tightly associated with IDH1 mutations, which are causative for the hypermethylation (see 1.3). Due to the hypermethylation phenotype, G-CIMP gliomas (as well as some others) exhibit methylation of the O6-methylguanine-DNA methyl-transferase (MGMT) promotor, thereby silencing MGMT, a DNA mismatch repair enzyme, leading to increased sensitivity towards alkalyting chemotherapy such as TMZ [74]. More recently, six different epigenetic subgroups among gliomas have been suggested, characterized by two mutations in the gene for histone H3.3 (*H3F3A*) occuring at young age (K27 belonging to the proneural class, and G34), IDH mutation (IDH, proneural class), PDGFRA amplification (RTK I PDGFRA, proneural class), mesenchymal and classical [75].

With this deeper understanding of heterogeneity and tumorigenic pathways of gliomas, not only biomarkers for diagnosis and prognosis have been identified, but also potential targets for specific treatment. Targeted therapy, however, will possibly remain a long-term goal in the next years.

1.3 The IDH mutations

Mutations in the *isocitrate dehydrogenase 1 (IDH1)* gene located on chromosome 2q33 were originally identified by an integrated genomic screen of glioblastoma multiforme [70]. Point mutations in the active site of the enzyme were found in 12 % of GBM patients and correlated with mutations in TP53, but not with PTEN, *retinoblastoma 1* (RB1), EGFR, or NF1 mutations, supporting the notion of distinct glioma subclasses (see 1.2). Isocitrate dehydrogenase isoforms are homodimeric enzymes catalyzing the oxidative decarboxylation of isocitrate to α-ketoglutarate (α-KG), producing nicotinamide adenine dinucleotide phosphate (NAD[P]H) [76]. Unlike the other isoforms, IDH1 is not located in the mitochondria, but in the cytoplasm and peroxisomes [77], where it plays an essential role in cellular regulation of oxidative stress by the generation of NADPH [78, 79]. IDH types 2 and 3 are located in the mitochondria and involved in the citric acid cycle and the generation of ATP.

IDH1 mutations occur in more than 70 % of diffuse and anaplastic astrocytomas, oligodendrogliomas, oligoastrocytomas, and secondary glioblastomas progressing from anaplastic astrocytomas [69, 71] and in all entities are associated with increased progression-free and overall survival and can thus be used as a prognostic marker for glioma patients. [70, 71, 75, 80]. However, no predictive value for treatment decisions has been shown for IDH1 mutations [80].

IDH mutations are an early – if not the earliest – event in gliomagenesis and probably occur before TP53 mutations or 1p/19q loss, because gliomas carrying only an IDH mutation are more frequent than those with only TP53 mutation or 1p/19q codeletion [67, 81]. Loss of 1p/19q appears later and may be the driving force toward oligodendroglioma differentiation [82-84].

Mutations in IDH1 almost uniformly affect amino acid 132, leading to an exchange of histidine to arginine (R132H), a critical residue in the catalytic site of the enzyme, forming salt bridges with the substrate isocitrate and mediating the hinge movements towards the active conformation [85]. The replacement with histidine leads to inability to bind the natural substrate. Most grade II and III gliomas as well as secondary glioblastomas which are negative for IDH1 mutations, harbor mutations in the IDH2 gene, uniformly affecting amino

acid arginine 172, which is the analogous amino acid to 132 of IDH1 [71]. Since their discovery not only in gliomas, but also other tumor entities such as acute myeloid leukemia (AML) [86-88], sarcomas like chondrosarcoma [89, 90], and intrahepatic cholangiocarcinomas [91], a large body of evidence has accumulated delineating the metabolic consequences of these monoallelic point mutations and their implications in tumorigenesis [92]. The amino acid exchange within the catalytic sites results in the inhibition of wt enzymatic function [93] and a neomorphic dominant enzymatic function that is associated with the reduction of α-KG to and the accumulation of the oncometabolite (R)-2-hydroxyglutarate (2-HG) (Fig. 1.3) [85, 88, 94].

IDH type 1 and 2 mutations and the consequences of 2-HG accumulation have been extensively studied. 2-HG accumulation is sufficient to alter the epigenome of glial and hematopoietic cells [95, 96] resulting in a hypermethylation phenotype [97, 98] by competitively inhibiting α-KG-dependent dioxygenases such as the methylcytosine hydroxylase TET2, which mediates DNA demethylation, and the histone demethylase JmjC [99]. These inhibitory mechanisms lead to DNA hypermethylation and therefore to the so-called G-CIMP. The IDH mutation is sufficient for establishment of this epigenetic phenotype [95], which leads to genetic instability, the subsequent acquisition of additional mutations and ultimately malignant transformation [100].

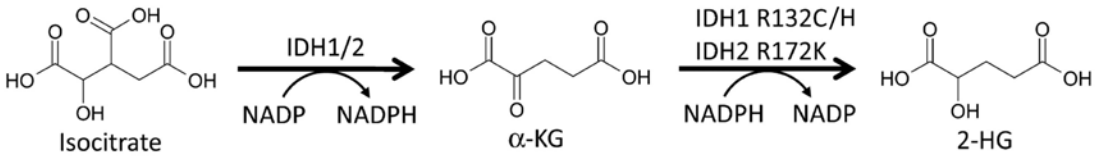

Fig.1.3. Chemical reactions catalyzed by IDH wt and IDH mutant enzymes. IDH1 and IDH2 convert isocitrate α-ketoglutarate by oxidative decarboxylation under the concomitant reduction of NADP to NADPH. Of note, IDH3 utilizes NAD+ to produce NADH. α-ketoglutarate serves as substrate for IDH mutant enzymes IDH1R132C, IDH1R132H, and IDH2R172K, which in turn reduce it to 2-hydroxyglutarate with accompanying oxidation of NADPH to NADP. The heterozygous nature of the mutation ensures sufficient α-KG levels. (Adapted from [94])

The identification of IDH1R132H has led to the epigenetic classification of gliomas according to promoter methylation patterns. Most GBM of the proneural subgroup carry the IDH1 mutation, which defines the G-CIMP methylation phenotype. The definition of six methylation clusters includes one so-called IDH subgroup (see 1.2) [75, 101].

The IDH1 mutation has been identified as a prognostic but not predictive marker in grade II – IV gliomas [80, 101-103]. Patients with IDH1R132H-mutated anaplastic glioma benefit from a better progression-free survival independent of treatment compared to patients with IDH1 wt anaplastic gliomas [104], together with the causality of mutation events supporting the notion that IDH1 mutation defines a distinct glioma entity.

In gliomas and other solid tumors the development of an antibody detecting IDH1R132H [105, 106] has not only been implemented in clinical routine diagnostics of gliomas [66] but also guided the concept that IDH1R132H is expressed in all tumor cells constituting this mutation an early event in gliomagenesis [107]. Beyond expanding the knowledge on the metabolic and epigenetic control of tumorigenesis, the discovery of IDH1 mutations bears important therapeutic implications. One route is the development of specific inhibitors of the neomorphic enzymatic function of IDH1 and IDH2, which are capable of suppressing tumor growth in preclinical cancer models of glioma and AML [108, 109]. As a specific and uniform hallmark of many gliomas and other tumors, IDH mutations might pave the way to a more targeted therapy for the hitherto believed to be highly heterogeneous glioma.

1.4 Immunotherapy for glioma patients

Improvements in standard therapy have not yet led to markedly enhanced survival, much less to cure of gliomas. In search of alternative and novel therapies to combat gliomas, immunological approaches, which have proven efficacious for other entities, have gained interest [110].

Gliomas are in general immunosuppressive tumors. Brain parenchyma as well as the tumor itself are characterized by soluble immunoinhibitory factors derived from microglia, astrocytes, and tumor cells, such as transforming growth factor β (TGF-β), which suppresses T cell proliferation and NK cell activity and induces T cell apoptosis [111], vascular endothelial growth factor (VEGF), and IL-10, as well as the expression of inhibitory enzymes, e.g. indoleamine 2,3-dioxygenase (IDO) by dendritic cells and tryptophan-2,3-dioxygenase (TDO) [112], impairing T cell functions, arginase, and nitric oxide synthase 2 (NOS-2) by tumor cells. In this regard, constitutive STAT-3 activation by tumor cells seems to be a central regulator in suppressing anti-tumor immune responses [113].

These immunosuppressive factors lead to impaired effector T cell (T_{eff}) proliferation and enhanced proliferation and recruitment of T_{reg}. Glioma cell expression of inhibitory surface molecules such as Fas ligand (FasL) and PD-1L (B7-H1) as well as the downregulation of MHC molecules contribute to weakened T cell proliferation and the induction of apoptosis [114]. The immunomedulatory microenvironment in glioma convert microglia and glioma-infiltrating monocytes to immunosuppressive phenotypes [115] and immunosuppressive monocytic cells, which have been termed myeloid-derived suppressor cells (MDSC) are found to inhibit T cell functions in glioma [116-119]. Hence, gliomas both directly inhibit T_{effs} and act immunosuppressive on other components of the immune system (Fig. 1.4)

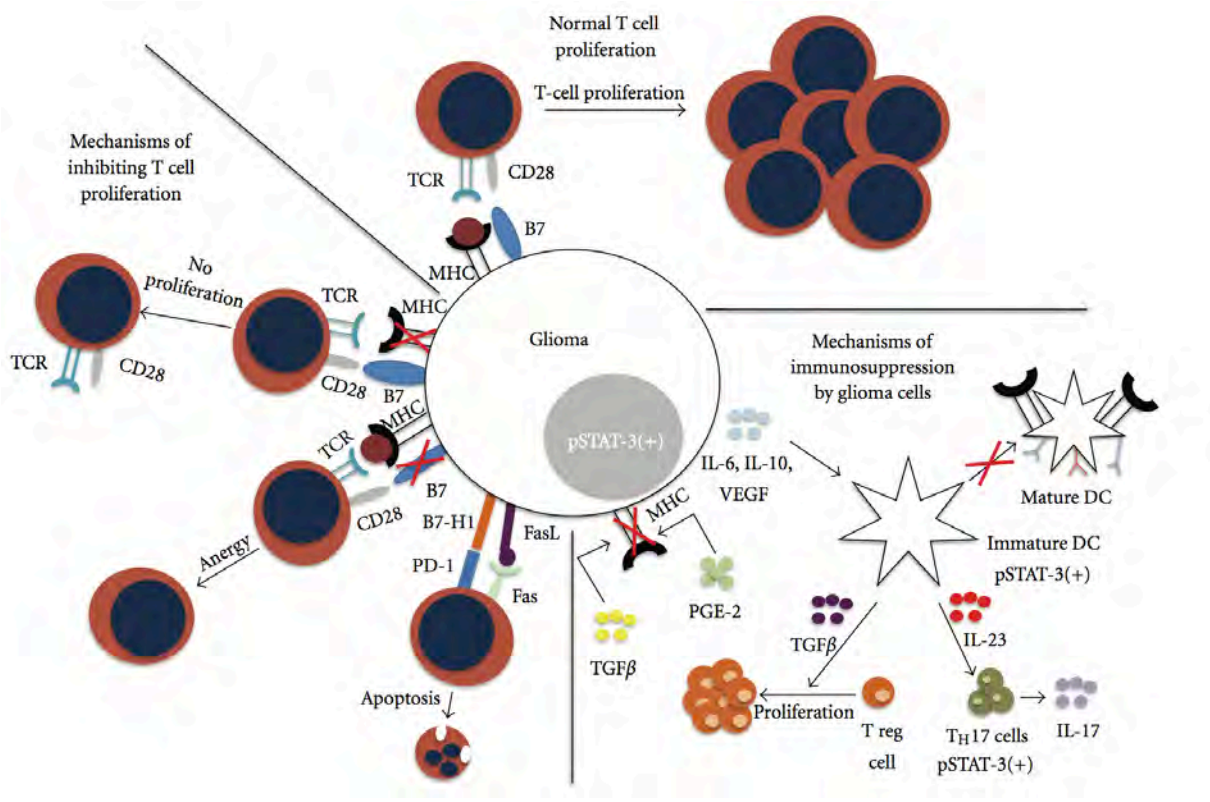

Fig. 1.4. Immunosuppressive mechanisms in glioma. [120]

The healthy brain is no longer regarded as a completely immunologically privileged organ, despite its intact BBB and lack of lymphatic vessels. Rather, the BBB allows tight regulation of immune responses in the brain by controlling the selective trafficking of immune infiltrates into the brain. Hence, under physiological conditions, the brain contains microglia, which are the brain-resident APCs contributing to 20% of CNS cells, macrophages and DCs [121]. The intact BBB results in the impairment of immune-mediated rejection at the time of malignant transformation and beginning of glioma growth. However, the necessity for a disruption of

the BBB for immune responses in the brain is a prevalent misconception that can be refuted by the fact that autoimmunity occurs in the brain without a primary BBB disruption, e.g. multiple sclerosis (MS) [122]. Actually, T cells constantly infiltrate and survey the brain to prevent inflammation of the CNS potentially caused by viral infections [123]. Moreover, during the course of tumor progression, the BBB becomes disrupted, making gliomas even more accessible for immune cell infiltrates and leading to chemokine-mediated attraction of immune cells into the brain tumor, including macrophages, DCs, and T cells [114], the latter consisting of both CD4+ and CD8+ T cells and constituting up to 3.2 % of tumor cells in high grade glioma [124, 125]. The finding that immunological synapses between T cells and glioma cells can form in the patient [126] leads to the assumption that infiltrating T cells are functional, targeting glioma cells.

Evidence that T cell-mediated immunitiy can play a role for glioma regression came from rat models of glioma, in which genetically modified glioma cells expressing IFN-γ implanted into the brain caused microglia priming with T cell infiltration and tumor rejection [127]. In glioma patients, tumor-infiltrating lymphocytes (TILs) are associated with longer survival and the extent of T cell infiltration correlates with a better outcome [128-131]. Importantly, glioma-infiltrating T cells were shown to be functional in exert tumor cell lysis *in vitro* [132], indicating that cytotoxic T cells are not only able to infiltrate gliomas, but also retain their functionality when not exposed to the immunosuppressive microenvironment of gliomas.

T cell-mediated anti-glioma immunity requires the presence of glioma-specific antigens. Although gliomas are heterogeneous tumors, several antigens have been identified, in part by mass spectrometry-based identification of HLA-bound epitopes, some of which shown to be immunogenic, such as IL13Rα2, EGFRvIII, gp100, and TRP2 [133], as well as survivin, SOX2, and MAGE1, [134-136]. Yet, a lot of clinical immunotherapy studies for glioma patients apply DC vaccination using autologous tumor lysate. In a study enrolling 23 patients with newly diagnosed glioblastoma, autologous tumor lysate loaded onto autologous and *ex vivo* matured DC, which were reinjected into the patient, led to CD8+ T cell infiltration into the recurrent tumor and – compared to historical controls – increased overall survival. Even more, this study identified glioblastoma of the mesenchymal subtype as the responding group susceptible to this type of immunotherapy, while patients with proneural GBM did not benefit from vaccination and did not show enhanced CD8+ T cell infiltration [137]. However, the uncontrolled and one-armed, non-blinded nature of this study makes conclusions on

effectiveness of such a vaccine difficult. In terms of glioma antigen-specific vaccination, EGFRvIII has probably gained most interest in recent years. Originally identified in primary human GBM, where it is expressed in 30 % of patients, EGFRvIII is a constitutively active, ligand-independent form of the EGFR that has been implicated in tumorigenicity via proliferation induction and inhibition of apoptosis [138, 139] as well as in resistance towards radiotherapy [140]. Thus, EGFRvIII represents a promising target and neoantigen, one of the few mutation antigens. Its immunogenicity arises from an in-frame deletion, leading to a truncated extracellular domain with creation of an antigenic junction harboring a novel glycine residue, and has led to the development of an EGFRvIII-specific peptide vaccine that has been extensively studied preclinically and clinically [141]. In a one-armed phase II trial, vaccination led to enhanced progression-free and overall survival compared to historical controls. Within the vaccinated patient group, responders measured by delayed-type hypersensitivity response and antibody development had a higher benefit than non-responding patients. However, patients eventually suffered from recurrence, which was associated with a loss of EGFRvIII expression [35]. Although this immunologic escape is an indicator for biological activity, these results might also be explained by the heterogeneity of gliomas, i.e. the presence of EGFRvIII-negative cells within the tumor, which are selected by immunotherapy.

With improved understanding of glioma immunobiology and immunosuppression, immunomodulation and targeting glioma-specific antigen might become part of combination therapy for glioma patients. In this regard, the homogeneous expression of the target is critical in a tumor entity that is characterized by regression and progression.

1.5 Objectives of this thesis

IDH1 mutations have proven to be effectively targeted by specific inhibitors, which change epigenetic characteristics and result in growth suppression [108, 109]. A different potential strategy may be to explore mutated IDH1 as a cancer immunotherapy target. From an immunological perspective the IDH1R132H mutation represents a potential target for active immunotherapy particularly of low grade and anaplastic gliomas as it is tumor specific, represents a potential neoantigen with high uniformity and penetrance and is expressed in all tumor cells [84, 106]. In addition, the development of a mutation-specific antibody in

mice [106] suggests that the immune system is – in principle – capable to discriminate between mutant and wt IDH1.

The present study aimed at evaluating the suitability of the IDH1R132H mutation as an immunotherapeutic target for gliomas and potentially other IDH1R132H-mutated tumors. To this end, analyses on the mutation-specific immunogenicity of potential epitopes in an MHC-humanized mouse model *in vivo*, spontaneous immune responses in glioma patients with IDH1R132H-mutated tumors, and the antitumor functionality of a peptide vaccine in MHC-humanized mice as well as the characterization of the immune response and possible effects of 2-HG on human T cells were included.

2 MATERIALS AND METHODS

2.1 Special materials

2.1.1 Mice

A2.DR1 mice B6.Tg(HLA-DRA*0101,HLA-DRB1*0101)1Dmz Tg(HLA-A/H2-D/B2M) 1Bpe H2-Ab1tm1Doi on C57BL/6J background are deficient for mouse MHC class I (H-2b) and class II (H-IAb) and transgenic for human MHC class I HLA-A*0201 and class II HLA-DRA*0101 and HLA-DRB1*0101 and were kindly provided by [142]. DR4 transgenic mice C57BL/6-Tg(HLA-IEd alpha/HLA-DRB1*0401-I-Ed beta)#39-2 are deficient for mouse MHC class II (H-2b) and transgenic for human MHC class II HLA-DRA*0101 and HLA-DRB1*0401 and were kindly provided by [143]. NOD/SCID mice were purchased from Charles River (Sulzfeld, Germany). Mice were bred according to local regulatory authorities.

2.1.2 Patients and patient samples

Patients were diagnosed at the Institute of Neuropathology, University Hospital Heidelberg. Blood samples were taken after patient agreement and approval of the local regulatory authorities. IDH1 mutation status was routinely determined by immunohistochemistry (IHC) and in exceptional cases by polymerase chain reaction (PCR) at the Institute of Neuropathology, University Hospital Heidelberg. Buffy coats of healthy donors were obtained from IKTZ Heidelberg. For patient characteristics, see 6.5, Table 6.1.

2.1.3 Peptides

Human IDH1wt and IDH1R132H amino acid sequences IDH1 p118-146 PRLVSGWVKPIIIGRHAYGDQYRATDFVV (wt) and PRLVSGWVKPIIIGHHAYGDQYRATDFVV (R132H), respectively, cover the amino acid exchange from arginine to histidine at position 132 and include all possible putatively processed 15-mer IDH1 peptides containing position 132 (Fig. 3.1). Mouse and human sequences are identical in this region except for amino acid 122 (serine in human, threonine in mouse). Peptide libraries for *ex vivo* and *in vitro* stimulation of IDH1wt and IDH1R132H of 10 amino acid long peptides with an overlap of 9

amino acids (10-mers) and 15 amino acid long peptides with an overlap of 13 amino acids (15-mers) contained the following peptides:

IDH1wt p123-132: GWVKPIIIGR;
IDH1wt p124-133: WVKPIIIGRH;
IDH1wt p125-134: VKPIIIGRHA;
IDH1wt p126-135: KPIIIGRHAY;
IDH1wt p127-136: PIIIGRHAYG;
IDH1wt p128-137: IIIGRHAYGD;
IDH1wt p129-138: IGRHAYGDQ;
IDH1wt p130-139: IGRHAYGDQY;
IDH1wt p131-140: GRHAYGDQYR;
IDH1wt p132-141: RHAYGDQYRA;
IDH1wt p118-132: PRLVSGWVKPIIIGR;
IDH1wt p120-134: LVSGWVKPIIIGRHA;
IDH1wt p122-136: SGWVKPIIIGRHAYG;
IDH1wt p124-138: WVKPIIIGRHAYGDQ;
IDH1wt p126-140: KPIIIGRHAYGDQYR;
IDH1wt p128-142: IIIGRHAYGDQYRAT;
IDH1wt p130-144: IGRHAYGDQYRATDF;
IDH1wt p132-146: RHAYGDQYRATDFVV;
IDH1R132H p123-132: GWVKPIIIGH;
IDH1R132H p124-133: WVKPIIIGHH;
IDH1R132H p125-134: VKPIIIGHHA;
IDH1R132H p126-135: KPIIIGHHAY;
IDH1R132H p127-136: PIIIGHHAYG;
IDH1R132H p128-137: IIIGHHAYGD;
IDH1R132H p129-138: IIGHHAYGDQ;
IDH1R132H p130-139: IGHHAYGDQY;
IDH1R132H p131-140: GHHAYGDQYR;
IDH1R132H p132-141: HHAYGDQYRA;
IDH1R132H p118-132: PRLVSGWVKPIIIGH;
IDH1R132H p120-134: LVSGWVKPIIIGHHA;

IDH1R132H p122-136: SGWVKPIIIGHHAYG;

IDH1R132H p124-138: WVKPIIIGHHAYGDQ;

IDH1R132H p126-140: KPIIIGHHAYGDQYR;

IDH1R132H p128-142: IIIGHHAYGDQYRAT;

IDH1R132H p130-144: IGHHAYGDQYRATDF;

IDH1R132H p132-146: HHAYGDQYRATDFVV.

For mouse vaccination and restimulation experiments, 20 amino acid long peptides

IDH1R132H p123-142 GWVKPIIIGHHAYGDQYRAT and

IDH1wt p123-142 GWVKPIIIGRHAYGDQYRAT and

25 amino acid long peptide

NY-ESO-1 p119-143 PGVLLKEFTVSGNILTIRLTAADHR

were used. As negative control peptide for *ex vivo* and *in vitro* stimulation, mouse myelin oligodendrocyte glycoprotein (MOG) p35-55 MEVGWYRSPFSRVVHLYRNGK was used. For ELISA establishment as negative control, MOG p35-55 and human immunodeficiency virus (HIV)-1 p17 gag p77-85 SLYNTVATL were used. In T2 binding assay, human T lymphotropic virus 1 (HTLV1) tax p11-19 LLFGYPVYV was used. MOG peptide was synthesised by Genscript. Tax, HIV, NY-ESO-1 p119-143, and IDH1 10-mer peptides were synthesized in house by DKFZ proteomics and genomics Core Facility, 15-mer and 20-mer peptides were synthesized by Bachem Distribution Services GmbH and jpt. Peptides were diluted in PBS 10% DMSO at 2.5 mg/ml and stored at -80°C.

2.1.4 2-hydroxyglutarate

(R)-2-hydroxyglutarate sodium salt was purchased from Sigma-Aldrich (order no. H8378).

2.2 Methods

2.2.1 MHC binding prediction

IDH1R132H p122-142 was subjected to HLA-A*0201 (HLA-A2) peptide binding prediction using NetMHC [144]. Algorithms for 8-mers, 9-mers, 10-mers, and 11-mers containing R132H were performed. Peptides with IC50 below 500 nM are defined as weak binders, those with IC50 below 50 nM are defined as strong binders. Prediction for binding of 10-mer peptides within the library to HLA-A2 was also performed using the SYFPEITHI algorithm [145].

MHC class II binding prediction for 15-mers within IDH1R132H p118-146 was done using the NetMHCII algorithm [146] to HLA-DRB1*0101 (HLA-DR1). Peptides with IC50 below 500 nM are defined as weak binders, those with IC50 below 50 nM are defined as strong binders.

2.2.2 T2 binding assay

T2 cells, which are HLA-A2+ transporter associated with antigen processing (TAP)-deficient cells expressing HLA-A2 stably on their surface only after peptide binding to HLA-A2, were treated with 5 µg/ml β2-microglobulin (BD Pharmingen) together with 10 µg/ml IDH1R132H peptides or tax as positive control peptide for 3h. As controls, cells were treated with equal volume of DMSO as vehicle with or without β2-microglobulin. Cells were washed and surface-stained with FITC-conjugated mouse anti-HLA-A2 antibody (BB7.2, 1 µl per test; BD Pharmingen) for 30 min and analyzed by flow cytometry. Binding values were calculated by subtraction of vehicle control and relative to positive control. Assay performed by Agnieszka Grabowska and Angelika Riemer.

2.2.3 Class II REVEAL™ MHC-Peptide Binding Assay

HLA-DRB1*01:01 binding assay was performed by ProImmune (quick check stability assay).

2.2.4 Tumor induction and generation of a syngeneic tumor cell line

500 µg 3-methylcholantrene (MCA) in peanut oil was injected s.c. into the flank of A2.DR1 mice. Tumor growth started after 60 to 90 days and was monitored daily. When tumors reached a maximum size of 1.5 cm, tumors were excised, cut into small pieces, embedded in Matrigel™ (BD Biosciences) and s.c. injected into the back of NOD/SCID mice. Established tumors were again excised, cut into small pieces and cultured in DMEM with 10% FBS (both PAA Laboratories), 50 µg/ml gentamycin, 10 mM HEPES, and 50 µM β-mercaptoethanol (all Sigma-Aldrich). When single cells grew out of tumor tissue, tissue pieces were removed and adherent single cells were obtained and grown as established cell line. Cells were s.c. injected into the flank of A2.DR1 mice and established tumors were excised for characterization by H&E staining. Tumor induction was done by Karin Müller-Decker, establishment of tumor cell line was done by Jasmin Quandt.

2.2.5 Stable overexpression of IDH1 and NY-ESO-1

A2.DR1 sarcoma cells were transduced with full-length cDNA of human *IDH1*R132H or *IDH1*wt (GenBank CR541695.1), or *CTAG1B* coding for human NY-ESO-1 (GenBank

AJ003149.1), provided by the DKFZ Genomics Facility, cloned in the retroviral vector pMXs-IRES-BsdR (Cell Biolabs, Inc.) (IDH1 by. S. Pusch, NY-ESO-1 by L. Bunse) using FuGene HD transfection reagent (Promega). Cells were selected with 9 µg/ml blasticidin (Sigma-Aldrich) 72 h after transfection. For therapeutic vaccination experiments, A2.DR1 IDH1R132H+ sarcoma cell clones were generated by limiting dilution and outgrowing clones were screened for IDH1R132H expression by 2-HG measurements (see 2.2.18) and immunofluorescent staining (see 2.2.22). Clone IVC1 was selected according to high and homogenous IDH1R132H expression. Clones of the human glioma cell line LN229 transfected with *IDH1*R132H (H3, H114) or *IDH1*wt (86) in pcDNA.3, selected with 1.5 mg/ml G418 (Sigma-Aldrich), and expressing endogenous IDH1wt protein levels (H114, 86) or half the amount (H3) were provided by J. Balß.

2.2.6 Peptide vaccination and tumor cell inoculation

A2.DR1 or DR4 transgenic mice were immunized with 100 µg IDH1R132H (p123-142; p122-136; p124-138) emulsified in complete Freund's adjuvant (CFA) or Montanide-ISA51® (Seppic). For CFA-vaccination, Freund's adjuvant was supplemented with mycobacteria (both from Difco) and emulsified with equal volume of peptide stock diluted in PBS or PBS with equal concentration of DMSO as sham control treatment. Final peptide concentration in the emulsion was 1 mg/ml. S. c. injections (50 µl each) were into the lateral pectoral region at both sides. For Montanide®-vaccination, peptide or DMSO at concentrations as above were emulsified in Montanide-ISA51® and injection was as above. In addition, Aldara® cream containing 5 % imiquimod (Meda Pharma) was applied at injection site. For this, mice were shaved before injections. 300 ng recombinant GM-CSF (Immunotools) in 50 µl PBS was s.c. injected medio-pectoral between emulsion injection sites. For both protocols, mice were boosted after 10 days. In case of Montanide®-vaccination, no GM-CSF was applied at boost. In vaccination only experiments, submandibular vein blood was taken and spleens were excised after 21 days. For tumor cell inoculation experiments, IDH1R132H (p123-142) was used with Montanide®/imiquimod.

For preventive vaccination, A2.DR1 mice were again boosted on day 21 by s.c. injection into the shaved back and imiquimod application. On day 25, $2*10^6$ syngeneic tumor cells expressing human IDH1R132H or IDH1wt were embedded in Matrigel™ and s.c. injected into the shaved right flank of A2.DR1 mice and tumor growth was measured regularly with a calliper in two dimensions. For therapeutic vaccination, $5*10^5$ syngeneic tumor cells

expressing human IDH1R132H (clone IVC1) were injected as above and tumor growth was measured regularly with a calliper in two dimensions. On day 6, when tumors were detectable in all mice, mice were divided into two groups according to tumor size and vaccinated with IDH1R132H (p123-142) or sham-treated using Montanide®/imiquimod as above. Mice were boosted on day 13. Therapeutic vaccination against NY-ESO-1 was done by injection of $8*10^5$ syngeneic tumor cells expressing NY-ESO-1 and vaccination with NY-ESO-1 (p119-143) or sham-treatment on day 6 using Montanide®/imiquimod as above. Mice were boosted on day 13.

Lymphocyte depletion was done by repeated i. p. injections of anti-CD4 (clone GK1.5, 1 mg / dose, every 3 days), anti-CD19 (clone 1D3, 500 µg / dose, every 5 days), or corresponding isotype controls (for anti-CD4, clone LTF-2, 1 mg / dose, every 3 days; for anti-CD19, clone 2A3, 500 µg / dose, every 5 days; all BioXcell). $8*10^5$ syngeneic tumor cells expressing human IDH1R132H were injected as above. On day 4, when tumors were detectable in all mice, mice were divided into groups according to tumor size and injected with depleting antibodies or controls. One group received specific antibodies and two were injected with isotype controls. On day 5, mice were vaccinated with IDH1R132H (p123-142) (depletion groups and one isotype control group) or sham treated (isotype control group) using Montanide®/imiquimod and boosted on day 13. On day 7 and 17, submandibular vein blood was taken from 2 mice of each group to verify depletion efficacy by flow cytometry (see 2.2.17).

2.2.7 Tumor cell vaccination

A2.DR1 transgenic mice were vaccinated by s.c. injection of 10^7 irradiated (100 Gy) syngeneic tumor cells overexpressing IDH1wt or IDH1R132H (clone IVC1) with 1 µg rGM-CSF in PBS into the neck. CFA was injected s.c. into the lateral pectoral region at both sides (50 µl each). Injection of 10^7 irradiated tumor cells only was repeated 4 times every 10 days and spleens were excised after 47 days.

2.2.8 Lymphocyte and bone marrow cell isolation

Spleens and lymph nodes (LN) were excised from vaccinated and sham-treated A2.DR1 or DR4 mice and bone marrow was isolated from hind limbs of naïve A2.DR1 mice. Organs were mashed through a 40 µm cell strainer. Blood lymphocytes were obtained from submandibular vein blood of lymphocyte-depleted mice. Erythrocytes in spleens, bone

marrow and blood were lysed with ACK buffer – containing 150 mM NH_4Cl, 10 mM $KHCO_3$, and 100 µM Na_2EDTA – and cells were washed twice with medium before culturing in RPMI1640 containing 10% FBS and 100 U/ml penicillin and 100 µg/ml streptomycin (all PAA Laboratories). For splenocytes and LN cells, medium was supplemented with 1 mM sodium-pyruvate, 2 mM glutamine (both PAA Laboratories), 100 µM non-essential amino acids (Lonza), and 50 µM β-mercaptoethanol (Sigma-Aldrich).

2.2.9 Isolation of tumor-infiltrating lymphocytes

Tumors were excised, washed in HBSS (Sigma-Aldrich) and cut into small pieces before tissue disruption in HBSS supplemented with 0.05 % collagenase, 0.1 µg/ml TLCK trypsin inhibitor, 10 µg/ml DNAse I, and 10 mM Hepes, pH 7.4, for 1 h under slow rotation at 37°C. Dispersed tissue was mashed through a 70 µm cell strainer and lymphocytes were isolated by density gradient centrifugation using Lympholyte® Mouse (Cedarlane).

2.2.10 Generation of antigen-specific T cells

Splenocytes from A2.DR1 mice vaccinated with IDH1R1232H (p123-142) in Montanide-ISA51® were stimulated with 10 µg/ml IDH1R132H (p123-142) peptide. After 7 days, medium was exchanged and supplemented with 3 % (v/v) ConA sup (kind gift from W. Osen) as an interleukin (IL)-2 source and 15 mM α-methylmannopyranoside (α-MM, Sigma-Aldrich). Medium was exchanged weekly including ConA sup and α-MM. Cells were restimulated every 4 weeks with autologous splenocytes irradiated with 30 Gy and loaded with 2 µg/ml IDH1R132H (p123-142) in ConA sup and α-MM-containing medium. Cells were used after two restimulations until the fifth restimulation. At the second restimulation, T cell clones were generated by limiting dilution (0.5 cells per well) and stimulation with IDH1R132H (p123-142)-loaded and irradiated autologous splenocytes. Reactive clones were picked according to polarized morphology after 4 weeks and restimulated. Medium was changed weekly and restimulation was every 4 weeks.

2.2.11 Peripheral blood mononuclear cell and T cell isolation

Peripheral blood mononuclear cells (PBMC) were isolated from buffy coats or heparin blood of glioma patients by density-gradient centrifugation using lymphocyte separation medium (LSM) 1077 (PAA Laboratories) and cultured in RPMI1640 containing 10% FBS or autologous serum (see below) and 100 U/ml penicillin and 100 µg/ml streptomycin, supplemented with

1 mM sodium-pyruvate, 2 mM glutamine, 100 µM non-essential amino acids, and 50 µM β-mercaptoethanol.

CD4+ or CD8+ T cells were isolated from PBMC by depletion of non-T cell populations using the CD4+ T cell isolation kit II and CD8+ T cell isolation kit (both Miltenyi Biotec, Bergisch Gladbach, Germany) according to manufacturer's instructions. Biefly, for CD4+ T cell isolation, cells were labeled with biotinylated antibody cocktail, magnetically labeled with anti-biotin beads, and subjected to magnetic separation. For CD8+ T cell isolation, cells were lebeled with CD8+ T cell biotin-antibody cocktail, magnetically labeled with CD8+ T cell microbead cocktail and subjected to magnetic separation. In both protocols, effluent cell population was the enriched T cell population. Purity was assessed by flow cytometry (see below) and T cells were cultured in RPMI1640 containing 10% FBS and 100 U/ml penicillin and 100 µg/ml streptomycin, supplemented with 1 mM sodium-pyruvate, 2 mM glutamine, 100 µM non-essential amino acids, and 50 µM β-mercaptoethanol.

2.2.12 IFN-γ ELISpot

ELISpot white bottom multiwell plates (Millipore) were coated with anti-mouse IFN-γ (AN18, Mabtech) or anti-human IFN-γ (1D1K, Mabtech) at 4°C overnight and blocked with RPMI1640 containing 10 % FBS and 100 U/ml penicillin and 100 µg/ml streptomycin. Human PBMC or mouse splenocytes or LN cells were seeded at $5*10^5$ to 10^6 per well and stimulated with 10 µg/ml peptide in case of cells from vaccinated mice or 20 µg/ml in case of human PBMC. As negative controls, MOG (p35-55) was used at equal concentrations and peptide diluent PBS 10 % DMSO was used at equal volume. Positive control was 20 ng/ml phorbol myristate acetate (PMA, Sigma-Aldrich) and 1 µg/ml ionomycin (Sigma-Aldrich). For T cell line and clone, antigen-presenting B cell blasts were generated from autologous (A2.DR1) splenocytes by stimulation with 25 µg/ml lipopolysaccharides (LPS, Sigma-Aldrich) and 7 µg/ml dextran-sulfate (Amersham Pharmacia Biotech AB) over 3 days, loaded with 0.1 µg/ml or 1.0 µg/ml peptides and seeded at $5*10^4$ cells per well together with $2.5*10^3$ T cells. CD4+ and CD8+ T cells from splenocytes of vaccinated mice were isolated by magnetic cell sorting (MACS) using the pan T cell isolation kit II, mouse, followed by CD4 (L3T4) MicroBeads, mouse (all Miltenyi Biotec) and $5*10^3$ T cells per well were stimulated with $5*10^4$ peptide-loaded (20 µg/ml) dendritic cells (DC) per well that had been derived from bone marrow cells by treatment with 20 ng/ml rGM-CSF (Immunotools) for 6 days. Peptide presentation

on MHC was blocked with blocking antibodies (1 µg per well) against HLA-A (W6/32, kindly provided by A. Riemer) or HLA-DR (L243, BioLegend).

After 36 h, IFN-γ-producing cells were detected with biotinylated anti-mouse IFN-γ (R4-6A2) or anti-human IFN-γ (7-B6-1), streptavidin-ALP (all Mabtech) and ALP color development buffer (Bio-Rad) and quantified using an ImmunoSpot Analyzer (Cellular Technology Ltd.).

2.2.13 Cytokine ELISA

Splenocytes from vaccinated and sham-treated mice were stimulated with 10 µg/ml IDH1R132H (p123-142), 20 ng/ml phorbol-12-myristate-13-acetate (PMA) and 1 µg/ml ionomycin as positive control, or peptide diluent PBS 10% DMSO (vehicle) as negative control (see above) for 3 days. Supernatants were used on cytokine-specific antibody-coated ELISA plates (Corning) and horseradish-peroxidase (HRP)-based cytokine detection was performed according to manufacturer's instructions (ebioscience) with TMB (ebioscience) and stopped with 1M H_2SO_4. OD at 450 nm was measured with an ELISA reader (Thermo Fisher). Cytokine concentrations were calculated using cytokine standard serial dilution. Cytokines detected were IFN-γ, TNF-α, IL-4, IL-6, and IL-17.

2.2.14 IgG ELISA

ELISA plates (Nunc or Corning) were coated with IDH1R132H and IDH1wt p123-142 for mouse IgG detection and p122-136 for patient IgG detection (10 µg per well in PBS), washed with PBS 0.05 % Tween 20, and blocked with 3 % FBS in PBS 0.05 % Tween 20. As negative controls, MOG p35-55 was used at equal concentrations and peptide diluent PBS 10% DMSO was used at equal volume. Positive control for patient serum was tetanus toxoid (0.25 µg per well; Merck Chemicals, Ltd). Mouse serum was obtained by puncture of the submandibular vein and centrifugation of whole heparin-mixed blood and diluted 1:50 in blocking solution. Patient serum was obtained from serum tubes by centrifugation and used undiluted. Monoclonal mouse anti-IDH1R132H (1:1000, H09, Dianova) was used as peptide coating control in human serum assays and as positive control in mouse serum assays. HRP-conjugated secondary antibodies were sheep anti-mouse IgG (1:5000, Amersham), goat anti-mouse IgG1, goat anti-mouse IgG2a, goat anti-mouse IgG2b, and goat anti-mouse IgG3 (all 1:10000, Bethyl Laboratories, Inc.) for mouse serum and control and goat anti-human IgG-Fc (1:10000, Bethyl Laboratories, Inc.), mouse anti-human IgG1, anti-human IgG2, anti-human IgG3, and anti-human IgG4 (all 1:500, Acris Antibodies, Inc.) for patient serum. Substrate was

TMB and reaction was stopped with 1M H_2SO_4. OD at 450 nm was measured with an ELISA reader. Data is shown in relation to MOG negative control.

2.2.15 IFN-γ secretion assay

PBMC isolated from glioma patients were stimulated with 40 µg/ml IDH1R132H (p123-142), equal concentration of MOG (p35-55) as negative, or 1 µg/ml staphylococcus-derived enterotoxin B (SEB, Sigma-Aldrich) as positive control and co-stimulated with 2 µg/ml anti-human CD28 (CD28.6, ebioscience) in medium containing 10 % autologous serum for 16 h. Splenocytes from vaccinated mice were stimulated with 20 µg/ml IDH1R132H (p123-142), equal volume of peptide diluent PBS 10% DMSO as negative, or 1 µg/ml SEB as positive control as above. Mouse T cells were stimulated with autologous splenocytes loaded with 10 µg/ml IDH1R132H (p123-142). Positive control was SEB (as above). IFN-γ secretion assay was performed according to manufacturer's instructions (IFN-γ Secretion Assay Cell Enrichment and Detection Kit (PE), human, 130-054-201; mouse, 130-090-517; Miltenyi Biotec). Briefly, cells were labelled with IFN-γ catch reagent and after secretion period IFN-γ caught on the cell surface was labelled with PE-conjugated antibody. For isolation and enrichment of IFN-γ-secreting cells, cells were incubated with anti-PE microbeads and subjected to magnetic separation. Separated cell populations were stained for flow cytometry (see 2.2.17). *Ex vivo* splenocytes were stained and analyzed without enrichment.

2.2.16 Mixed leukocyte reaction

As an *in vitro* model of allogeneic T cell stimulation in response to (R)-2-HG-treatment, mixed leukocyte reactions (MLR) were performed. PBMCs of two non-related donors were isolated, cells from one donor were irradiated with 30 Gy and mixed with non-irradiated cells of the second donor at $2*10^5$ cells per donor and per well. Cells were treated with increasing concentrations of (R)-2-HG for five days. Alternatively, cells were seeded on $6*10^3$ LN229 overexpressing IDH1wt or IDH1R132H per well, which had been seeded one day before for adherent growth, or in supernatant of these cells For collecting supernatant, LN229 were cultured in RPMI1640 containing 10% FBS and 100 U/ml penicillin and 100 µg/ml streptomycin for two days. MLR were pulsed with [^{3}H]-methylthymidine (Amersham Radiochemical Centre, Buckinghamshire, U.K.) for 20h and frozen. Incorporated [^{3}H]-methylthymidine was harvested (Tomtec Cell Harvester, Tomtec, Hamden, CT, USA) and

measured in a scintillation counter (Wallac Micro Beta TriLux Scintillation Beta Counter, Perkin Elmer, Waltham, MA, USA). Proliferation was given as counts per minute (cpm).

2.2.17 Flow cytometry

Purity of isolated T cell subsets from PBMC was assessed by staining of negative and positive cell fractions for CD3, CD4, and CD8. Cells were blocked with autologous serum and stained with FITC-conjugated mouse anti-human CD3 (SK7), eFluor450®-conjugated mouse anti-human CD4 (RPA-T4), and APC-conjugated mouse anti-human CD8 (SK1; all 1 µl/well, ebioscience).

Subsequent to IFN-γ secretion assay, positively selected cell populations from patient PBMC were blocked with autologous serum and stained with FITC-conjugated mouse anti-human CD3 (SK7, 1 µl/well), eFluor450®- or PerCP-conjugated mouse anti-human CD4 (RPA-T4, 1 µl/well, and SK3, 5 µl/well, respectively), and APC-conjugated mouse anti-human CD8 (SK1, 1 µl/well, all ebioscience). Selected mouse T cells were blocked with rat anti-mouse CD16/32 (93, 0.5 µg/well, ebioscience) and stained with FITC-conjugated rat anti-mouse CD3 (17A2), Pacific Blue™-conjugated rat anti-mouse CD4 (RM4-5, both BioLegend), and APC-conjugated rat anti-mouse CD8 (53-6.1, ebioscience; all 0.5 µl/well). Propidium iodide (PI, 1 µg/ml, Sigma-Aldrich) was used to exclude dead cells. Live single cells were gated on IFN-γ+ CD3+ T cells and analyzed for CD4 and CD8 expression.

For IDH1R132H-specific T cell phenotype characterization, splenocytes from vaccinated or sham-treated mice were *ex vivo* stimulated with 10 µg/ml IDH1R132H (p123-142) or equal volume of DMSO as vehicle control for 4 days. For T cell line, DC were loaded with 4 µg/ml IDH1R132H (p123-142) or equal volume of DMSO as vehicle control. After stimulation of splenocytes or T cells for 4 days, cells were restimulated as before and treated with 5 µg/ml brefeldin A (Sigma-Aldrich) for 4.5 h to inhibit secretion of cytokines. Alternatively, T cell line was stimulated with 20 ng/ml PMA and 1µg/ml ionomycin for 4.5 h in the presence 5 µg/ml brefeldin A. Cells were blocked as above and stained with Pacific Blue™-conjugated rat anti-mouse CD4, APC-conjugated rat anti-mouse CD8, and PE-conjugated rat anti-mouse CD25 (all 0.5 µl/well, BioLegend). For intracellular staining, cells were fixed and permeabilized with cytofix/cytoperm solution (BD Bioscience) and stained in perm/wash buffer (BD Biosciences) with PE-conjugated rat anti-mouse IFN-γ (XMG1.2), APC-conjugated rat anti-mouse IL-17 (17B7), FITC-conjugated rat anti-mouse IL-4 (BVD6-24G2), and APC-conjugated rat-anti-mouse FoxP3 (FJK-16s, all 1 µl/well, ebioscience).

For NY-ESO-1-specific T cell phenotype characterization, splenocytes from vaccinated or sham-treated mice were *ex vivo* stimulated with 10 µg/ml NY-ESO-1 (p119-143) or MOG (p35-55) as negative control. After stimulation for 4 days, cells were restimulated as before and treated with 5 µg/ml brefeldin A (Sigma-Aldrich) for 4.5 h to inhibit secretion of cytokines. Cells were blocked as above and stained with eFluor450®-conjugated rat anti-mouse CD3 (17A2), APC-conjugated rat anti-mouse CD4 (RM4-5), and PE-conjugated rat anti-mouse CD8 (53-6.1, all 0.5 µl/well, ebioscience). For intracellular staining, cells were fixed and permeabilized as above and stained with FITC-conjugated rat anti-mouse IFN-γ (XMG1.2, 1 µl/well, ebioscience).

Tumor-infiltrating lymphocytes were stained for IDH1R132H-specific T helper cells using an HLA-DRB1*01:01 MHC class II tetramer bound to IDH1R132H p123-142 (kindly provided by the National Institute of Health [NIH] tetramer core facility). Cells were blocked with rat anti-mouse CD16/32, stained with APC-conjugated IDH1R132H- or class II-associated invariant chain peptide (CLIP)-bound control tetramer (15 µg/ml, 37°C, 1h; NIH) in RPMI1640 containing 10 % FBS and 100 U/ml penicillin and 100 µg/ml streptomycin, washed and stained with Pacific Orange™-conjugated rat anti-mouse CD45 (30-F11, 1 µl/well, Life technologies, Invitrogen), PE-Cy7-conjugated rat anti-mouse CD3, FITC-conjugated rat anti-mouse CD4, and PE-conjugated rat anti-mouse CD8 (all 1 µl/well, ebiosciences). PI (1 µg/ml) was used to exclude dead cells. Cells were subsequently gated on CD45+ leukocytes, CD3+ T cells, and CD4+ T cells to analyze tetramer+ T helper cells.

For verification of T cell depletions, submandibular vein blood lymphocytes were blocked with rat anti-mouse CD16/32 and stained with PE-conjugated rat anti-mouse CD3 (17A2), pacific blue™-conjugated rat anti-mouse CD4, and APC-conjugated rat anti-mouse CD8 (ebioscience; all 0.5 µl/well). Cells were gated on CD3+ T cells and analyzed for CD4 and CD8 expression. For verification of B cell depletions, submandibular vein blood lymphocytes were blocked with rat anti-mouse CD16/32 and stained with eFluor450®-conjugated rat anti-mouse CD3 and APC-conjugated rat anti-mouse CD19 (1D3; all 0.5 µl/well, ebioscience).

HLA-expression in A2.DR1 sarcoma cells was analyzed after stimulation with 50 or 100 ng/ml recombinant mouse IFN-γ (Peprotech GmbH) for 48 h. Cells were stained with FITC-conjugated mouse anti-human HLA-A2 (BB7.2, 1 µl/well, BD Biosciences) and APC-conjugated mouse anti-human HLA-DR1 (T36, 2 µl/well, Southern Biotechnology Assoc. Inc.)

For activation and phenotype characterization of 2-HG-treated T cells, CD4+ or CD8+ T cells were treated with 50 or 100 µM 2-HG and stimulated via the TCR using anti-human CD28 (CD28.6, 2 µg/ml), anti-human CD3 (OKT3, 1.5 µg/ml, both ebioscience) and recombinant human IL-2 (100 U/ml, Proleukin, Novartis AG, Basel, Switzerland) for 10 days. Cells were blocked with autologous serum and stained for activation markers with PE-conjugated mouse anti-human CD45RO (UCHL1, 5 µl/well, Biolegend) and APC-conjugated mouse anti-human CD69 (FN50, 2 µl/well, Biolegend). For phenotype characterization, cells were restimulated with 20 ng/ml PMA and 1 µg/ml ionomycin and treated with GolgiStop (1:1500, BD Biosciences, order no. 554724) for 4.5 h to inhibit secretion of cytokines before blocking with autologous serum. CD4+ T cells were stained with PerCP-conjugated mouse anti-human CD4 (SK3, 5µl/well, ebioscience) and APC-conjugated mouse anti-human CD25 (4E3, 5 µl/well, Miltenyi Biotec). CD8+ T cells were stained with PE-conjugated mouse anti-human CD8 (SK1, 0.5 µl/well, ebioscience). T cells were fixed and permeabilized using the Transcription Factor Buffer Set (BD Pharmingen™) according to manufacturer's instructions and stained in Perm/Wash buffer with eFluor450®-conjugated mouse anti-human IFN-γ (4S.B3, 1 µl/well). CD4+ T cells were in addition stained with AlexaFluor488®-conjugated mouse anti-human IL-17 (eBio64DEC17, 5 µl/well, both ebioscience), PE-Cy7-conjugated mouse anti-human IL-4 (8D4-8, 5 µl/well, Novus Biologicals), and PE-conjugated mouse anti-human FoxP3 (236A/E7, 2.5 µl/well, ebioscience).

In all experiments, corresponding isotype controls were used. Cells were measured on a FACS Canto II (BD Biosciences). For intracellular flow cytometry for detection of cytokines, a minimum of 10^5 cells was recorded. Data analysis was done using FlowJo software.

2.2.18 2-HG measurement

2-HG production in cells and tumors was analyzed by Jörg Balß [147]. 50% confluent cells were collected, dissolved in 220 µl cell lysis buffer (Cell signaling, Danvers, MA, USA) and freeze-thawed three times. To remove cell debris samples were centrifuged for 5 min at 13000 *g*. (R)-2-HG standard was prepared with concentrations of 0.5, 1, 2.5, 5, 7.5, 10, 25 and 50 µM (R)-2-HG in ddH_2O. 10 ml of assay solution containing 100 mM HEPES pH 8.0, 100 µM NAD^+ (Applichem, Darmstadt, Germany), 0.1 µg HGDH, 5 µM resazurin (Applichem) and 0.01 U/ml diaphorase (0.01 U/ml, MP Biomedical, Irvine, CA, USA) was prepared freshly for each assay. Just before use 75 µl of assay solution were added to 25 µl sample volume and incubated at RT in the dark for 30 min in black 96-well plates (Thermo Scientific).

Fluorometric detection was carried out in triplicate with 25 µl deproteinized sample analyzed in each reaction with excitation at 540+/-10 nm and emission of 610+/-10 nm (FLUOstar Omega, BMG Labtech, Offenburg, Germany).

Measured 2-HG concentrations were compared to 2-HG concentrations found in patient tumors, which range from 1 to 30 mM [92, 147].

2.2.19 Pathological organ analysis

Organs from A2.DR1 mice preventively or therapeutically vaccinated with IDH1R132H (p123-142) or sham treated using Montanide® were excised, fixed with Roti®-Histofix 4,5% (Carl Roth GmbH + Co. KG), paraffin-embedded and cut to 3 µm sections which were stained using hematoxylin and eosin and analyzed microscopically at the Freie Universität Berlin, Institute of Veterinary Pathology.

2.2.20 IDH enzymatic activity assay

IDH activity was measured based on NADPH production using the Isocitrate Dehydrogenase Activity Colorimetric Assay Kit (BioVision). Liver and brain from A2.DR1 mice therapeutically vaccinated with IDH1R132H (p123-142) or sham treated using Montanide® were cryopreserved, homogenized in IDH assay buffer, and subjected to IDH1/2 activity measurement using NADP+ as cofactor according to manufacturer's instructions. NADPH production was colorimetrically followed for 30 min after initial 30 min incubation at 37 °C. IDH activity was analysed after subtraction of background without external substrate or NADP+ and calculated according to manufacturer's instructions using an NADH standard curve.

2.2.21 Western Blot

Total protein was isolated by cell lysis with with ice cold tris (hydroxymethyl) aminomethane hydrochloride (TRIS-HCl, 50 mM, pH 8,0; Carl Roth) containing 150 mM NaCl (J.T. Baker, Deventer, Netherlands), 1 % Nondiet P-40 (Genaxxon Bioscience, Ulm, Germany), 10 mM ethylenediaminetetraacetic acid (EDTA) (GerbuBiotechnik, Gaiberg, Germany), 200 mM dithiothreitol (Carl Roth), 100 µM phenylmethylsulphonyl fluoride (PMSF) and complete EDTA-free (1:50, Roche, Mannheim, Germany) for 20 min and centrifuged to pellet debris. Protein concentrations were measured via the Bio-Rad protein assay (Bio-Rad, Hercules, CA, USA) at 595 nm and 30 µg of protein diluted in Laemmli sample buffer were denatured at 95 °C for 5 min and electrophoretically separated on 12 % acrylamide-polyacrylamide SDS-

containing gels. Proteins were blotted onto nitrocellulose membranes by wet blot at 1.5 mA/cm^2 for 1 h. After blocking with 5 % milk powder in 0.5 M Tris-based saline (TBS), pH 7.4, 1.5 M NaCl, 0.05 % Tween 20, membranes were incubated consecutively with primary monoclonal mouse anti-IDH1R132H (1:500, H09, Dianova), monoclonal rat anti-panIDH1 (1:500, W09, Dianova) for detection of wt and R132H IDH1, or monoclonal mouse anti-NY-ESO-1 (1:500, E978, Sigma-Aldrich) overnight at 4 °C, and mouse anti-α-tubulin (1:5000, Sigma-Aldrich) as loading control for 1 h at room temperature (RT). Staining with secondary HRP-conjugated anti-rat (1:(1000xF), Dako) or anti-mouse (1:5000, GE Healthcare, Buckinghamshire, UK) antibodies was performed at RT for 1 h and was followed by chemoluminescent development using ECL or ECL prime (both Amersham).

2.2.22 Immunofluorescence

For immunoflourescent staining cells were seeded on glass coverslips, grown until 70 – 90 % confluent and fixed and permeabilized with Cytofixx Pump Spray (Cell Path) and subsequent 4 % PFA. For blocking and staining, 5 % FBS in PBS was used. Primary antibodies were mouse anti-IDH1R132H (1:50, H09, Dianova) and mouse anti-NY-ESO-1 (1:100, E978, Sigma-Aldrich) and secondary antibody was donkey anti-mouse AlexaFluor® 488 (1:300, Molecular Probes, Invitrogen). Vectashield HardSet Mounting Medium with DAPI (Vector laboratories) was used for mounting and nuclear staining. Images were taken on LEICA DM IRB microscope.
IDH1R132H Immunofluorescent stainings were performed by Lukas Bunse.

2.2.23 Immunohistochemistry

A2.DR1 mouse tumor tissue was fixed with Roti®-Histofix 4.5 % (Carl Roth GmbH + Co. KG), paraffin-embedded, cut to 3 µm sections and processed using a Ventana BenchMark XT® immunostainer. Tissue was deparaffinized with HistoClearTMII and rehydrated. Antigen retrieval was performed using Cell Conditioning Solution CC1 (Ventana Medical Systems) for 30 min. Endogenous peroxidase activity was blocked by 3 % hydrogen peroxide in PBS for 10 min. Blocking was performed using 5 % FBS in PBS for 30 min. N-Histofine® mousestain kit (Nichirei Biosciences, Inc.) was used to reduce unspecific binding of monoclonal mouse anti-IDH1R132H (1:50, H09, Dianova) and rat anti-CD3 (1:300, Dako) in mouse tissue according to manufacturer´s instructions. Briefly, before adding primary antibody, endogenous mouse tissue IgG was blocked using reagent A and Fab´ was blocked with reagent B prior to incubation with Simple Stain Mouse MAX PO. Counterstaining was performed with hemalum

(Carl Roth GmbH + Co. KG) for 2 min. Stained tissue was dehydrated and mounted with Histomount™ (National Diagnostics). H&E-staining was performed using hematoxylin and bluing reagent for 4 min.

Immunohistochemistry was performed by Lukas Bunse.

2.2.24 Image analysis

20 images per tumor were randomly taken of the tumor bulk with 20x objective using LEICA DM LB2 microscope. IDH1R132H+ A2.DR1 tumor cells and CD3+ T cells were counted by ImageJ with an algorithm using background subtraction and color deconvolution plugin (see 6.4 Fig. 6.1). IDH1R132H+ and CD3+ cell counts of 20 images were set in relation to calculated tumor volume in mm^3. Image analysis was performed by Lukas Bunse.

2.2.25 Statistics

The mean of variables was compared with Student‘s t test, assuming unequal variances, or Welch‘s ANOVA, when more than two groups were compared. In that case, a pairwise t test with Bonferroni correction was performed afterwards. Data shown in Fig. 3.15d were log2 transformed prior to analysis. The area under the curve (AUC) of tumor area over time was calculated through the MIfuns package, and median AUC was compared with the Wilcoxon rank-sum test. Odds were compared with Fisher‘s exact test. The Bonferroni method was applied to adjust for type I error inflation due to multiple testing and $p < 0.05$ was considered statistically significant (http://www.R-project.org/). All tests were two-sided. Analyses were carried out using R version 2.15.2 by Benedikt Wiestler.

3 RESULTS

3.1 MHC binding studies reveal IDH1 epitopes

In order to generate an efficient antigen-specific T cell response, peptides derived from the antigen need to be presented on MHC molecules and are then called epitopes. Whereas epitopes are presented to CD8+ T cells on MHC class I, MHC class II molecules present epitopes to CD4+ T cells.

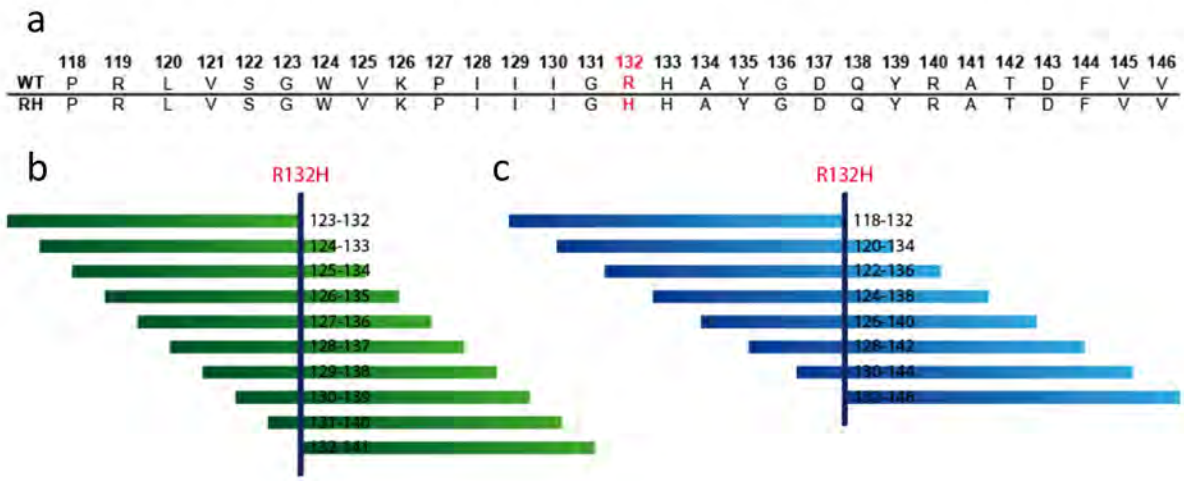

Fig. 3.1. Overlapping IDH1 peptide libraries. a, Human IDH1wt (WT) and IDH1R132H (RH) amino acid sequences covering the mutated residue indicate the amino acid exchange from arginine to histidine at position 132. Mouse and human sequences are identical in this region except for amino acid 122 (serine in human, threonine in mouse). **b** and **c**, Peptide libraries of IDH1wt and IDH1R132H covering the sequences shown in a and containing peptides of 10 (b), or 15 (c), amino acids were generated by an overlap of 9 or 13 amino acids, respectively.

Peptides presented on MHC class I can be 8 to 11 amino acids long, whereas those presented on MHC class II contain 15 or more amino acids. Hence, IDH1R132H and IDH1wt amino acid sequences (118-146) were analyzed, which cover the amino acid exchange from arginine to histidine at position 132 and include all possible putatively processed 15-mer IDH1 peptides containing position 132 (Fig. 3.1a). Mouse and human sequences are identical in this region except for amino acid 122, which is a serine in human and a threonine in mouse (see 6.3.3). For *in vitro* binding studies, IDH1R132H and wt peptide libraries containing 10-mer peptides with an overlap of 9 amino acids encompassing the mutated IDH1R132H for MHC class I binding (Fig. 3.1b) and containing 15-mer peptides overlapping

by 13 amino acids for MHC class II binding (Fig. 3.1c) were generated.

3.1.1 IDH1R132H peptides do not bind to HLA-A2

To assess the immunogenic potential of the IDH1R132H mutation *in situ*, the amino acid sequences encompassing the mutated (R132H) and corresponding wt residue of IDH1 were subjected to MHC binding prediction algorithms.

Because CD8+ T cells are the main cytotoxic T cells with a high importance in anti-tumor immunity, first, IDH1R132H 8-, 9-, 10-, and 11-mers were subjected to MHC I binding prediction to the most common HLA-A type in Caucasians, HLA-A*0201 (HLA-A2) [148], using the NetMHC algorithm (Fig. 3.2a) [144] or SYFPEITHI database (Fig. 3.2b) [145]. None of the peptides were predicted to bind, although SYFPEITHI binding scores above 10 were predicted for some peptides, which, compared to positive controls, might be considered as positive binding to HLA-A2. To verify the *in silico* results, the IDH1R132H 10-mer peptide library (Fig. 3.1b) was tested for binding to HLA-A2 *in vitro* by T2 binding assay, which makes use of the fact that T2 cells are deficient of transporter associated with antigen-processing (TAP) and express HLA-A2 on their surface only when peptide is bound to HLA, and is based on flow cytometric detection of surface HLA-A2. In line with the prediction results, none of the 10-mer IDH1R132H peptides was bound by and presented on HLA-A2 (Fig. 3.2c).

3.1.2 IDH1 peptides bind to HLA-DR1

As CD4+ T cells also have a great potential for anti-tumor immunity [149-151], IDH1R132H peptides were in addition tested for binding to MHC class II. 15-mers were subjected to MHC II binding prediction to one of the five most common HLA-DR types in Caucasians [148], HLA-DRB1*0101 (HLA-DR1), using NetMHCII and SYFPEITHI. Some of the peptides were predicted to bind by both algorithms; however, binding predictions for none of the peptides correlated between both algorithms, which was also true for positive control peptides (Fig 3.3a). Considering the inefficient reliability and accordance of MHC class II peptide binding prediction algorithms, IDH1 peptides were tested for binding to HLA-DR1 *in vitro*. To this end, the IDH1R132H and wt 15-mer peptide libraries (Fig. 3.1c) were tested for immediate binding to HLA-DR1 as well as stability in a class II REVEAL™ peptide binding assay. IDH1 peptides bound to HLA-DR1 irrespective of the R132H mutation with various binding

efficiency (p122-136 > p124-138 > p126-140 > 128-142), which was for the strongest binding peptide comparable to the positive control concerning both immediate binding and stability of the MHC:peptide complex after 24 h (Fig 3.3b, c).

a

8mers

sequence	position	IC50 (nM)
VKPIIIGH	125-132	24777
KPIIIGHH	126-133	24681
PIIIGHHA	127-134	19387
IIIGHHAY	128-135	22419
IIGHHAYG	129-136	22809
IGHHAYGD	130-137	24403
GHHAYGDQ	131-138	24929
HHAYGDQR	132-139	24528

10mers

sequence	position	IC50 (nM)
GWVKPIIIGH	123-132	35385
WVKPIIIGHH	124-133	33983
VKPIIIGHHA	125-134	31124
KPIIIGHHAY	126-135	35984
PIIIGHHAYG	127-136	29845
IIIGHHAYGD	128-137	23076
IIGHHAYGDQ	129-138	33505
IGHHAYGDQR	130-139	36979
GHHAYGDQRA	131-140	35797
HHAYGDQRAT	132-141	30943

9mers

sequence	position	IC50 (nM)
WVKPIIIGH	124-132	23076
VKPIIIGHH	125-133	24843
KPIIIGHHA	126-134	23178
PIIIGHHAY	127-135	24897
IIIGHHAYG	128-136	19210
IIGHHAYGD	129-137	24150
IGHHAYGDQ	130-138	24885
GHHAYGDQR	131-139	24872
HHAYGDQRA	132-140	24254

11mers

sequence	position	IC50 (nM)
SGWVKPIIIGH	122-132	24016
GWVKPIIIGHH	123-133	24813
WVKPIIIGHHA	124-134	11094
VKPIIIGHHAY	125-135	24765
KPIIIGHHAYG	126-136	24420
PIIIGHHAYGD	127-137	25023
IIIGHHAYGDQ	128-138	21476
IIGHHAYGDQR	129-139	24073
IGHHAYGDQRA	130-140	24655
GHHAYGDQRAT	131-141	23643
HHAYGDQRAT	132-142	23989

b

9mers

sequence	position	score
WVKPIIIGH	124-132	6
VKPIIIGHH	125-133	9
KPIIIGHHA	126-134	6
PIIIGHHAY	127-135	5
IIIGHHAYG	128-136	9
IIGHHAYGD	129-137	16
IGHHAYGDQ	130-138	10
GHHAYGDQR	131-139	2
HHAYGDQRA	132-140	1

10mers

sequence	position	score
GWVKPIIIGH	123-132	6
WVKPIIIGHH	124-133	9
VKPIIIGHHA	125-134	6
KPIIIGHHAY	126-135	5
PIIIGHHAYG	127-136	9
IIIGHHAYGD	128-137	16
IIGHHAYGDQ	129-138	10
IGHHAYGDQR	130-139	2
GHHAYGDQRA	131-140	1
HHAYGDQRAT	132-141	6
GLCTLVAML	EBV	28
GILGFVFTL	Influenza	30

c

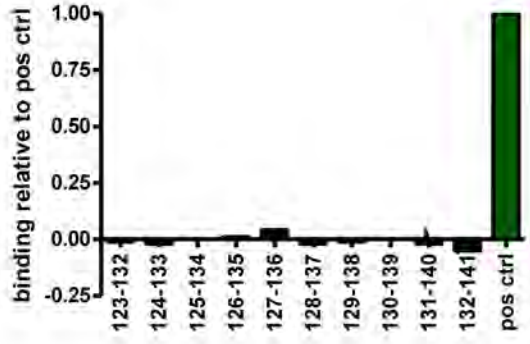

Fig. 3.2. IDH1R132H peptides do not bind to HLA-A2. a and **b**, MHC peptide binding predictions for IDH1R132H peptides to HLA-A*0201. NetMHC algorithm was used to predict binding of 8-, 9-, 10-, and 11-mers (a). Peptides with IC50 below 500 nM are defined as weak binders, those with IC50 below 50 nM are defined as strong binders, and those with IC50 above 500 nM are defined as non-binders. 9- and 10-mers were also tested with SYFPEITHI (b). For comparison, positive control peptides from Epstein-Barr-virus (EBV) and influenza are shown. **c**, IDH1R132H 10-mer peptide binding to HLA-A2 *in vitro* in a T2 binding assay. T2 cells were loaded with individual peptides from the IDH1R132H 10-mer peptide library (Fig. 3.1b) and surface HLA-A2 was determined by flow cytometry. Fluorescence intensities (black) are depicted after background subtraction and relative to a positive peptide control (tax, green).

a

15mers		NetMHCII	SYF
sequence	position	IC50 (nM)	score
PRLVSGWVKPIIIGH	118-132	39,1	16
RLVSGWVKPIIIGHH	119-133	60,4	20
LVSGWVKPIIIGHHA	120-134	193,3	0
VSGWVKPIIIGHHAY	121-135	490,1	15
SGWVKPIIIGHHAYG	122-136	508,2	15
GWVKPIIIGHHAYGD	123-137	518,9	25
WVKPIIIGHHAYGDQ	124-138	566,6	10
VKPIIIGHHAYGDQY	125-139	407,3	11
KPIIIGHHAYGDQYR	126-140	308,7	18
PIIIGHHAYGDQYRA	127-141	485,8	8
IIIGHHAYGDQYRAT	128-142	564,9	8
IIGHHAYGDQYRATD	129-143	920,1	1
IGHHAYGDQYRATDF	130-144	2525,1	8
GHHAYGDQYRATDFV	131-145	2693,5	1
HHAYGDQYRATDFVV	132-146	3332,1	16
VAMNNGMEDLLIWEP	MPT63	561,7	16
AVIPGYPVAGQVWEA	MPT63	392,9	16
TADGINYRVLWQAAG	MPT63	32,1	0

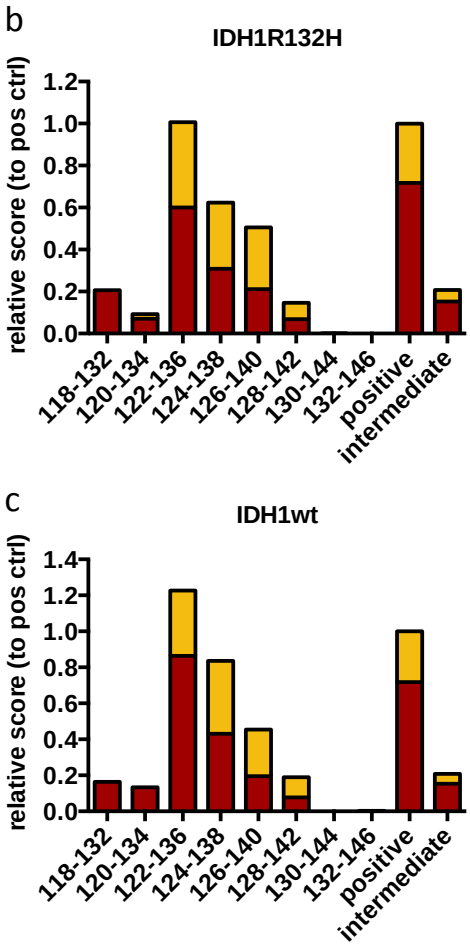

Fig. 3.3. IDH1 peptides bind to HLA-DR1 *in silico* and *in vitro*. a, MHC peptide binding predictions for IDH1R132H peptides to HLA-DRB1*0101. NetMHCII and SYFPEITHI algorithms were used to predict binding of 15-mers. In NetMHCII, peptides with IC50 below 500 nM are defined as weak binders, those with IC50 below 50 nM are defined as strong binders, and those with IC50 above 500 nM are defined as non-binders. MPT63, control peptides; SYF, SYFPEITHI. **b** and **c**, HLA-DR1-binding IDH1R132H (b), and IDH1wt (c), 15-mer epitopes were identified by Reveal Class II™ binding assay (ProImmune) using the peptide libraries from Fig 3.1c. Immediate binding (0 h, yellow) and stability after 24 h (red) were tested.

Collectively, the obtained *in situ* and *in vitro* data indicate that the IDH1R132H region contains epitopes that bind to MHC class II HLA-DR1, but not to MHC class I HLA-A2 and that binding efficiency depends on amino acid residues 125/126 to 135/136, but is not affected by the mutation.

3.2 IDH1R132H is immunogenic in MHC-humanized mice

A suitable *in vivo* system to evaluate if epitope presentation on HLA molecules is associated with an antigen-specific T cell response is the MHC-humanized mouse model, which allows

for the analysis of adaptive immune functions in the context of human MHC in immunocompetent mice. Human MHC expression is particularly important because, as mentioned above, the ability of an epitope to be presented and therefore induce an adaptive immune response heavily depends on the effective binding to an MHC, which in turn can be restricted to a certain HLA-type. A2.DR1 mice are devoid of mouse MHC class I (H-2b) and class II (H-IAb) and at the same time transgenic for the human MHCs HLA-A2 and HLA-DR1 [142] and were used to study IDH1R132H-specific cellular and humoral adaptive immune responses after vaccination. This allowed for evaluation of both CD4+ and CD8+ T cell functions in the context of epitope presentation on human MHC class I and II.

3.2.1 IDH1R132H peptide vaccination using complete Freund's adjuvant induces mutation-specific T helper responses in A2.DR1 mice

To induce antigen- and potentially mutation-specific adaptive immune responses in MHC-humanized mice, peptide vaccination was chosen as active immunization approach using a 20-mer IDH1R132H peptide (p123-142), which encompasses all R132H-containing and HLA-DR1-binding epitopes, but omits residue 122, which is distinct in human and murine IDH1. Peptide was emulsified in complete Freund's adjuvant (CFA), which is a potent adjuvant, e.g. used for *in vivo* models of T helper cell-mediated autoimmune diseases such as experimental autoimmune encephalomyelitis (EAE).

Page 38:

Fig. 3.4. IDH1R132H peptide vaccination using CFA induces mutation-specific T helper responses in A2.DR1 mice. a, ELISpot analysis of mutation-specific IFN-γ response to HLA-DR1-binding IDH1R132H 15-mer epitopes (upper panel) and IDH1R132H peptides of the 10-mer library (lower panel) after vaccination of A2.DR1 mice with p123-142 (R132H) (vacc) or vehicle control (sham) in CFA and restimulation of splenocytes with indicated peptides (white, negative controls; MOG, MOG (p35-55); red, p123-142 [R132H]; blue, p123-142 [wt]; black, R132H library peptides). (p123-142 [R132H vs. wt], Welch t test; 10-, 15-mers, ANOVA; *n* = 3). Error bars, mean + SEM. **b**, Splenocytes from p123-142 (R132H)-CFA vaccinated (red) or sham-treated (black) A2.DR1 mice were tested for production of T helper cytokines IFN-γ, TNFα, IL-4, IL-6, and IL-17 after *ex vivo* stimulation with p123-142 (R132H) or vehicle in cytokine ELISA (Welch t test; *n* = 3). Error bars, mean + SEM. **c**, Representative intracellular flow cytometry of splenocytes from three vaccinated (upper panel) and three sham-treated mice (lower panel) after IDH1R132H (p123-142)-stimulation or vehicle treatment gated on CD4+ cells. Red numbers, populations in percent.

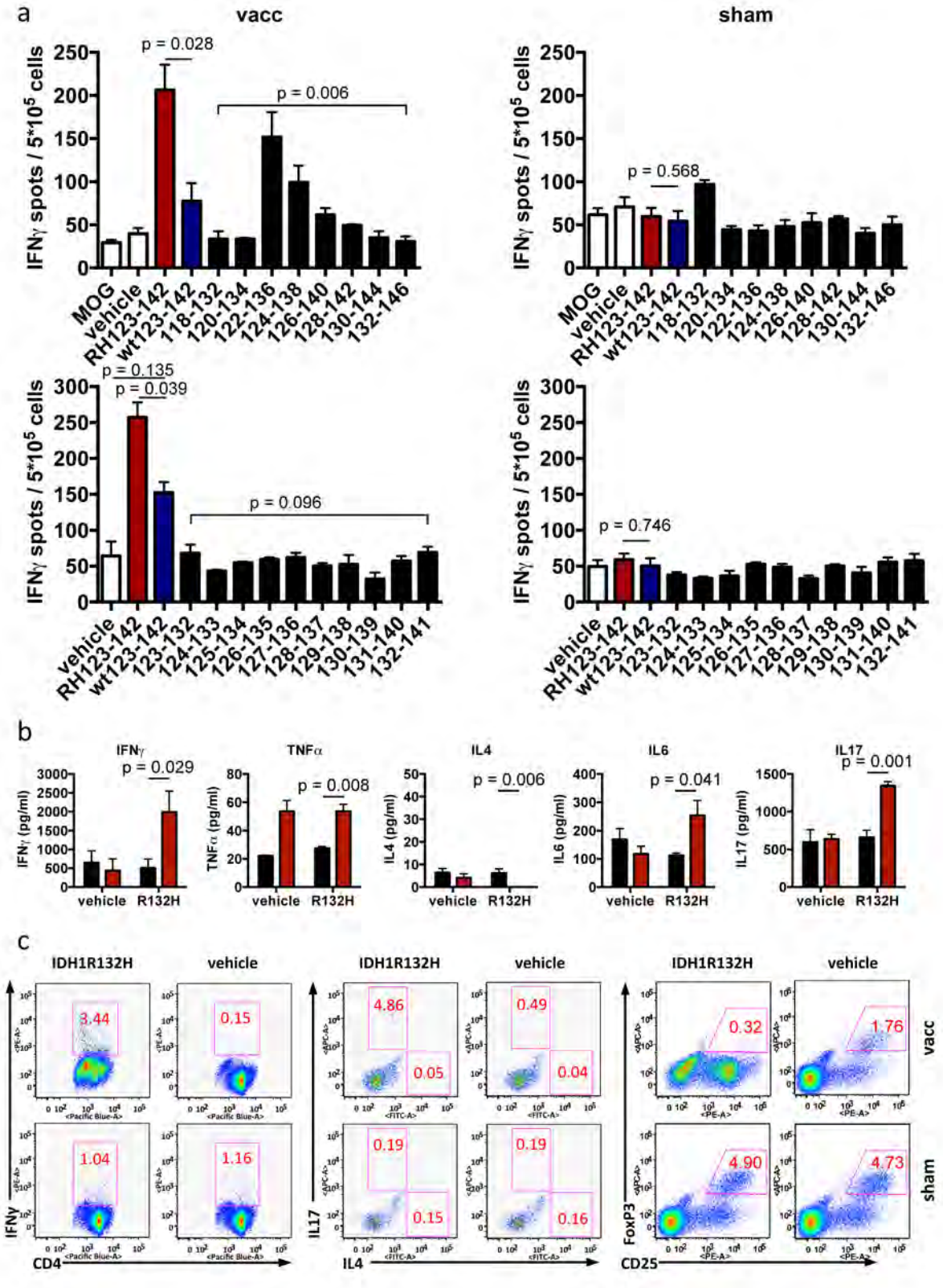

Fig. 3.4. IDH1R132H peptide vaccination using CFA induces mutation-specific T helper responses in A2.DR1 mice. See page 37 for details.

In contrast to the control treatment without IDH1R132H peptide (sham), IDH1R132H peptide vaccination with the 20-mer resulted in a robust IDH1-specific T cell response as measured by IFN-γ enzyme-linked immunoadsorbent spot assay (ELISpot) after restimulation of splenocytes with IDH1 20-mer peptides. Importantly, the T cell response discriminated between mutated and wildtype IDH1 peptides (Fig 3.4a), suggesting the induction of a mutation-specific T cell response after immunization with the p123-142 (R132H) peptide. Moreover, *ex vivo* restimulation with individual peptides of the 15-mer IDH1 peptide library induced IFN-γ responses, whose magnitude strongly correlated with the peptide HLA-DR1 binding strength (p122-136 > p124-138 > p126-140 > 128-142) (Fig. 3.4a; see Fig. 3.3b,c). T cell responses were restricted to 15-mer and 20-mer peptides and not induced by IDH1R132H peptides of the 10-mer library (Fig. 3.4a), suggesting predominant class II-restricted CD4+ T cell responses.

Especially CD4+ T cells are functionally diverse and even more importantly, regulatory T cells (T_{reg}) might be induced, which inhibit effector immune responses. The nature and phenotype of the induced T cell response were analyzed in more detail by measuring signature cytokines by enzyme-linked immunoadsorbent assay (ELISA) and intracellular flow cytometry including the signature transcription factor FoxP3, which is characteristic for T_{reg}, after restimulation with IDH1R132H p123-142 peptide *ex vivo*. In addition to confirmation of IFN-γ secretion, which is characteristic for T helper 1 (Th1) and CD8+ cytotoxic T lymphocytes (CTL), the Th2 cytokine IL-6, but not IL-4, and the Th17 cytokine IL-17 were induced by IDH1R132H peptide stimulation in splenocytes from vaccinated mice, but not sham-treated mice (Fig. 3.4b,c). However, no IDH1R132H-specific TNF-α, which is the second Th1 cytokine, was detected (Fig. 3.4b). Of note, no T_{reg} were induced after vaccination, as evidenced by FoxP3 positivity (Fig. 3.4c).

3.2.2 Combined adjuvant Montanide®/imiquimod shifts the IDH1R132H T helper response and induces CTL responses in A2.DR1 mice

CFA is typically used to induce T helper responses and in this vaccination protocol, which has been established for EAE induction, induces mainly Th1 and Th17 [152, 153]. For these reasons, and to be able to transfer these findings to the clinic by vaccinating glioma patients, the clinically approved cancer vaccine adjuvant Montanide-ISA51® combined with the TLR-7 agonist imiquimod (Aldara®), which is suitable also for poorly immunogenic tumors and

induction of CD4+ T cell-mediated antitumor immune responses and approved in a commercial lung cancer vaccine [154, 155], and recombinant GM-CSF [47, 156, 157] was applied for IDH1R132H peptide vaccination of A2.DR1 mice.

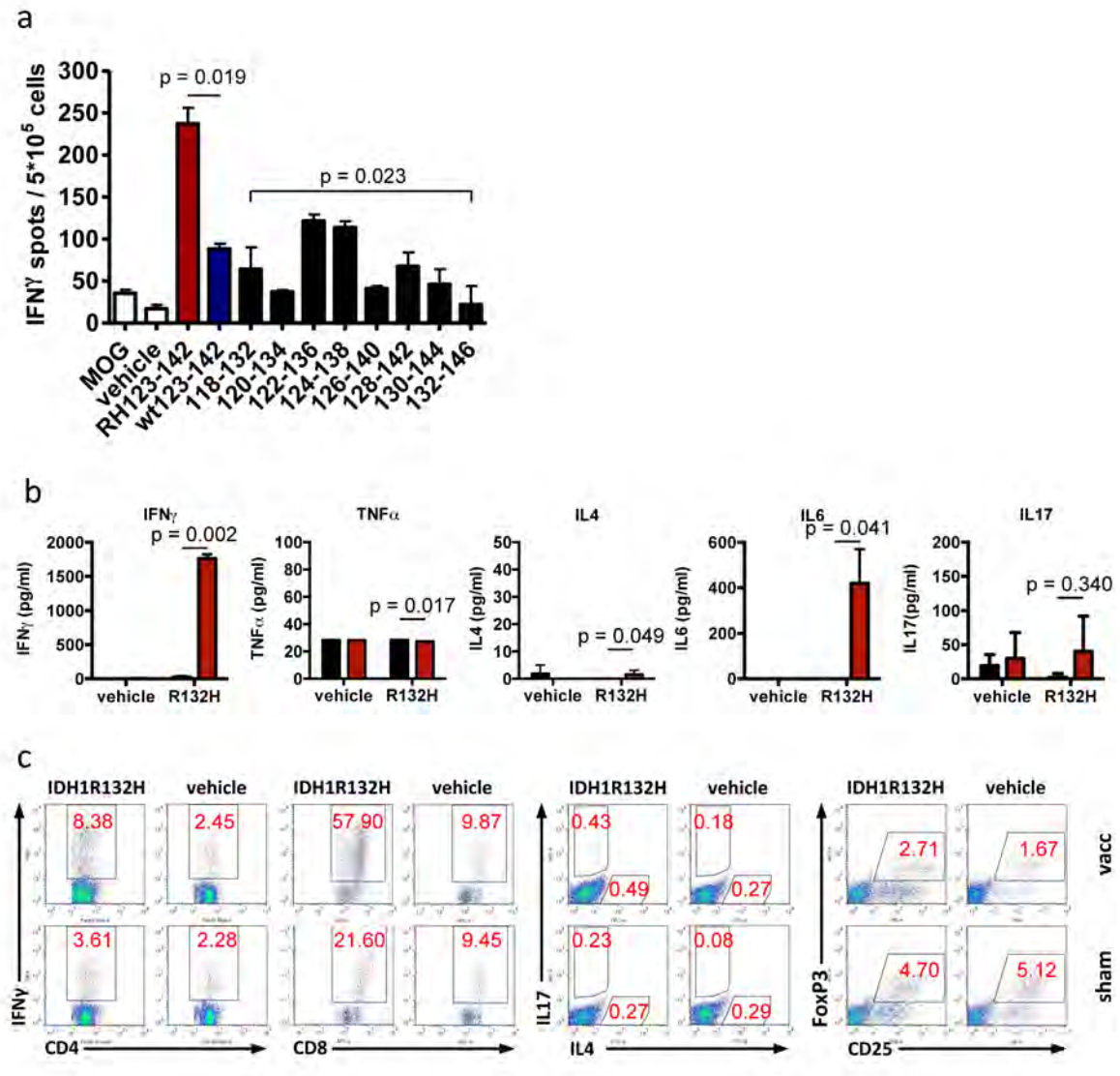

Fig. 3.5. Combined adjuvant Montanide®/imiquimod shifts the IDH1R132H T helper response and induces CTL responses in A2.DR1 mice. a, ELISpot analysis of mutation-specific IFN-γ response to IDH1 peptides of HLA-DR1-binding IDH1R132H 15-mer epitopes after vaccination of A2.DR1 mice with p123-142 (R132H) and restimulation of splenocytes with indicated peptides (white, negative controls; red, p123-142 [R132H]; blue, p123-142 [wt]; black, R132H library peptides). (p123-142 [R132H vs. wt], Welch t test; 15-mers, ANOVA; *n* = 3) Error bars, mean + SEM. **b**, Splenocytes from p123-142 (R132H)-Montanide®/imiquimod vaccinated (red) or sham-treated (black) A2.DR1 mice were tested for production of T helper (Th) cytokines IFN-γ, TNF-α, IL-4, IL-6, and IL-17 after *ex vivo* stimulation with p123-142 (R132H) or vehicle in cytokine ELISA (Welch t test; *n* = 3). Error bars, mean + SEM. **c**, Representative intracellular flow cytometry of splenocytes from three vaccinated (upper panel) and three sham-treated mice (lower panel) after p123-142 (IDH1R132H)-stimulation or vehicle-treatment gated on CD4+ (left and two right panels) or CD8+ (second left panel) cells. Red numbers, populations in percent.

This clinically approved cancer vaccine adjuvant was equally capable of inducing a mutation-specific T cell IFN-γ response in IDH1R132H peptide-vaccinated mice with the same congruence of the peptide MHC class II binding strength and the magnitude of the T cell response after stimulation with 15-mer library peptides (Fig 3.5a). With this regimen, the Th1 profile which was induced by CFA-vaccination persisted with strong induction of IL-6 but not tumor necrosis factor (TNF)-α, but the Th17 cytokine IL-17 was not induced (Fig. 3.5b,c). In addition to IFN-γ and IL-6-producing CD4+ T cells, also IFN-γ-producing cytotoxic CD8+ T cells were generated by vaccination (Fig. 3.5c).

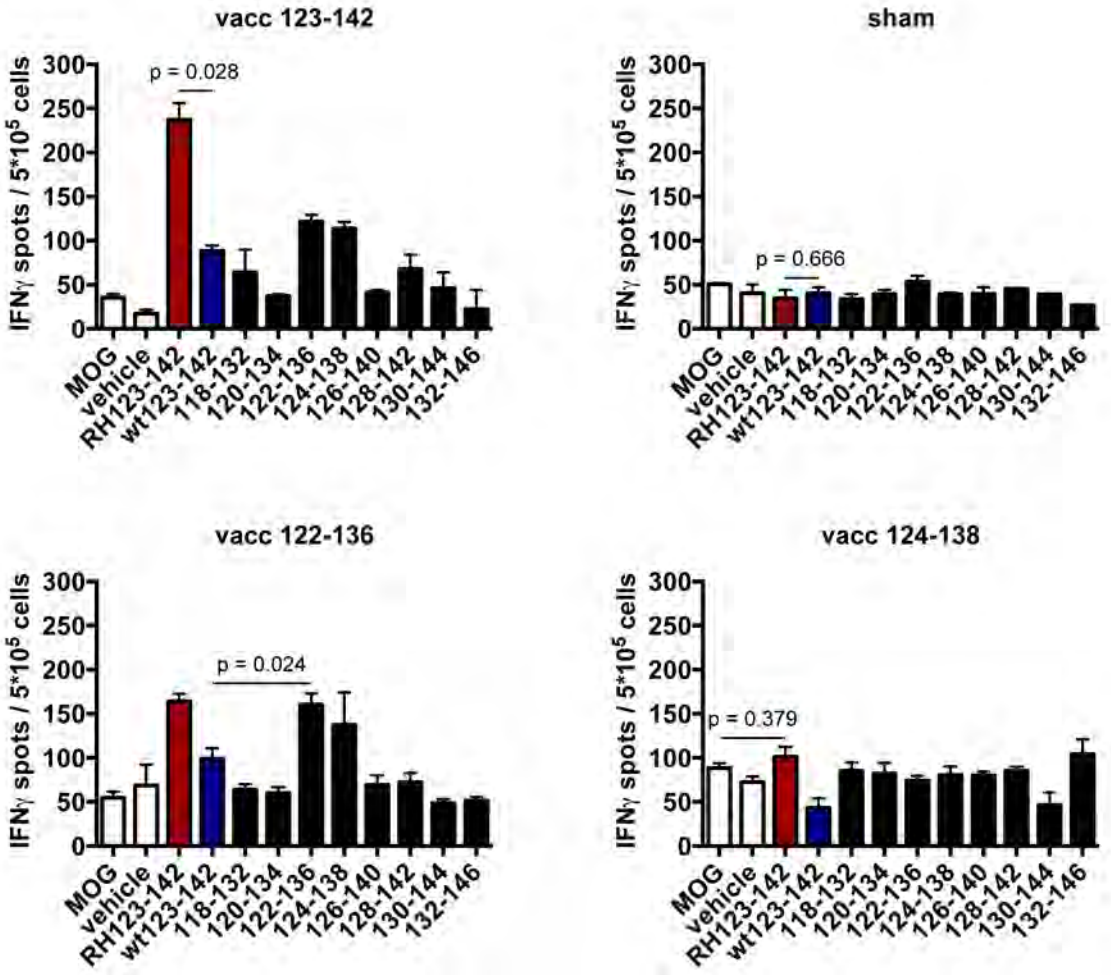

Fig. 3.6. The strongest HLA-DR-binding IDH1R132H epitope is equally capable of inducing IDH1R132H-specific T cell responses with combined adjuvant Montanide®/imiquimod in A2.DR1 mice. ELISpot analysis of mutation-specific IFN-γ response to IDH1 peptides after vaccination of A2.DR1 mice with IDH1R132H (vacc) (p123-142), (p122-136), (p124-138), or vehicle control (sham) using Montanide®/imiquimod and restimulation of splenocytes with indicated peptides (white, negative controls; red, p123-142 [R132H]; blue, p123-142 [wt]; black, R132H library peptides). (p123-142 [R132H vs. wt], Welch t test; 15-mers, ANOVA; *n* = 3). Error bars, mean + SEM.

When A2.DR1 mice were in addition to IDH1R132H (p123-142) 20-mer peptide vaccinated with HLA-DR1-binding IDH1R132H 15-mers (p122-136) and (p124-138) using Montanide®/imiquimmod, IDH1R132H (p122-136), but not (p124-238), induced a mutation-specific IFN-γ response to the 20-mer and HLA-DR1 15-mer epitopes (p122-136) and (p124-138) with an extent comparable to the vaccination with the 20-mer (p123-142) (Fig. 3.6). These results indicate that for priming T cells *in vivo*, IDH1R132H amino acid residue 123 is required to induce the response.

Nevertheless, for further vaccination experiments, IDH1R132H (p123-142) was used, because it induced the strongest and most mutation-specific IFN-γ response. Moreover, amino acid 122 differs in mouse and human IDH1, thus immune responses after vaccination with IDH1R132H (p122-136) might be a result of foreign protein rather than mutation-specific (Fig. 3.6, lower left panel).

3.2.3 Generation and characterization of IDH1R132H-specific A2.DR1 T cell line and clone

For a more detailed analysis of the nature of the IDH1R132H-specific T cell response and potential cloning of the IDH1R132H-binding T cell receptor (TCR), an IDH1R132H (p123-142)-specific CD4+ T cell line was generated from IDH1R132H (p123-142)-stimulated splenocytes of Montanide®/imiquimod-vaccinated A2.DR1 mice. T cells were expanded by four-weekly restimulation rounds with peptide-loaded irradiated autologous splenocytes from naïve A2.DR1 mice as antigen-presenting cells (APC).

Using the above described protocol, a highly antigen-specific T cell line was established, as shown by robust mutation-specific responses to low concentrations of IDH1R132H (p123-142) peptide in IFN-γ ELISpot analysis with peptide-loaded autologous B cell blasts as APC (Fig 3.7a). IFN-γ production was efficiently inhibited with an MHC class II HLA-DR-blocking antibody, but not by an HLA-A-blocking antibody (Fig. 3.7b), nor by MHC class II HLA-DP- nor HLA-DQ-blocking antibodies (Fig. 3.7c), proving the dependency of the T cell line on peptide presentation on HLA-DR1. Direct evidence for IFN-γ secretion by CD4+ T cells came from IFN-γ secretion assay after stimulation of the T cell line with IDH1R132H (p123-142)-loaded autologous splenocytes (Fig. 3.7d). In line with the characterization of the T cell response *ex vivo* after vaccination (see Fig. 3.5), the IDH1R132H-specific T cell line had a Th1 phenotype and secreted IL-17 in addition after stimulation with the phorbol ester phorbol-12-myristate-13-acetate (PMA) together with the ionophore ionomycin (Fig. 3.7e). However, the Th17

phenotype did not persist after antigen-specific stimulation with peptide-loaded autologous dendritic cells (DCs) (Fig. 3.7f). This discrepancy can be explained by the mode of action of PMA and ionomycin, which bypass the TCR-specific stimulation by activation of protein kinase C and hence the MAPK and NF-κB pathways and permeability increase and therefore Ca^{2+} influx, respectively [158]. Therefore, PMA and ionomycin do not reflect antigen-specific stimulation.

During development, genetic rearrangement within the variable region leads to a variety of 25 million TCRs [159], among which more than one might be able to bind a specific antigen with varying affinity and avidity, hence a diverse ability to effectively stimulate the T cell upon antigen encounter. Pursuing the aim to isolate and clone an IDH1R132H-specific TCR with a high activation capacity, CD4+ T cell clones were established from the IDH1R132H-specific T cell line by limiting dilution. In line with the phenotype of the T cell line (see Fig 3.7), the one out of four T cell clones which was reactive against IDH1R132H was mutation-specific and dependent on peptide-presentation on HLA-DR (Fig. 3.8).

Page 44:

Fig. 3.7. IDH1R132H-specific CD4+ T cell line is mutation-specific, dependent on HLA-DR presentation and has a Th1 phenotype. a – c, ELISpot assays of T cells stimulated with peptide-loaded autologous APC (a, Welch t test; *n* = 3; error bars, mean ± SEM) and treated with HLA-blocking antibodies (b, HLA-A and HLA-DR, *n* = 2; c, HLA-DP, HLA-DQ, and HLA-DR, *n* = 3; pairwise Welch t test with Bonferroni correction; error bars, mean + SEM) (white, MOG; black, vehicle; red, p123-142 [R132H]; blue, p123-142 [wt]). **d**, IFN-γ secretion assay of T cells stimulated with peptide-loaded autologous APC followed by CD4 and CD8 surface staining and flow cytometry (flow through, IFN-γ-negative fraction; SEB, staphylococcus enterotoxin B, positive control; IDH1R132H, p123-142; upper left panel, T cell line alone). **e** and **f**, Intracellular cytokine flow cytometry of T cells after stimulation with PMA and Ionomycin (e) or with IDH1R132H (p123-142)-loaded or vehicle-treated DC (f). Gated on CD4+ T cells. Red numbers, populations in percent.

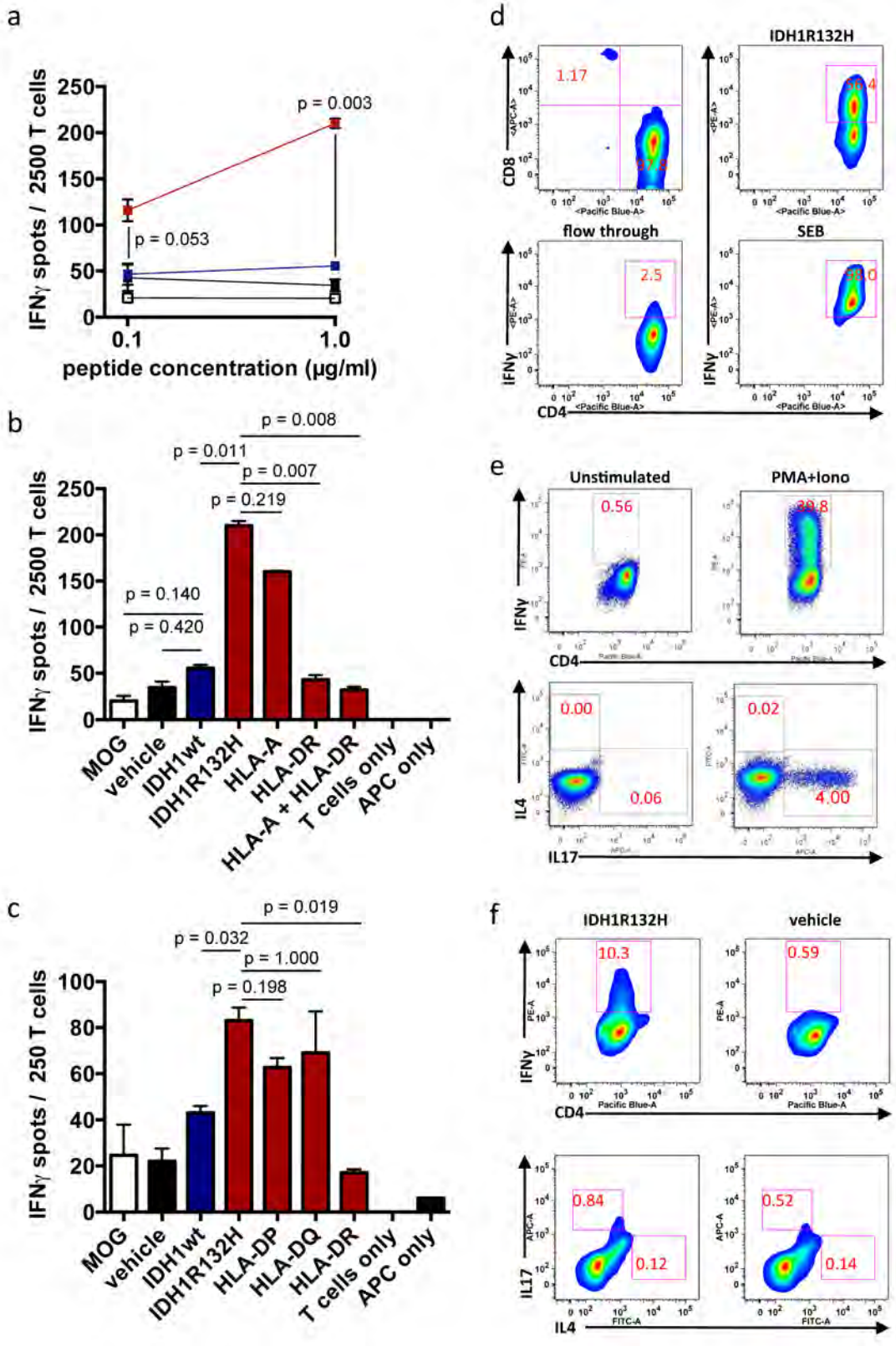

Fig. 3.7. IDH1R132H-specific CD4+ T cell line is mutation-specific, dependent on HLA-DR presentation and has a Th1 phenotype. See page 43 for details.

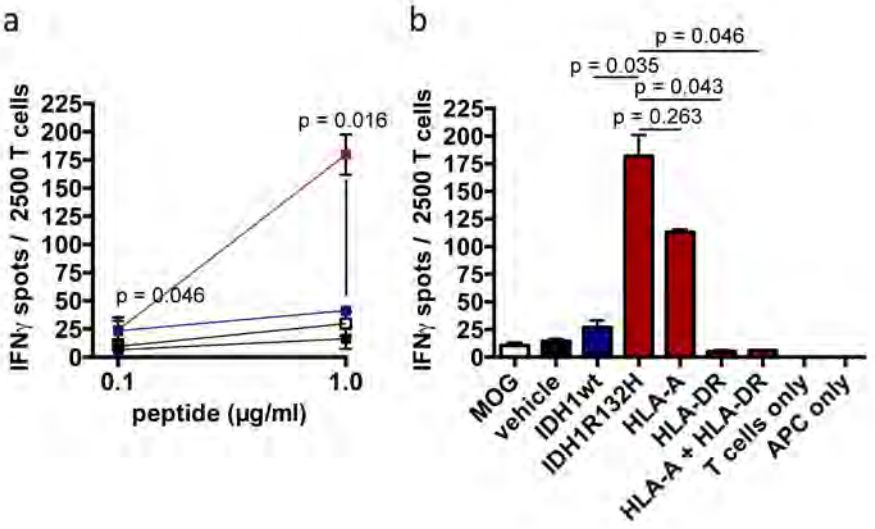

Fig. 3.8. IDH1R132H-specific CD4+ T cell clone is mutation-specific and dependent on HLA-DR presentation. a, ELISpot analysis of IFN-γ production by T cells after stimulation with peptide-loaded autologous B cell blasts (white, MOG; black, vehicle; blue, p123-142 [wt]; red, p123-142 [R132H]) (Welch t test; *n* = 3). Error bars, mean ± SEM. **b**, p123-142 (R132H)-specific IFN-γ production after treatment with blocking antibodies against HLA-DR- and HLA-A in ELISpot with peptide-loaded autologous B cell blasts (white, vehicle; black, MOG; blue, p123-142 [wt]; red, p123-142 [R132H]) (Pairwise Welch t test with Bonferroni correction; *n* = 3). Error bars, mean + SEM.

3.2.4 Cellular IDH1R132H responses are not restricted to HLA-DR1 in MHC-humanized mice

The hitherto collected data on the immunogenicity of IDH1R132H were restricted to one of the most common HLA-DR types within the Caucasian population. However, only about 10 % of this population are positive for serotype HLA-DR1, including HLA-DR1*0101, *0102, and *0103 [148]. Consequently, in a potential clinical study, the possibility to enroll patients with other HLA-DR types would be of high value and advantage. Therefore, the potential of IDH1R132H-encompassing peptides to bind another HLA-DR type and induce a specific T cell response was evaluated.

The class II MHC serotype HLA-DR4 accounts for about 11 % of all HLA-DR types in the Caucasian population and is therefore more common than HLA-DR1 [148]. DR4 mice are like A2.DR1 mice deficient for mouse MHC class II (H-IAb), but proficient for mouse MHC class I (H-2b) and transgenic for human HLA-DRA*0101 and HLA-DRB1*0401 (HLA-DR4) [143].

Vaccination of DR4 mice with IDH1R132H (p123-142) with Montanide®/imiquimod resulted in mutation-specific IFN-γ responses to IDH1R132H (p123-142) (Fig 3.9a). In concordance with T cell responses in A2.DR1 mice (see 3.2.2), this vaccination regimen induced mainly

Th1 responses, with IDH1R132H-induced secretion of IFN-γ and to a lesser extent IL-6, but not TNF-α nor IL-17 (Fig. 3.9b,c). No FoxP3+ T_{reg} were induced by the vaccination (Fig 3.9c).

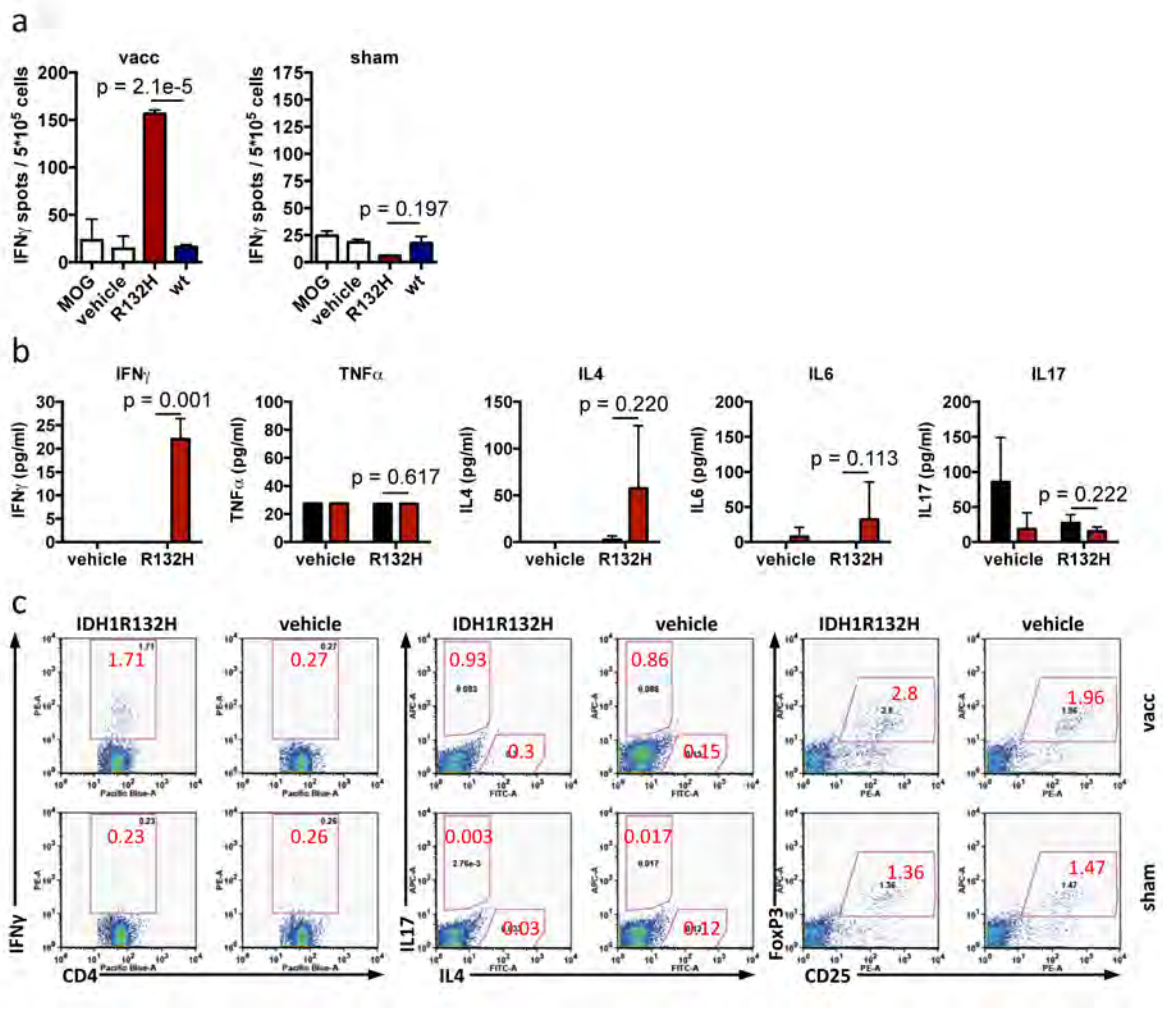

Fig. 3.9. IDH1R132H peptide vaccination using Montanide®/imiquimod induces Th1 responses in HLA-DR4+ humanized mice. a, ELISpot analysis of mutation-specific IFN-γ response to IDH1 (p123-142) after vaccination of DR4 mice with p123-142 (R132H) (vacc) or vehicle control (sham) using Montanide®/imiquimod and restimulation of splenocytes with indicated peptides (white, negative controls; red, p123-142 [R132H]; blue, p123-142 [wt]). (Welch t test; *n* = 3) Error bars, mean + SEM. **b**, Splenocytes from p123-142 (R132H)-Montanide®/imiquimod vaccinated (red) or sham-treated (black) DR4 mice were tested for production of T helper (Th) cytokines IFN-γ, TNF-α, IL-4, IL-6, and IL-17 after *ex vivo* stimulation with p123-142 (R132H) or vehicle in cytokine ELISA (Welch t test; *n* = 3). Error bars, mean + SEM. **c**, Representative intracellular flow cytometry of splenocytes from three vaccinated (upper panel) and three sham-treated mice (lower panel) after p123-142 (IDH1R132H)-stimulation or vehicle-treatment gated on CD4+ cells. Red numbers, populations in percent.

3.2.5 IDH1 peptide-coated serum ELISA allows detection of IDH1R132H-binding antibodies in IDH1R132H peptide-vaccinated A2.DR1 mice

Since one of the functions of antigen-reactive T helper cells is to stimulate B cells to produce and secrete antigen-specific antibodies, T helper cell responses are usually associated with the production of antigen-binding antibodies, which can be detected in serum. With this rationale, the consequent aim was the detection of IDH1R132H-specific antibodies in A2.DR1 mouse serum after vaccination. To this end, a peptide ELISA using IDH1R132H peptides was established to detect IDH1R132H-binding immunoglobulin G (IgG) in mouse serum.

IDH1 peptides of the 15-mer library as well as the 20-mer (p123-142) were coated on ELISA plates, serum was added and peptide-bound IgG were detected with a horseradish peroxidase (HRP)-conjugated secondary antibody and TMB as a substrate (Fig. 3.10a). The ELISA system was established with the IDH1R132H-specific antibody, which has been developed and is routinely used at the University Hospital Heidelberg and internationally for diagnosis of the IDH1 mutation status in glioma patients [105, 106]. Using this antibody, peptide concentration, buffer system, and surface of the ELISA plate were optimized. In accordance with the immunogenic peptide used for production of the IDH1R132H-specific antibody (p125-137), the antibody bound to IDH1R132H (p122-136, p124-138, and p126-140) (Fig. 3.10b). A lower detection limit of about 4 µg/ml IgG was determined by titration of the antibody using plate-bound IDH1R132H (p122-136) (Fig. 3.10c). Importantly, the ELISA system was suitable to discriminate between IDH1R132H and wt, i. e. antibody binding only to the mutated IDH1, but not wt IDH1 was detectable (Fig. 3.10b,d). In addition to the measurement of total IgG, detection of mouse IgG subtypes IgG1, IgG2a, IgG2b, and IgG3 was tested with subtype-specific secondary antibodies. As expected from the antibody subtype, only IgG2a binding to IDH1R12H was detected, verifying the specificity of secondary antibodies in this system (Fig.3.10d).

With the established IDH1 peptide ELISA system, IDH1R132H (p123-142)-binding IgG were detected in serum of some, but not all A2.DR1 mice which had been vaccinated with IDH1R132H (p123-142) with Montanide®/imiquimod. Of note, responding mice developed antibodies which discriminated between wt and mutated IDH1 (Fig. 3.11a). These antibodies were mainly of IgG1 subtype (Fig. 3.11b).

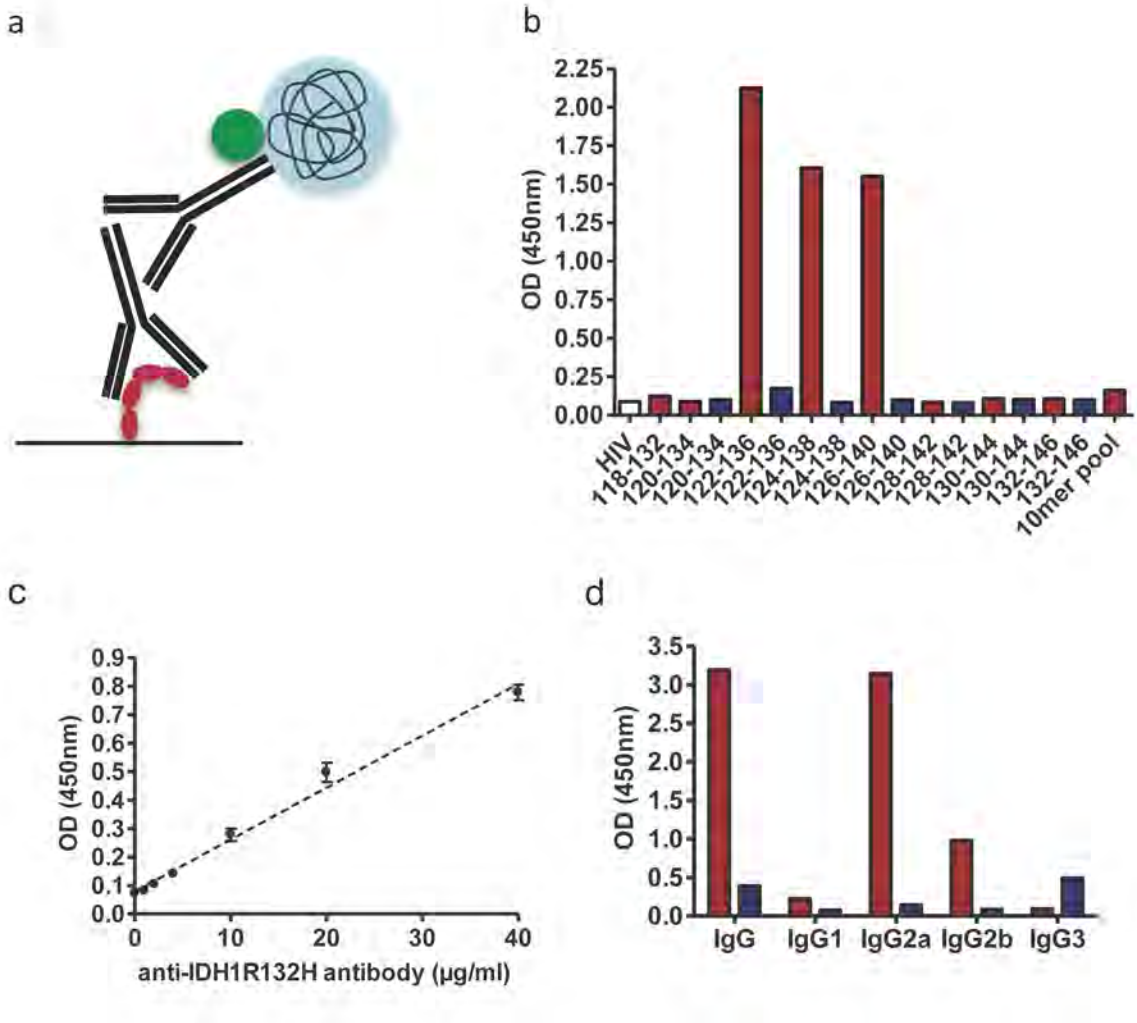

Fig. 3.10. IDH1 peptide-coated ELISA is established for detection of IDH1-specific IgG in mouse serum. a, ELISA plates are coated with IDH1R132H, IDH1wt, or control peptides, washed, blocked, and incubated with human serum or serum from vaccinated mice. Bound IgG are detected using horseradish peroxidase (HRP)-conjugated anti-mouse or anti-human total IgG, IgG1, IgG2a, IgG2b, or IgG3, respectively and subsequent addition of TMB. Colour reaction is stopped with H_2SO_4 and measured at 450 nm. **b – d**, ELISA IDH1R132H specificity and applicability were tested using mouse anti-IDH1R132H antibody as serum substitute. **b**, ELISA on indicated peptides of the 10-mer and 15-mer libraries (blue, IDH1wt; red, IDH1R132H; 10-mer pool, all library peptides) and a negative control peptide (white, HIV). **c**, p122-136 (IDH1R132H) was used to titrate the anti-IDH1R132H antibody. **d**, IgG subtype-specific secondary antibodies were used with IDH1R132H-specific antibody on p122-136 (IDH1R132H).

The results described here show that peptide vaccination with IDH1R132H induces mutation-specific T helper 1-mediated cellular responses and IgG production in MHC-humanized mice and that this immunogenicity is restricted to MHC class II, but not to HLA-DR1. Potent IFN-γ T cell responses are induced not only by CFA, but also with a clinically approved adjuvant. The established peptide ELISA allows mutation-specific detection of IDH1R132H-binding epitopes in mouse serum.

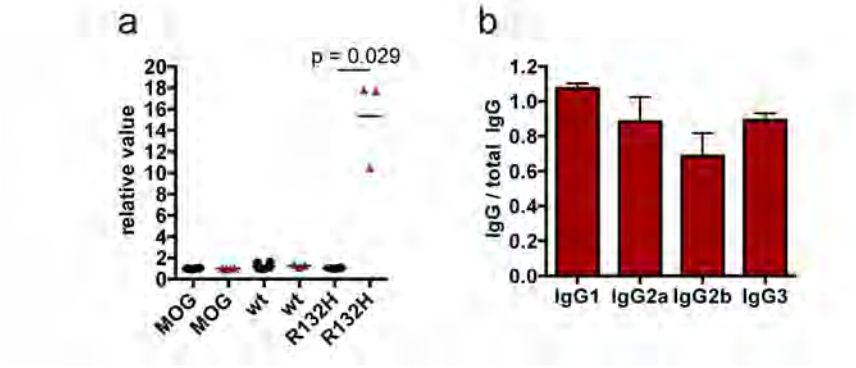

Fig. 3.11. IDH1R132H peptide vaccination using Montanide®/imiquimod induces IDH1-specific antibodies in A2.DR1 mice. a, Detection of IDH1R132H-specific antibodies by MOG-, p123-142 (R132H, wt) peptide-coated ELISA in serum of A2.DR1 mice immunized with p123-142 (R132H) (red), but not sham-treated (black). OD values are depicted relative to negative control (MOG) OD (Welch t test; *n* = 3). Scatter plot showing individual values for each mouse and the mean. **b**, Detection of IDH1R132H-specific IgG subclasses IgG1, IgG2a, IgG2b, and IgG3 with 123-142 (R132H)-peptide-coated ELISA in serum of vaccinated mice bearing IDH1R132H-specific IgG. Values are depicted relative to total IgG.

3.3 Spontaneous IDH1R132H cellular and humoral responses are detected in glioma patients

The *ex vivo* results obtained from the vaccination experiments in MHC-humanized mice indicate that the IDH1 mutation is immunogenic in a way that an epitope harboring the mutated residue is presented on MHC class II to induce an IDH1R132H-specific T cell response that is able to stimulate the production of IDH1R132H-binding IgG antibodies. Nevertheless, these results are not empowered to prove the processing of the immunogenic epitope from the IDH1R132H protein.

To pursue the question of epitope processing, but even more to analyze the clinical relevance of an IDH1R132H-specific immune response, IDH1R132H-positive glioma patients were tested for spontaneous responses against the mutated IDH1. It has been shown for other tumor entities and antigens that patients can harbor spontaneous tumor antigen-specific humoral and cellular immune responses, e.g. against the cancer testis antigen NY-ESO-1 [40, 41]. In high-grade glioma, spontaneous immune reactions against the tumor-associated antigens IL13Rα2 and EphA2, as indicated by specific T cells in the peripheral blood, correlated with prolonged survival [160]. Therefore, it was hypothesized that an immunogenic IDH1R132H epitope might spontaneously induce specific immunity in glioma patients with IDH1R132H-mutated tumors.

3.3.1 IDH1R132H-positive glioma patients harbor spontaneous IDH1R132H-specific T helper responses

IDH1R132H-positive patients were screened for IDH1R132H-induced IFN-γ secretion in peripheral blood mononuclear cells (PBMC) using library peptides in ELISpot analysis. Four out of 25 patients (16 %) with IDH1-mutated tumors, but none of 29 glioma patients with an IDH1 wt status showed IDH1R132H-specific IFN-γ responses against the 20-mer IDH1R132H peptide 123-142, which had been used for vaccination studies in MHC-humanized mice, in the periphery. These responses were mutation-specific (Fig. 3.12a-c). Notably, no response against IDH1R132H peptides of the 10-mer library (see Fig. 3.1b) was detectable in any of 23 IDH1R132H-positive patients tested, including one patient with a response against IDH1R132H (p123-142) (Fig. 3.12d), pointing towards the notion that immune responses are not MHC class I-mediated.

Supporting this idea and in line with the induced IDH1R132H-specific T cell responses in vaccinated MHC-humanized mice, specific IFN-γ secretion was abrogated by the HLA-DR-blocking antibody in responsive patients (Fig. 3.12e), indicating the presentation of the IDH1R132H epitope on HLA-DR and a CD4+ T cell response. To further characterize the phenotype of the T cell response, IFN-γ secretion assays were performed enabling the enrichment and flow cytometric analysis of IFN-γ-producing T cells from ELISpot positive patients. In line with the results of the immunizations of MHC-humanized mice, IDH1R132H-specific IFN-γ-producing T cells were predominantly CD4+ in two patients tested positive for IDH1R132H-specific IFN-γ responses (data shown for one patient, Fig. 3.12f).

Notably, the spontaneous antigen-specific T cell responses were of very low frequency compared to those detected in vaccinated mice; however, this can be expected due to immunosuppressive properties of the tumor [114] and an impaired antigen encounter as a consequence of the blood brain barrier. In addition, no IDH1R132H-induced IFN-γ secretion was detectable in patients with an IDH1 wt status (Fig. 3.12c), indicating that these cellular responses are specific and of clinical relevance and that an IDH1R132H-positive tumor might induce specific responses by stimulating the immune system.

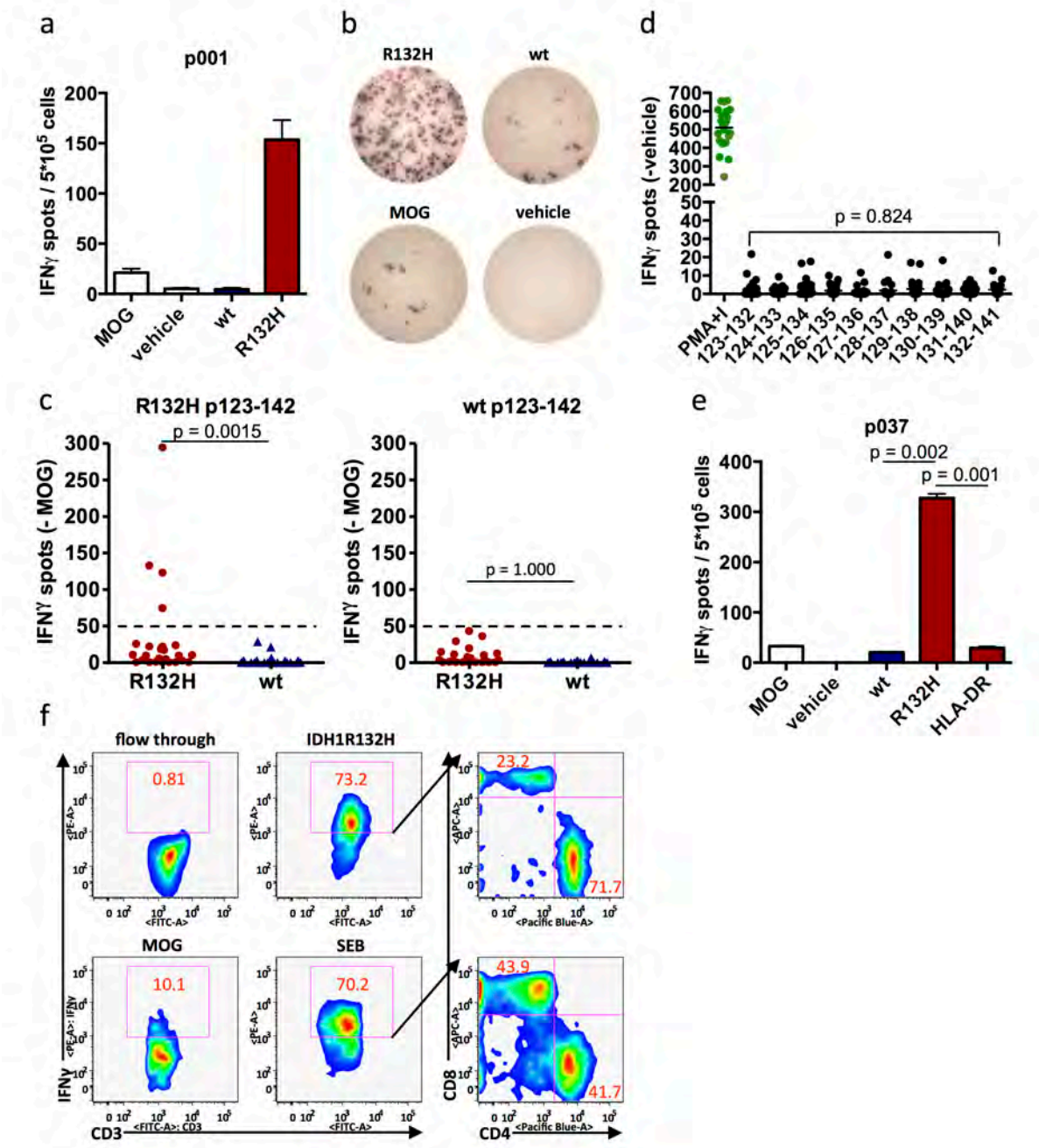

Fig. 3.12. Spontaneous IDH1R132H-specific CD4+ T cell responses are detected in some IDH1R132H-positive glioma patients. a and **b**, Representative IFN-γ ELISpot analysis of PBMC from patients p001 (a) and p037 (b), stimulated with IDH1R132H p123-142 (a, red), IDH1wt p123-142 (a, blue), and negative controls (MOG p35-55 and vehicle; a, white). a, error bars, mean + SEM, *n* = 2. **c** and **d**, IFN-γ ELISpot analyses of PBMC from patients with IDH1R132H-mutated gliomas (c, red, *n* = 25; d, *n* = 23) or IDH1wt gliomas (c, blue, *n* = 29), stimulated with IDH1 (p123-142) R132H or wt (c) or indicated 10-mer peptides (d; black; green, positive control PMA+I, phorbol myristate acetate + ionomycin. (c, Wilcoxon rank-sum test; Fisher's exact test of odds, p = 0.043; d, Welch ANOVA) Data are depicted as specific spots after subtraction of background spots (MOG, negative values set to zero) in a scatter plot showing values for each patient. Dashed line, cut-off for positivity set to 50 in c. **e**, IFN-γ production by PBMC of patient p037 in response to p123-142 (R132H) as in a including an HLA-DR-specific blocking antibody (Welch t test; *n* = 3). Error bars, mean + SEM. **f**, IFN-γ secretion assay of (p123-142)-stimulated PBMC from patient p037 (flow through, IFN-γ-negative fraction; MOG, negative control; SEB, positive control; IDH1R132H, p123-142). Red numbers, populations in percent. Data in b, c, e, and f collected and analyzed by L. Bunse.

3.3.2 IDH1R132H-specific antibodies can be detected in the serum of IDH1R132H-positive glioma patients

The results obtained from glioma patient peripheral blood described above (see 3.3.1) show that an immunogenic IDH1R132H epitope induces an IDH1R132H-specific cellular response only in those patients harboring IDH1-mutated tumors. Moreover, the cellular response was restricted to CD4+ T helper cells. Consequently, as in vaccinated mice, spontaneous IDH1R132H-specific T cell responses might be accompanied by humoral responses in these patients as well.

Before glioma patients were screened, IDH1 peptides of the 15-mer library and the 20-mer peptides were tested for binding to serum IgG from IDH1R132H glioma patients using the established ELISA system (see 3.2.5). IDH1R132H-specific IgG bound exclusively to one 15-mer peptide (p122-136) (Fig 3.13a), which was subsequently used for screening.

IDH1R132H-positive glioma patients who were tested with the ELISA had significantly higher IgG IDH1R132H-peptide binding values than patients with IDH1wt gliomas. The obtained data from 89 patients in total was used to define a binding capacity threshold for positivity, which was defined as a five-fold IDH1R132H-binding value relative to the negative control peptide (Fig. 3.13b). According to this threshold, compliant with the vaccination studies in MHC-humanized mice, IDH1R132H-specific antibodies were detected in 4 of 42 patients with IDH1R132H-mutated but not in 47 patients with IDH1wt tumors and not in healthy donors, indicating the presence of IDH1R132H-specific antibodies in a fraction (9.5 %) of glioma patients with IDH1R132H-mutated tumors. Of note, as opposed to IDH1R132H T cell and antibody reactivity, there was no difference between patients with IDH1wt and IDH1R132H-mutated tumors nor IDH1R132H-responders and non-responders in their ability to react to the foreign positive control antigen tetanus toxoid with specific antibody production (Fig.3.13c), indicating that the difference is not due to a different ability to react to a neoantigen in general between the groups. Serum of 10 patients with IDH1R132H+ tumors, who had been shown to have elevated IDH1R132H-specific IgG levels, was tested for IDH1R132H-binding IgG subtypes. In correlation with vaccination-induced specific IgG production in mice, patient IDH1R132H-binding IgG were of IgG1 subtype (Fig. 3.13d).

Collectively, screening of glioma patients harboring IDH1wt or IDH1R132H tumors revealed that spontaneous mutation-specific IDH1R132H-directed T cell and humoral responses are rare, but detectable in IDH1R132H-positive patients, but not in IDH1wt patients, indicating

that R132H-mutated IDH1 is naturally processed in glioma patients to present an immunodominant epitope in the p123-142 region on MHC class II molecules to CD4+ T cells to induce a spontaneous mutation-specific Th1-polarized response and the production of mutation-specific antibodies detectable in patients with IDH1R132H-mutated but not IDH1 wt gliomas.

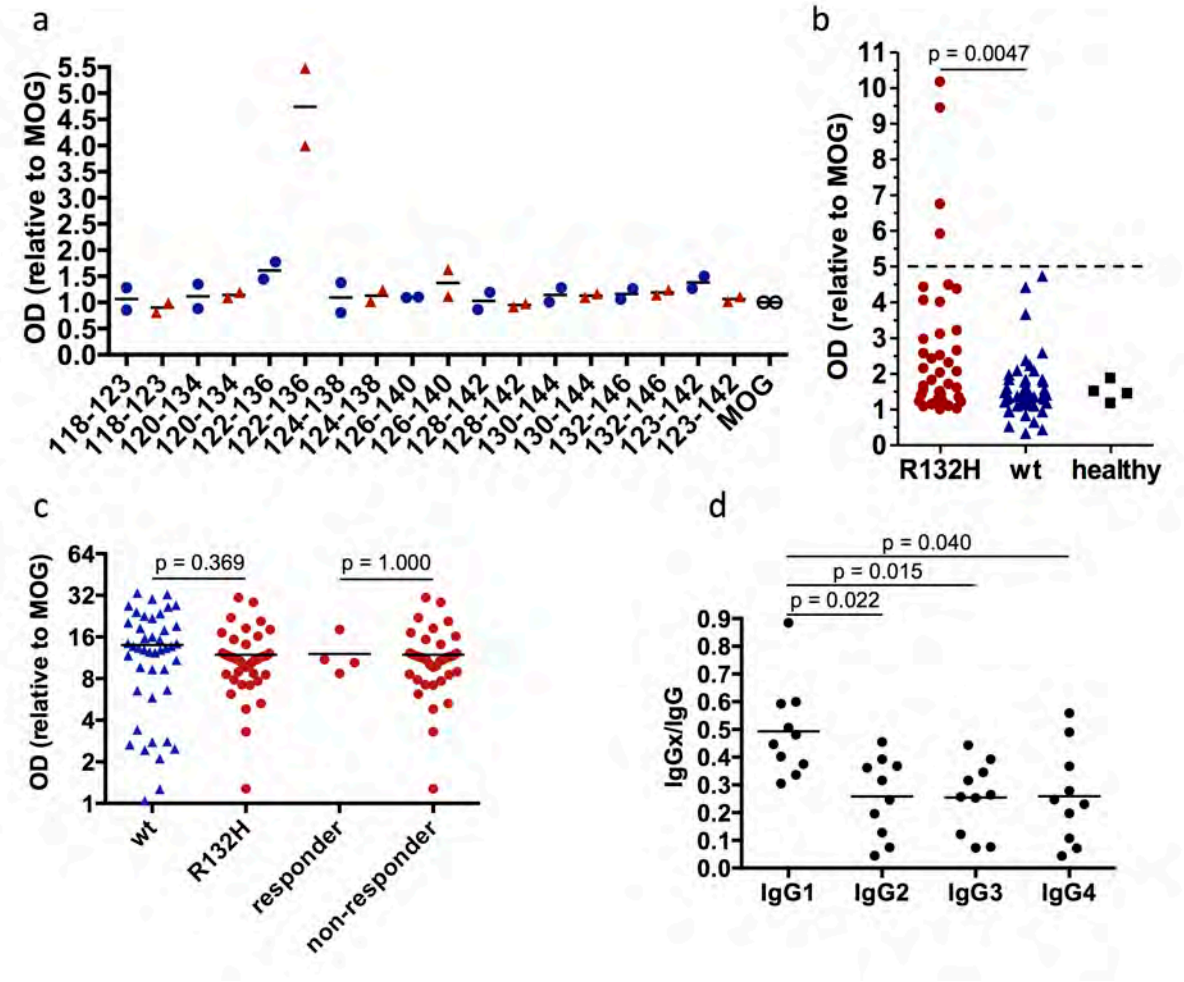

Fig. 3.13 IDH1R132H-specific antibodies can be detected in some IDH1R132H-positive glioma patients. a, Peptide-coated ELISA analyzing IDH1-specific IgG in serum of 2 IDH1R132H-positive patients using indicated IDH1 15-mer library and 20-mer peptides (blue, IDH1wt; red, IDH1R132H; white, MOG negative control). Data are presented relative to MOG. **b**, Peptide-coated ELISA analyzing IDH1R132H-specific IgG in serum of 42 IDH1R132H-positive patients, 47 IDH1wt patients, and 4 healthy donors. (Wilcoxon rank-sum test; Fisher's exact test of odds, p = 0.043) Data are depicted relative to MOG. Dashed line, cut off for positivity set to 5. **c**, Detection of tetanus toxoid-specific IgG in serum of IDH1wt patients (blue, *n* = 44) and IDH1R132H-positive patients (red, *n* = 40). IDH1R132H-positive patients are grouped into IDH1R132H-IgG positive (responder, *n* = 4) and negative (non-responder, *n* = 36) according to b (Wilcoxon rank-sum test). Data are depicted relative to MOG. **d**, IDH1R132H-specific IgG and IgG subtypes IgG1, IgG2, IgG3, and IgG4 were detected in serum of IDH1R132H-positive glioma patients (Pairwise Welch t test with Bonferroni correction; *n* = 10). Data are depicted relative to total IgG. Scatter plots showing values for each patient (and the mean in a, c, d). Data in b – d collected and analyzed by L. Bunse.

3.4 IDH1R132H vaccination specifically reduces IDH1R132H tumor growth in A2.DR1 mice

3.4.1 Establishment of a syngeneic MHC-humanized tumor model for vaccination

An essential but hitherto open question was the therapeutic relevance and functionality of the IDH1R132H-specific immune response, which is spontaneously detectable in IDH1R132H-positive glioma patients and inducible by peptide vaccination in MHC-humanized mice. To address this question, which is, in other words, the question if the specific anti-IDH1R132H CD4+ T helper cell response after vaccination is capable of inducing an effective anti-tumor immune response, a syngeneic tumor mouse model for preventive and therapeutic vaccination studies was required. Since vaccination studies were performed with MHC-humanized mice and the human MHC context was to be retained, a syngeneic model in A2.DR1 mice was established. To this end, sarcomas were chemically induced in A2.DR1 mice, excised and passaged through immunodeficient NOD/SCID mice to increase the HLA expression for establishment of a sarcoma cell line suitable for vaccination studies (J. Quandt, Fig. 3.14a,b). Notably, sarcoma cells upregulated the surface expression of HLA-A2, but not HLA-DR1 after passage through NOD/SCID mice (Fig. 3.14c). Cells were retrovirally transduced with human IDH1R132H or IDH1wt as control for stable antigen expression (Fig. 3.14a,d) to generate 2-HG levels comparable to human gliomas endogenously expressing IDH1R132H, which lie between 1 and 30 mM [69], as an indicator for clinically relevant antigen expression levels (Fig.3.14e). These levels were maintained in clone IVC1, which was generated by limiting dilution and selected for homogenous IDH1R132H expression (Fig. 3.14d,e). Interestingly, when cells (R132H line) were implanted s.c. into the flank of A2.DR1 mice, IDH1R132H-overexpressing tumors grew slower than tumors lacking the mutation (Fig. 3.14f). Principally, this is in line with the clinical situation, in which glioma patients with IDH1R132H-expressing tumors show a longer overall and progression-free survival than patients with IDH1wt tumors [70, 71, 75, 80].

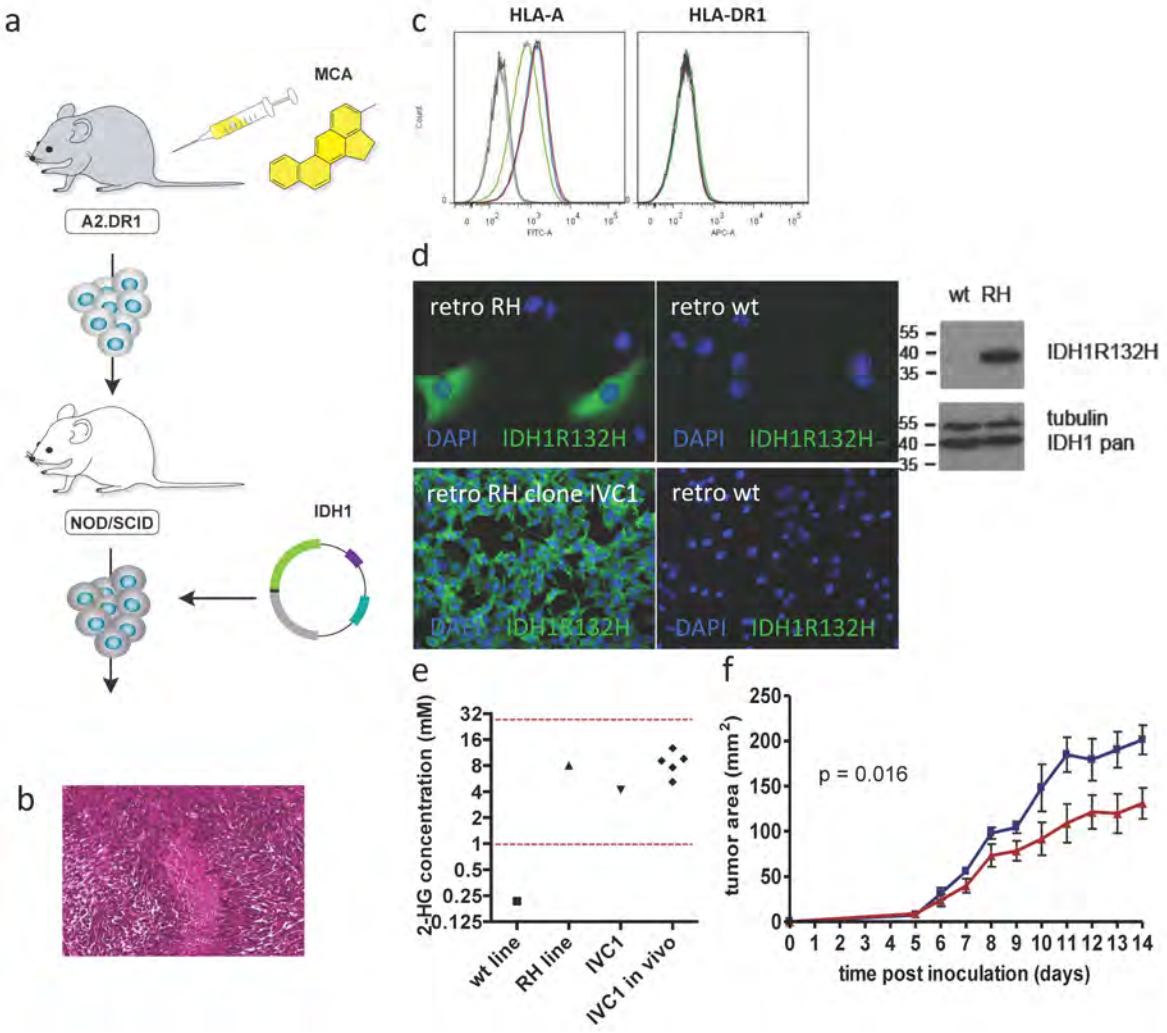

Fig. 3.14. Establishment of a syngeneic MHC-humanized tumor model for vaccination. a, 3-methylcholantrene (MCA) was injected s. c. into flanks of A2.DR1 mice and spontaneously developing tumors were excised, passaged once through NOD/SCID mice by s. c. injection and excised to expand a cell line. Cells were retrovirally transduced with human IDH1R132H or IDH1wt for implantation into A2.DR1 mice. **b**, H&E staining of MCA-induced and NOD/SCID-passaged established A2.DR1 sarcoma cell line. A2.DR1 sarcoma cells were implanted into A2.DR1 mice, tumors were excised and H&E-stained. **c,** HLA-expression of A2.DR1 sarcoma cell line. Cells were stimulated with different concentrations of IFN-γ for 48h, stained for HLA-A and HLA-DR1 and analyzed by flow cytometry. dark grey, unstained; light grey, isotype control; red, 100 ng/ml IFN-γ; blue, 50 ng/ml IFN-γ; green, untreated. **d,** IDH1R132H-expression in transduced A2.DR1 sarcoma cells. Cells were retrovirally transduced with IDH1wt (wt) or IDH1R132H (RH) and selected for stable expression. IDH1R132H protein detection in IDH1R132H-expressing and IDH1wt-expressing cell lines and IDH1R132H clone IVC1 by immunofluorescent staining (left; green, IDH1R132H; blue, nuclei) and by western blot in cell lines (right). **e**, 2-HG concentrations in A2.DR1 syngeneic sarcoma cells *in vitro* and IVC1 tumor *in vivo* measured by enzymatic assay. Red dashed lines mark the range of 2-HG concentrations found in patient tumors. **f**, IDH1R132H- (red) and wt-expressing (blue) A2.DR1 sarcoma cells were implanted into A2.DR1 mice and tumor growth was measured (Wilcoxon rank-sum [WRS] test for median area under the curve [AUC]; *n* = 5 mice per group). Error bars, mean ± SEM. A2.DR1 sarcoma cell line and data in b provided by J. Quandt. Scheme in a by J. Jung. Establishment and analysis of clone IVC1 by L. Bunse. Data in e provided by J. Balß.

3.4.2 Preventive IDH1R132H peptide vaccination reduces IDH1R132H, but not IDH1wt tumor growth

To evaluate whether IDH1R132H is endogenously processed and presented in a human HLA-DR1 context, which is a prerequisite for exerting antigen-specific anti-tumor immune responses, A2.DR1 mice were vaccinated by injection of irradiated syngeneic tumor cells overexpressing IDH1wt or IDH1R132H (clone IVC1) as a whole tumor cell vaccine. Vaccination with IDH1R132H but not IDH1wt A2.DR1 sarcomas induced a robust T cell response to IDH1R132H, but not wt IDH1 p123-142 epitope suggesting that IDH1 is endogenously processed to present the R132H-containing epitope on HLA-DR1 (Fig. 3.15a).

For assessment of a functional anti-tumor immune response in the HLA-DR1 context *in vivo*, A2.DR1 mice were vaccinated with IDH1R132H (p123-142) using Montanide®/imiquimod as an adjuvant or adjuvant only (sham) and subsequently, IDH1R132H- or IDH1wt-transduced sarcoma cell lines were s. c. transplanted into the flank (Fig. 3.15g). Peptide vaccination of A2.DR1 mice with IDH1R132H (p123-142) resulted in a growth suppression of IDH1R132H but not IDH1wt tumors (Fig. 3.15b) although vaccination efficacy was comparable if not higher in mice with IDH1wt tumors evidenced by IDH1R132H-specific IFN-γ secretion measured by ELISA (Fig 3.15e) and ELISpot (Fig. 3.15f). Importantly, IDH1R132H tumors which resisted IDH1R132H-specific peptide vaccination, displayed greatly and significantly reduced IDH1R132H expression while sarcomas in the control group retained their IDH1R132H expression (Fig. 3.15c,d). The loss of antigen expression after specific vaccination indicates the biological activity and effectiveness of vaccination and can explain the limited success of vaccination with an outgrowth of mostly IDH1R132H-negative tumor cells, which were enclosed among the IDH1R132H-transduced sarcoma cells (Fig. 3.14d, upper left), and display a growth advantage over IDH1R132H-expressing cells *per se* (Fig. 3.14f) after two weeks of tumor challenge.

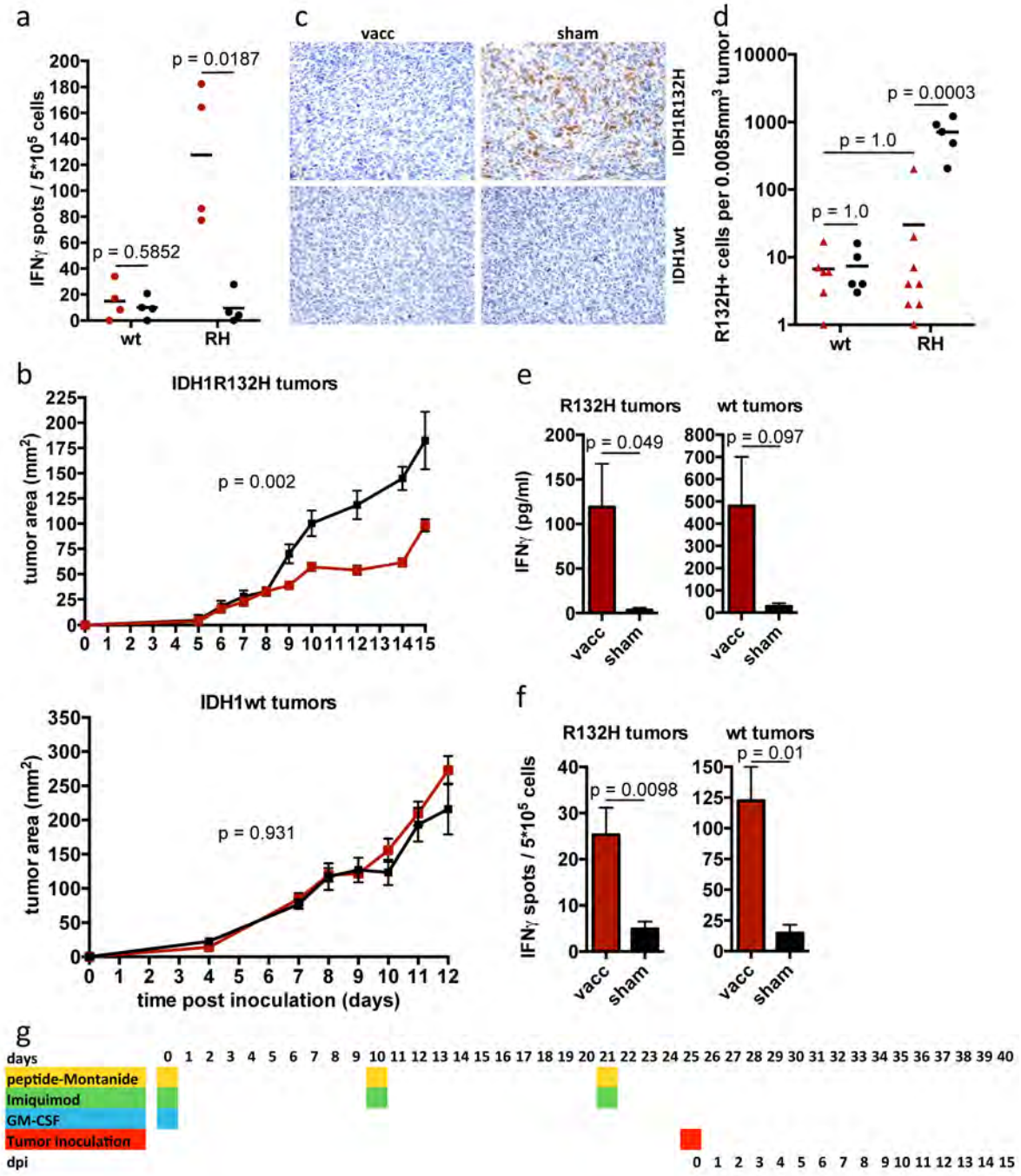

Fig. 3.15. Preventive IDH1R132H peptide vaccination reduces IDH1R132H+, but not IDH1wt tumors. **a**, IFN-γ ELISpot of splenocytes from A2.DR1 mice vaccinated with IDH1R132H (red) or IDH1wt (black) sarcoma cells after stimulation with IDH1 p123-142 (R132H, RH) or wt. (Welch t test; *n* = 4 mice) Data are depicted as specific spots after subtraction of background spots (MOG, negative values set to zero) in a scatter plot showing values for each mouse and the mean. **b**, Growth of IDH1R132H and wt tumors after vaccination with IDH1R132H p123-142 (vacc, red) or vehicle (sham, black) (WRS test for median AUC). Error bars, mean ± SEM. **c** and **d**, IDH1R132H IHC of IDH1R132H (RH) and wt tumors after vaccination (vacc, red) or sham (black). c, representative images; d, scatter plot showing values for each tumor and the mean (Welch one-way ANOVA, pairwise Welch t tests with Bonferroni correction after log2 transformation). **e** and **f**, IDH1R132H p123-142 immune responses of vaccinated (vacc) or sham-treated mice by ELISA (e) and ELISpot (f, spot counts are depicted after subtraction of background spots [MOG]) (Welch t test). Error bars, mean + SEM. b – f; *n* = 8 IDH1R123H tumors, vacc; *n* = 6 IDH1R132H tumors, sham; *n* = 5 IDH1wt tumors **g**, Schedule for tumor cell inoculation into vaccinated mice. dpi, days post inoculation. Data in c and d collected and analyzed by L. Bunse.

3.4.3 Therapeutic IDH1R132H peptide vaccination reduces IDH1R132H tumor growth

Taken together, the hitherto obtained data indicate that the immunogenic epitope is processed and presented in an IDH1R132H-positive tumor and that a peptide vaccine targeting IDH1R132H induces a mutation-specific immune response restricted to human MHC, which is able to trigger an effective anti-tumor immune response in a syngeneic mouse model *in vivo*. However, the preventive vaccination study is limited in that it does not reflect the patient situation – apart from the fact that a sarcoma model is used – in two ways. First, the vaccination was preventive, which is the reason why a therapeutic vaccination at a time point when tumors were established was conducted (see Fig. 3.16e). Second, sarcoma cells were heterogeneous in terms of IDH1R132H expression, leading to antigen loss in vaccinated tumors (Fig. 3.15c,d). Although this finding is important as it clearly demonstrates biological functionality of the vaccine, this setting does not reflect the homogenous expression of IDH1R132H within the tumor that is found in patients with IDH1-mutated gliomas [107]. Therefore, a more homogenous sarcoma cell line was required for the therapeutic vaccination study, which is why clone IVC1 was selected for *in vivo* experiments by immunofluorescent staining according to homogenous IDH1R132H expression (see Fig. 3.14d,e and 3.4.1) and used to test whether the peptide vaccine would also be able to control pre-established tumors in a clinically relevant treatment setting.

For this purpose, vaccination was initiated 6 days after the inoculation of an IDH1R132H-positive sarcoma cell clone (IVC1) after measurable tumors had formed (Fig.3.16e). In line with the preventive vaccination results, therapeutic IDH1R132H peptide vaccination of mice bearing established IDH1R132H-positive sarcomas efficiently suppressed the growth of these tumors (Fig. 3.16a). Vaccination went along with high vaccination efficiencies shown by systemic specific T cell-mediated IFN-γ responses in all vaccinated mice (Fig.3.16b) and antibody production by 5 out of 7 vaccinated mice (Fig.3.16c).

Of note, the IDH1R132H peptide vaccine did not cause any overt toxicity compared to the sham-treated animals as evidenced by histopathological organ analysis (Table 3.1), nor did it impair IDH1wt enzymatic function, verified by biochemical assay for enzymatic activity in liver and brain (Fig. 3.16d).

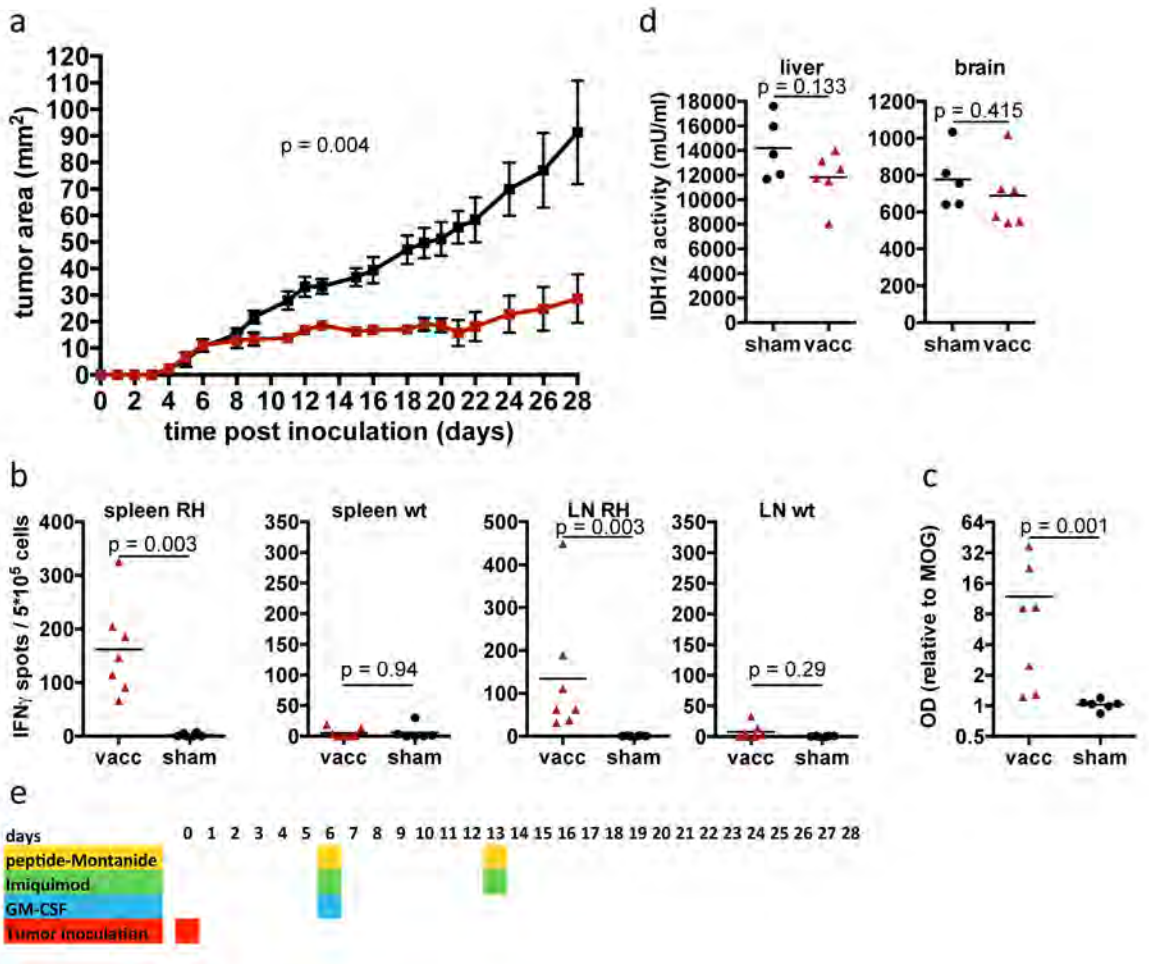

Fig. 3.16. Therapeutic IDH1R132H peptide vaccination suppresses IDH1R132H+ tumor growth. a, Growth of subcutaneous tumor clone IVC1 in A2.DR1 mice immunized on day 6 with IDH1R132H p123-142 (vacc, red) or vehicle (sham, black) using Montanide®/imiquimod (WRS test for median AUC, *n* = 7 for each group. Error bars, mean ± SEM. **b** and **c**, Systemic immune responses in therapeutically vaccinated A2.DR1 mice. Splenocytes (spleen) and lymph node cells (LN) were analyzed for IFN-γ production after *ex vivo* stimulation with p123-142 (R132H [RH] and wt) by ELISpot (b, spot counts are depicted after subtraction of MOG negative control-induced spots) and IDH1R132H-specific serum IgG were detected by ELISA (c, OD values are depicted relative to negative control [MOG]) (Welch t test; *n* = 7 vacc mice, *n* = 6 sham mice). **d**, IDH1/2 enzymatic activity was measured in liver and brain homogenates of A2.DR1 mice vaccinated with IDH1R132H (p123-142) (vacc, red) or sham-treated (sham, black) using Montanide®/imiquimod (Welch t test; *n* = 6, vacc; *n* = 5, sham). b – d, scatter plots showing values for each mouse and the mean. **e**, Schedule for tumor cell inoculation and vaccination.

Aiming at benchmarking the quality of the IDH1R132H neoantigen in order to classify the relevance of vaccination efficacy, A2.DR1 sarcomas were transduced with the well-established and clinically relevant tumor-associated antigen human NY-ESO-1 [37, 43, 161] (see 1.1), which contains a 41 % sequence homology to mouse CTAG2, which has the highest similarity with the epitope used for therapeutic vaccination (59 % for the DR1 epitope) (Fig.

3.17a,b). NY-ESO-1 is an antigen that not only elicits CTL responses, but also CD4+ T helper cell activity [40, 41]. Six days after implantation of NY-ESO-1+ sarcomas, after measurable

ID	treatment	heart	lung	liver	kidney	stomach	intestine	brain
384	sham	-	-	minimal multifocal single-cell necrosis	n.d.	-	-	-
386	sham	-	-	-	n.d.	-	-	-
394	vacc	-	-	-	-	-	-	-
395	vacc	-	-	minimal extramedullary hematopoiesis	-	-	-	-
399	vacc	-	-	-	-	-	-	-
400	vacc	-	-	-	-	-	-	-
413	sham	-	-	-	-	-	-	-
419	sham	-	-	-	-	-	-	-
421	sham	-	-	-	-	-	-	-
431	vacc	-	-	-	n.d.	-	-	-
432	vacc	-	-	minimal extramedullary hematopoiesis	-	-	-	-
434	vacc	-	-	-	-	-	-	-
435	vacc	-	-	-	-	-	-	-

Table 3.1. Pathological analysis of organs from IDH1R132H (p123-142) vaccinated and sham-treated A2.DR1 mice. n.d., not determined.

tumors had formed, A2.DR1 mice were vaccinated with the NY-ESO-1 peptide (p119-143), which represents an HLA-DR1-restricted immunodominant epitope [162], with Montanide®/imiquimod as an adjuvant or adjuvant only (sham). The vaccine efficiently induced an NY-ESO-1-specific T helper cell response in A2.DR1 mice (Fig. 3.17d,e) and resulted in the control of NY-ESO-1+ sarcomas (Fig. 3.17c). Thus, the therapeutic effect of the IDH1R132H peptide vaccine compared well with another HLA-DR1-restricted, clinically relevant peptide vaccine (growth suppression by 58.8 % for p123-142 [R132H] vs. 65.4 % for p119-143 [NY-ESO-1]) (Fig. 3.16a and 3.17c). This underlines both the suitability of the A2.DR1 syngeneic tumor model for MHC class II and CD4+ T cell-mediated therapeutic vaccination and the relevance of IDH1R132H as an immunogenic neoantigen.

Collectively, these data suggest that a peptide vaccine targeting IDH1R132H induces a mutation-specific immune response restricted to human MHC class II capable of triggering an effective anti-tumor immune response *in vivo* in a therapeutic setting comparable to a clinically relevant benchmark vaccine.

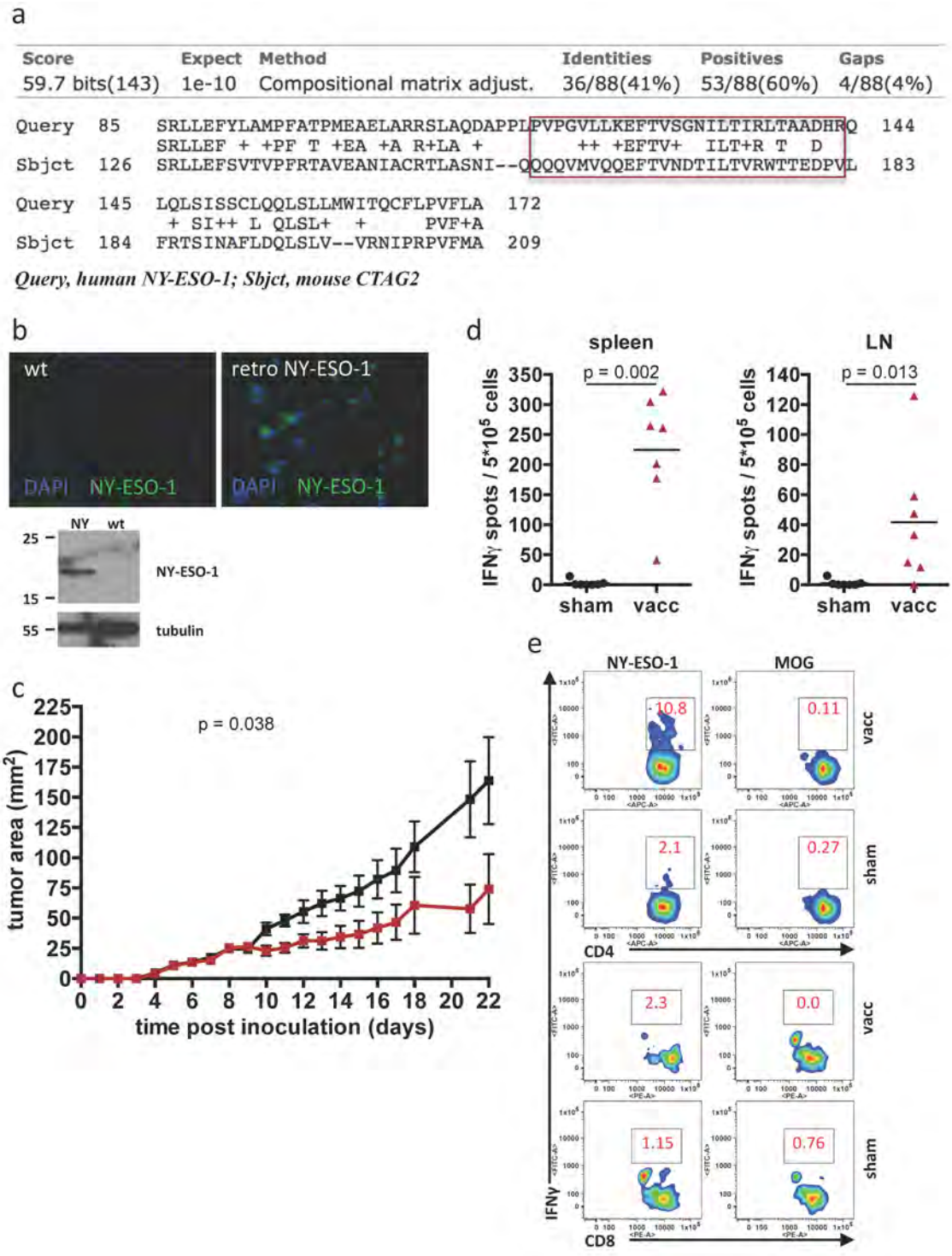

Fig. 3.17. NY-ESO-1 is a suitable antigen for HLA-DR1-dependent, CD4+ T cell-mediated therapeutic peptide vaccination in A2.DR1 mice. a, Protein alignment of hNY-ESO-1 with mCTAG2. HLA-DR1 epitope NY-ESO-1 p119-143 (red box) was blasted against murine proteome for maximal score, CTAG2 was identified, proteins were aligned. Sbjct, subject. **b**, NY-ESO-1 protein detection by IF and western blot in NY-ESO-1 (NY) and wt sarcoma cells. **c**, Growth of NY-ESO-1 tumors after vaccination with NY-ESO-1 p119-143 (vacc, red) or sham (black) (WRS test for median AUC). Error bars, mean ± SEM. **d** and **e**, Splenocytes (spleen, d and e) and LN cells (d) from NY-ESO-1 (p119-143)-vacc or sham mice were *ex vivo* stimulated with NY-ESO-1 (p119-143) and MOG and subjected to IFN-γ ELISpot (d, spot counts depicted after subtraction of MOG-induced spots in scatter plot showing values for each mouse and the mean) (WRS test) and flow cytometry gated on CD4+ T cells (upper panel) or CD8+ T cells (lower panel) (e). Representative plots are shown. Red numbers, populations in percent. *n* = 7.

3.4.4 IDH1R132H peptide vaccination-induced tumor growth suppression depends on IDH1R132H-specific CD4+ T cells and B cells

Although there is increasing evidence that antigen-specific cytotoxic CD4+ T cells are in principle capable and sufficient to exert antitumor immunity [151], the relevance of a CD4+ T cell-mediated antitumor immune response in the absence of an MHC class I-restricted CD8+ T cell response is still controversial. Consequently, the functional contribution of IDH1R132H-specific CD4+ T cells to control tumor growth was delineated. Analyses of splenocytic T cells recovered from IFN-γ secretion assays after immunization of A2.DR1 mice with IDH1R132H (p123-142) and Montanide®/imiquimod confirmed that antigen-specific T cells, responding to IDH1R132H (p123-142) with high IFN-γ production, were CD4+ but not CD8+ T cells (Fig. 3.18a). This finding was verified by the separation of CD4+ and CD8+ T cells from spleens of IDH1R132H (p123-142)-vaccinated A2.DR1 mice and stimulation with IDH1R132H (p123-142)-loaded autologous dendritic cells. CD4+, but not CD8+ T cells produced IFN-γ specifically in response to IDH1R132H (p123-142) (Fig. 3.18b).

Tumors from vaccinated mice were highly infiltrated by pan T cells compared to sham-treated mice (Fig. 3.18 c,d). In order to assess if these T cells included T helper cells specific for IDH1R132H, IDH1R132H (p123-142) HLA-DR1 tetramers were used to stain tumor-infiltrating lymphocytes (TILs), which allowed confirmation that IDH1R132H-expressing A2.DR1 sarcomas were indeed infiltrated by IDH1R132H HLA-DR1 tetramer-positive T helper cells only after vaccination with IDH1R132H (p123-142) (Fig. 3.18e).

This result proved the induction of – and infiltration of tumors with – IDH1R132H-specific T helper cells after vaccination, but not the requirement for this T cell population for tumor growth suppression in the therapeutic vaccination.

To address this question, CD4+ T cells and B cells were depleted from A2.DR1 mice using antibodies and therapeutic vaccination of pre-established syngeneic IDH1R132H-positive A2.DR1 sarcomas was performed (Fig. 3.19f). Depletion of CD4+ T cells abrogated the therapeutic effects of the IDH1R132H (p123-142) Montanide®/imiquimod vaccine, signifying that the therapeutic efficacy is dependent on CD4+ T cells (Fig. 3.19a,b). Interestingly, the vaccine-mediated control of tumor growth was also abrogated when CD19+ B cells were depleted (Fig. 3.19c,d), although T cell responses were strongly induced by vaccination (Fig. 3.19e), suggesting a major contribution of B cells to the therapeutic efficacy of the IDH1R132H vaccine.

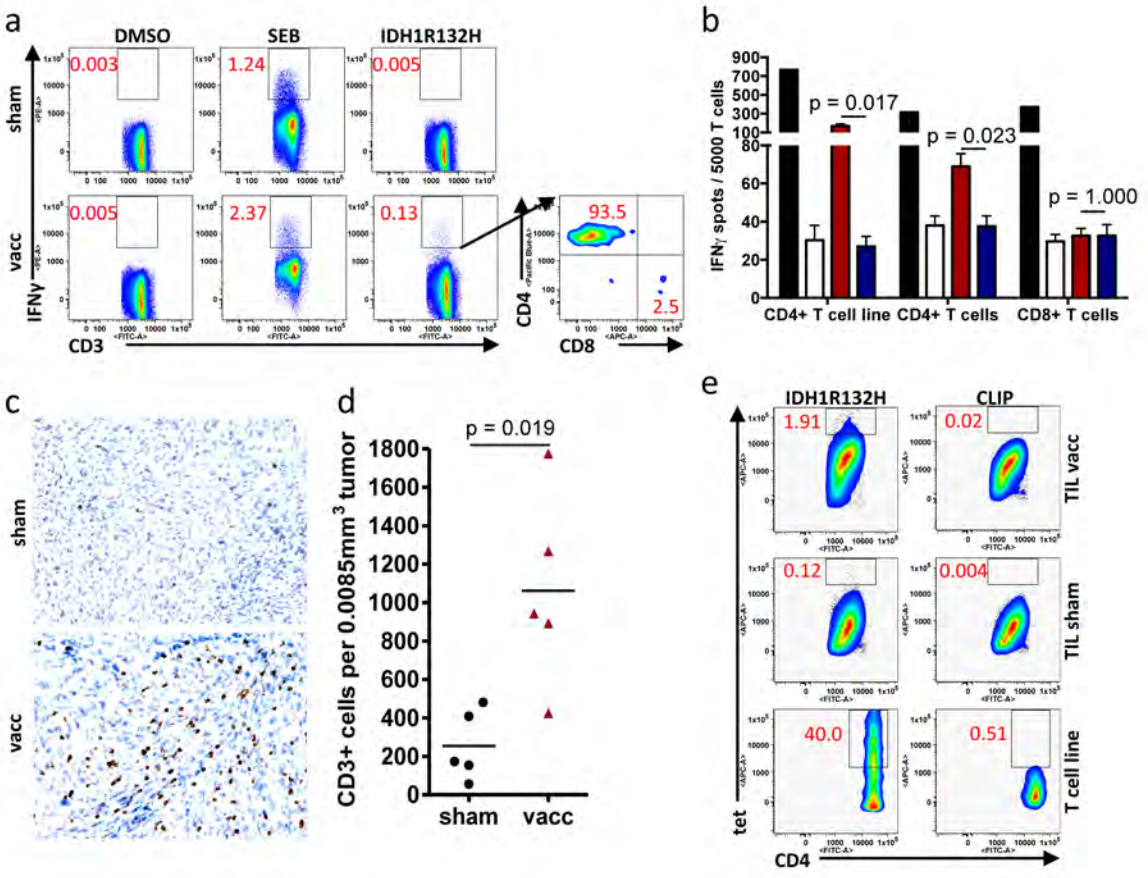

Fig. 3.18. Therapeutic IDH1R132H peptide vaccination induces specific T helper cells, but not cytotoxic T cells, which are recruited into the tumor. a, IFN-γ secretion assay followed by CD3, CD4, and CD8 surface staining and flow cytometry (DMSO, negative control; SEB, positive control; IDH1R132H, p123-142) of *ex vivo* stimulated splenocytes from 5 A2.DR1 mice immunized with p123-142 (R132H) (vacc, lower panel) or sham-treated (sham, upper panel). **b**, ELISpot analysis of mutation-specific IFN-γ response to IDH1 p123-142 of isolated CD4+ or CD8+ T cells from A2.DR1 mice vaccinated with IDH1R132H p123-142 using Montanide®/imiquimod or established T cell line, stimulated by autologous dendritic cells loaded with IDH1 p123-142 (R132H, red; wt, blue) or MOG (white), or with PMA and ionomycin (black) (Welch t test; *n* = 3). Error bars, mean + SEM. **c** and **d**, Immunohistochemistry for CD3 expression in tumors expressing IDH1R132H after therapeutic vaccination with IDH1R132H p123-142 (vacc, red) or sham treatment (sham, black) shown as representative images (c) and scatter plot showing individual values of CD3 expression for each tumor and the mean (d, Welch one-way ANOVA and pairwise Welch t tests; *n* = 5 per group). **e**, Flow cytometric analysis of IDH1R132H-specific CD4+ T cells in IDH1R132H+ tumors (tumor-infiltrating lymphocytes, TIL) after vaccination with IDH1R132H p123-142 (vacc) or sham treatment (sham) in comparison to IDH1R132H-specific T cell line stained with IDH1R132H (p123-142)- and control (CLIP)-tetramer. Data in c and d collected and analyzed by L. Bunse.

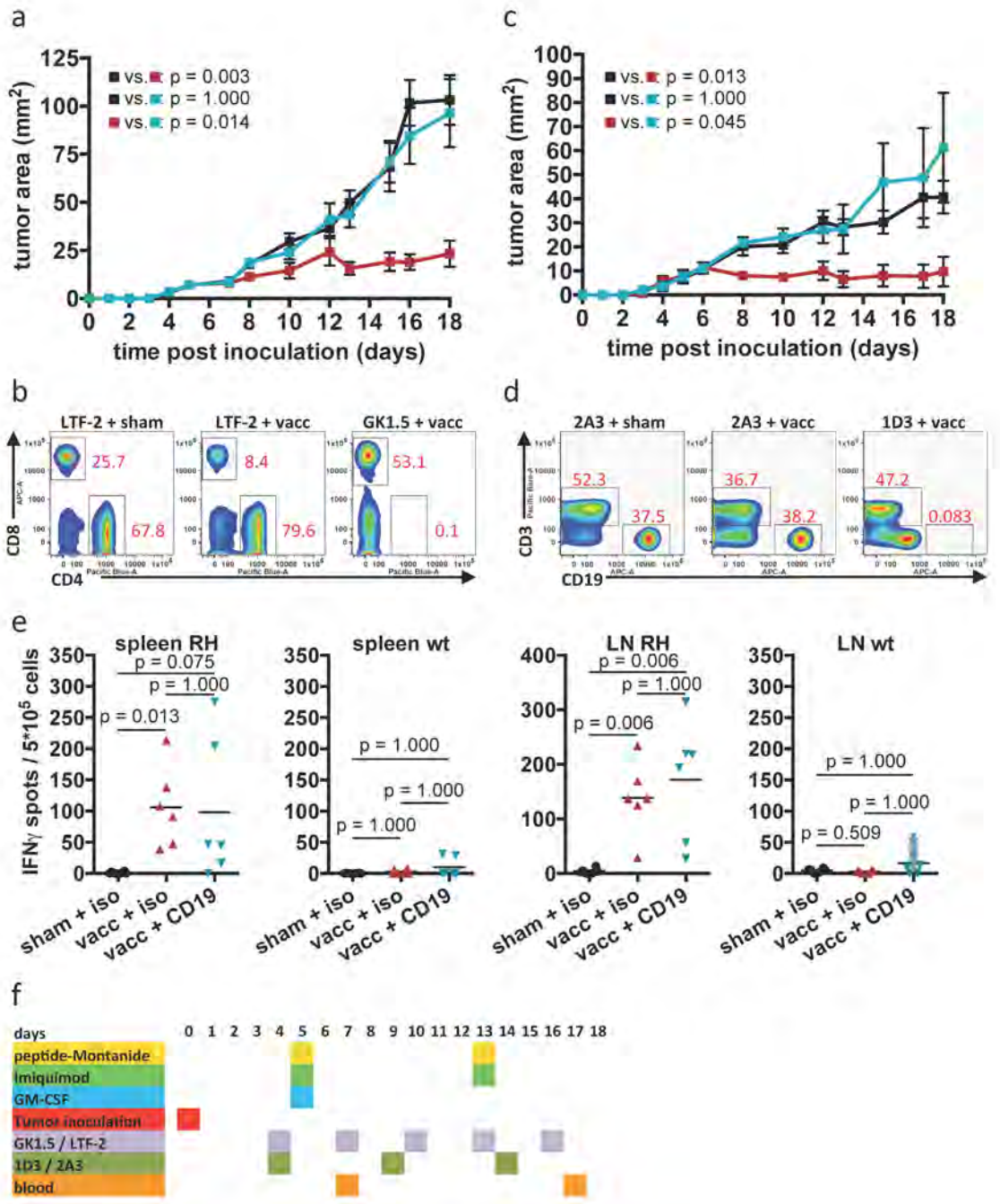

Fig. 3.19. IDH1R132H+ tumor growth suppression by therapeutic IDH1R132H peptide vaccination is dependent on T helper and B cells. a and **c**, Growth of IDH1R132H+ tumors in A2.DR1 mice depleted of CD4+ T cells (a) or CD19+ B cells (c) (blue) and vaccinated with IDH1R132H p123-142 in comparison to non-depleted, vaccinated (red) and sham-treated (black) mice (WRS test for median AUC with Bonferroni correction; *n* = 6 per group; *n* = 7, vacc without depletion). Error bars, mean ± SEM. **b** and **d**, CD4 / CD8 staining gated on CD3+ T cells (b) and CD3 / CD19 staining (d) of blood lymphocytes (b; GK1.5, anti-CD4; LTF-2, isotype control; d; 1D3, anti-CD19; 2A3, isotype control) from mice in a and c. Samples were taken from two mice per group on day 7 and day 17. Representative plots are shown for day 17. Red numbers, populations in percent. **e**, IFN- γ ELISpot of splenocytes (spleen) and LN cells from mice depleted of B cells and vacc (blue), control-treated and vacc (red) or sham-treated (black), after *ex vivo* stimulation with IDH1 p123-142 (R132H [RH] and wt). Spot counts are depicted after subtraction of background spots (MOG) (Welch one-way ANOVA and pairwise Welch t tests with Bonferroni correction; *n* = 6). Scatter plots showing values for each mouse and the mean. **f**, Schedule for tumor cell inoculation, lymphocyte depletion, and vaccination.

The inhibition of IDH1R132H-expressing tumor growth in MHC-humanized mice by antigen-specific peptide vaccination demonstrates the functional relevance and therapeutic efficiency of active immunotherapy targeting IDH1R132H as a novel antigen. The systemic cellular and humoral IDH1R132H-specific responses that are induced by vaccination are not only accompanied by an increased overall T cell infiltration, but also by the recruitment of IDH1R132H-specific T helper cells into the tumor. This observation and the loss of efficacy after depletion of CD4+ T cells suggests that antigen-specific T helper cells are responsible for combatting the tumor leading to growth reduction. However, the roles of cytotoxic T cells that might be locally but unspecifically activated by bystander effect after vaccination and of antibody responses – and other B cell functions – require further clarification.

To recapitulate the previous results obtained by peptide vaccination of MHC-humanized mice and patient screening, IDH1R132H represents a tumor-specific neoantigen recognized by CD4+ IFN-γ-producing T cells in patients with IDH1R132H-positive tumors and in vaccinated mice. An IDH1R132H vaccine induces both specific cellular and humoral immune responses that in addition are effective against IDH1R132H-mutated tumors in an MHC-humanized animal model. These data underline that mutant IDH1 may serve as a therapeutic target not only through drug-mediated inhibition of the neomorphic enzymatic function [108, 109] but also through T cell-based targeting of the mutant epitope.

3.5 The IDH1R132H-derived cancer metabolite 2-hydroxyglutarate does not influence T cells

IDH1 and IDH2 point mutations that have been described mainly in gliomas and acute myeloid leukemia (AML) uniformly occur in the catalytic pocket, impairing enzymatic function and leading to a neomorphic enzymatic function in terms of the conversion of the natural product α-ketoglutarate (α-KG) to the oncometabolite R-2-hydroxyglutarate (2-HG). The molecular consequences of this metabolic shift have been extensively studied. The accumulation of 2-HG has been shown to be sufficient to alter the epigenome of glial and hematopoietic cells [95, 96] resulting in a hypermethylation phenotype [97, 98], genetic instability, the subsequent acquisition of additional mutations and ultimately malignant transformation [100]. However, these analyses have mostly focused on autocrine effects on

tumor and tumor-initiating cells. One study on differentiation analyzed 2-HG effects with a model of adipocyte differentiation [95]. Until now, no evidence has been published on the paracrine effects of the accumulation of 2-HG in the tumor stroma on cells of the innate and adaptive immune system. Although AML studies on the effects of the IDH2 mutation R172K revealed changes in cells of the haematopoietic system, these studies focus on the respective tumor entity [96].

Nevertheless, the effects of the IDH mutation and 2-HG accumulation described for haematopoietic cells led to the assumption that 2-HG produced by IDH1R132H-positive glioma cells might have consequences for functionality or phenotype of infiltrating or peripheral T cells. This potential influence can be of particular importance when aiming at the application of an IDH1R132H-targeted vaccination for stimulation of directed T cell function.

3.5.1 Peripheral T cell proliferation is not altered by exogenous 2-hydroxyglutarate

First, 2-HG effects on human T cell proliferation were analyzed by mixed leukocyte reactions (MLRs), which reflect mainly CD8+ T cell proliferation. To this end, MLRs were performed on top of IDH1wt or 2-HG-producing, R132H-overexpressing human glioma cells (Fig. 3.20a,d) or in supernatant of these cells (Fig 3.20b), but T cell proliferation was not affected. To exclude other factors potentially overriding the 2-HG effects, MLRs were exogenously treated with 2-HG, but one-week treatment did not affect proliferation in this setting either (Fig. 3.20c).

3.5.2 Peripheral T cell activation is not altered by exogenously administered 2-hydroxyglutarate

To gain deeper insights into 2-HG effects on T cell functionality, isolated human CD8+ T cells were treated with 2-HG. Several surface T cell activation markers serve as indicators for T cell functionality, since they are differentially expressed after stimulation. Regulation of these activation markers by CD8+ T cells after TCR-mediated stimulation was not affected by treatment of T cells with 2-HG (Fig. 3.21a), indicating that 2-HG does not influence T cell activation. Extending these findings to IDH1R132H-responsive T cells, CD4+ T cell activation as defined by stimulation-mediated regulation of surface expression of activation markers was not altered by 2-HG treatment either (Fig. 3.21b).

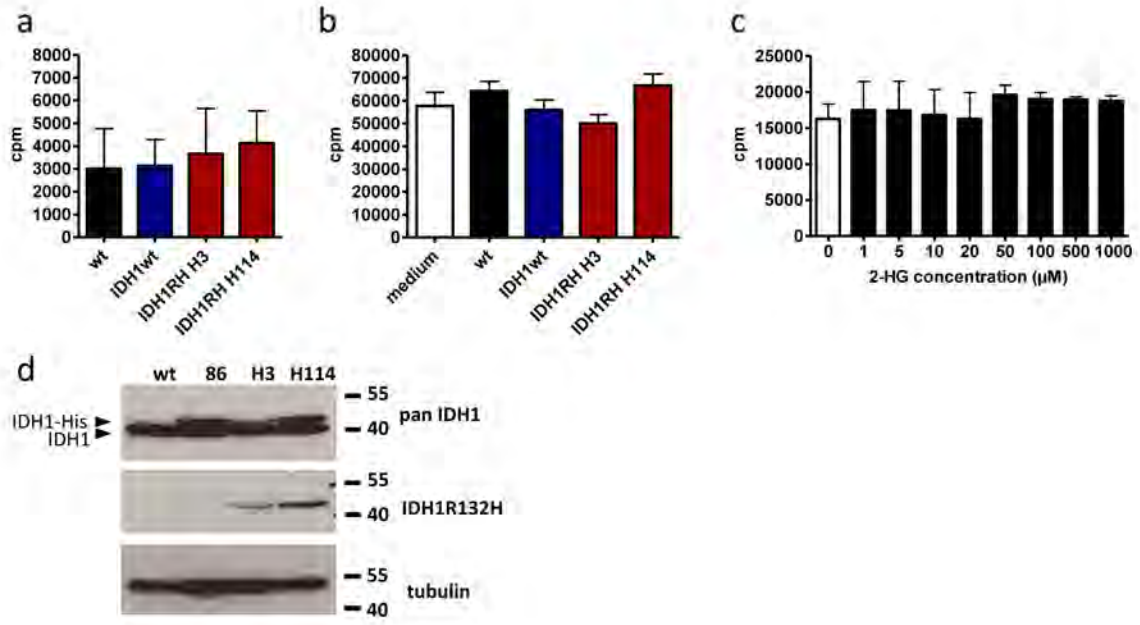

Fig. 3.20. Exogenous 2-hydroxyglutarate does not affect T cell proliferation in an MLR. a, Mixed leukocyte reactions were performed with PBMCs from two unrelated donors on LN229 glioma cells overexpressing IDH1. black, empty vector control; blue, IDH1wt; red, IDH1R13H, clone H3, and clone H114. **b**, Mixed leukocyte reactions were performed with PBMCs from two unrelated donors in supernatant of LN229 glioma cells overexpressing IDH1. White, medium; black, empty vector control; blue, IDH1wt; red, IDH1R13H, clone H3, and clone H114. **c,** Mixed leukocyte reactions were performed with PBMCs from two unrelated donors. Cells were stimulated with indicated concentrations of 2-HG. Proliferation was measured after 7 days by ^{3}H-thymidine incorporation. **d**, Western Blot of LN229 transfected with IDH1. LN229 clone H3 expresses half the amount of endogenous IDH1 protein, clone H114 expresses the same protein amount.

For an effective tumor immunotherapy by vaccination, the phenotype of the responding T cells is of particular importance, especially in the case of T helper cell responses, because CD4+ T helper cells are the most diverse and plastic cells in the haematopoietic system. For this reason, the phenotype of activated T cells must be taken into account when studying 2-HG effects on this cell population. Thus, in addition to surface activation markers, cytokine profiles as indicator for T cell phenotypes were analyzed to rule out that these are altered by 2-HG. Indeed, no 2-HG-mediated effect was detectable after 10-day treatment of CD8+ or CD4+ T cells. Activated T cells showed identical IFN-γ, IL-4, and IL17 production. Hence, neither the frequency of cytotoxic T cells (CTL) (Fig. 3.22a), nor Th1 (Fig. 3.22b), Th2, nor Th17 (Fig. 3.22c) was altered by 2-HG treatment. Moreover, no change in the frequency of inhibitory CD4+ T_{reg} was observed (Fig. 3.22d).

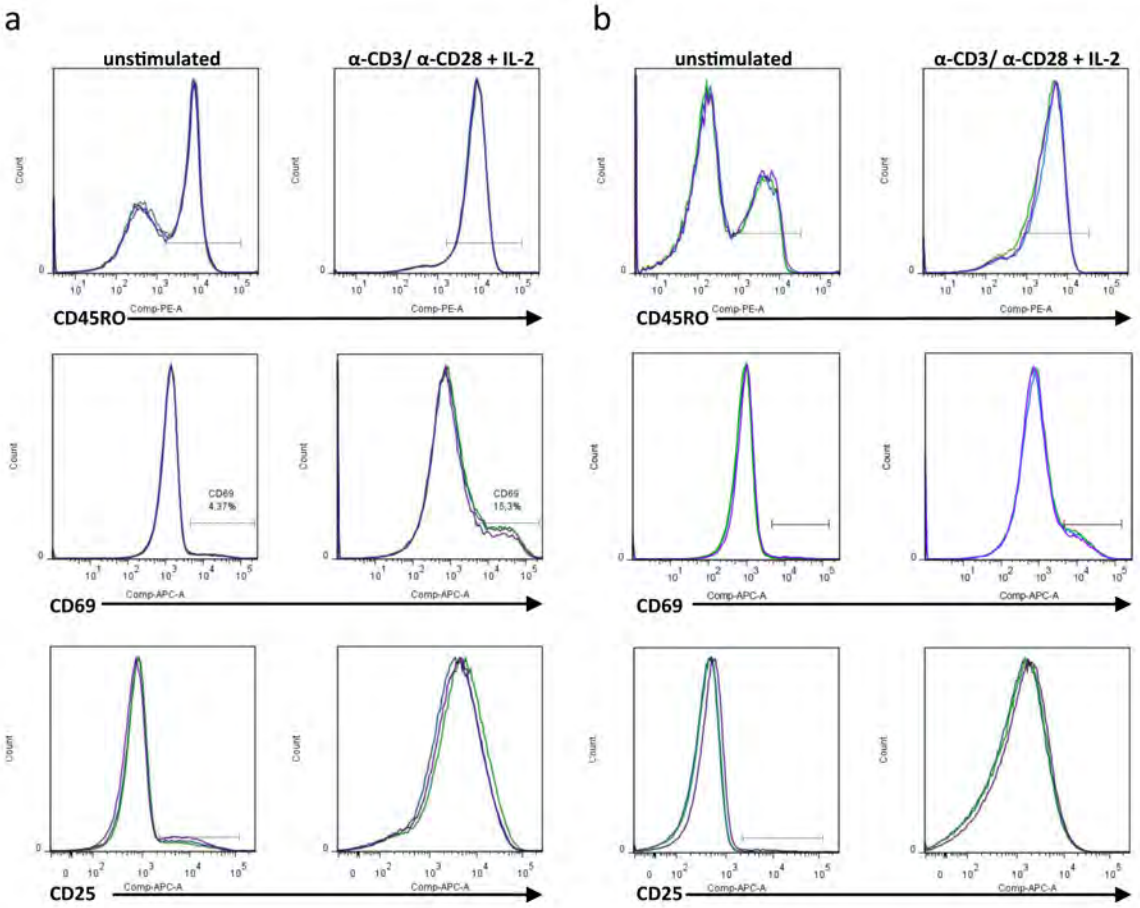

Fig. 3.21. Peripheral T cell activation is not altered by exogenously administered 2-hydroxyglutarate. a and **b**, Activation of CD8+ (a), or CD4+ (b) human T cells after 6 day-treatment with 2-HG and TCR-mediated stimulation with anti-CD3 and anti-CD28 antibodies and recombinant IL-2 was analyzed by flow cytometry. Blue, untreated; green, 50 µM 2-HG; purple, 100 µM 2-HG.

Page 69:

Fig. 3.22. Peripheral T cell phenotypes are not altered by exogenously administered 2-hydroxyglutarate. a, Human cytotoxic T cells (CTL) were analyzed by flow cytometry after 6 day-treatment of CD8+ T cells with 2-HG and TCR-mediated stimulation with anti-CD3 and anti-CD28 antibodies and recombinant IL-2 and TCR-independent stimulation with PMA and ionomycin. **b** and **c**, Cytokine analysis by flow cytometry of human CD4+ T cells after 6 day-treatment with 2-HG and TCR-mediated stimulation with anti-CD3 and anti-CD28 antibodies and recombinant IL-2 and TCR-independent stimulation with PMA and ionomycin. Th1 (b), Th2 and Th17 (c) phenotypes were analyzed. **d**, T_{reg} analysis after treatment of CD4+ T cells with 2-HG for 6 days.

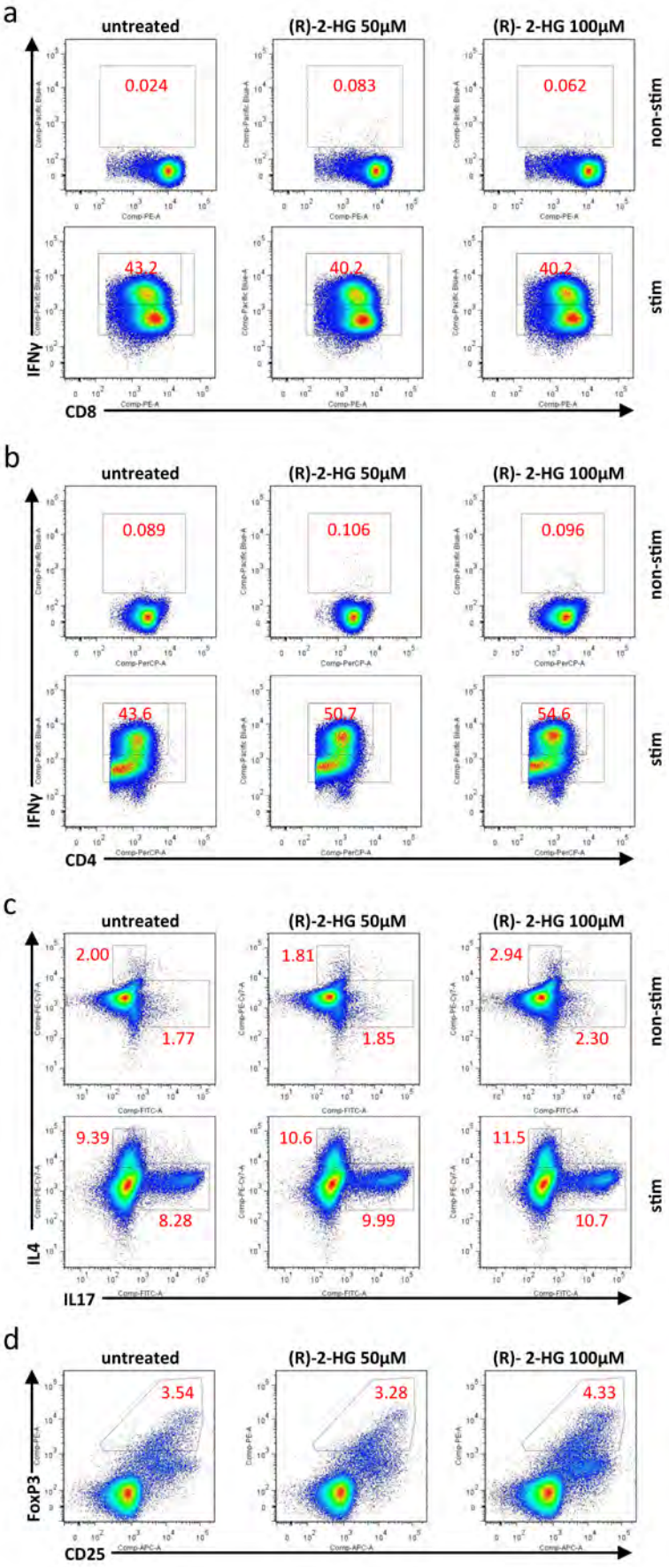

Fig. 3.22. Peripheral T cell phenotypes are not altered by exogenously administered 2-hydroxyglutarate. See page 68 for details.

Taken together, exogenously administered 2-HG does not seem to influence human peripheral T cell proliferation, activation, nor phenotype of activated T cells in this system. In this context, it is noteworthy that the metabolite 2-HG is not tumor cell permeable, which might be the reason why T cells in the periphery or within the tumor microenvironment are not directly affected by exogenous or tumor cell-derived 2-HG.

4 DISCUSSION

4.1 Targeting IDH1R132H as a novel immunotherapeutic approach for glioma

Despite 50 years of extensive research in the field of neurooncology and glioma therapy to improve standard of care and to prolong survival also for patients with low-grade and anaplastic gliomas, overall survival in these patients is still limited with a five-year survival rate of 45 to 60 % for grade II gliomas and only 25 % for anaplastic astrocytoma (grade III) [55, 60].

The standard of care for low-grade and anaplastic gliomas is defined as maximal tolerable resection followed by postoperative radiotherapy or alkylating chemotherapy [66, 104]. As opposed to glioblastoma, the beneficial effect of concomitant chemotherapy has not been demonstrated in controlled clinical trials. Only in anaplastic oligodendroglioma with a combined deletion of chromosomes 1p/19q, the combined therapy with procarbazine, lomustine, and vincristine (PCV) in addition to radiotherapy improves overall survival compared to radiotherapy alone [163, 164]. A major characteristic of low-grade and anaplastic gliomas is inevitable recurrence, and there is currently no standard treatment during remission or at recurrence. Participation in clinical trials using anti-angiogenic, anti-invasive, differentiating or immune-modulatory compounds are the best option for these patients [66].

Conceptually, patients with low-grade and anaplastic gliomas represent a patient population, which may particularly benefit from a tumor vaccine, as these tumors may remain stable or minimally growing for several years but will inevitably recur, often with a more malignant phenotype, and as there is currently no maintenance therapy available preventing recurrence in this relatively young and immunologically competent patient population [165]. As these tumors have a high prevalence of the IDH1R132H mutation, IDH1R132H represents an ideal target for active immunotherapy.

Active immunotherapy trials using autologous tumor lysates [137] and also targeting mutated antigens such as EGRRvIII [35] for glioma patients have been conducted. Mutated antigens are attractive and clinically relevant targets in gliomas and other types of tumors in general, because they have the advantage of being highly specific for the target cells as they

do not occur in healthy cells and hence, minimize autoimmunity. In fact, IDH1R132H-positive cells are used histopathologically to define tumor cells and identify distant brain manifestations of macroscopically circumscript tumors [107]. Specificity of a vaccination is not guaranteed by the exclusive expression of the target antigen alone, but requires specificity of reactive T cells. This is particularly important when targeting mutation antigens, because T cells must not react against the wt protein. In the case of EGFRvIII, T cell specificity, which is the specific binding of the TCR to a given epitope presented on MHC molecules, arises from the generation of a completely novel epitope. An in-frame deletion leads to a truncated extracellular domain with creation of an antigenic junction harboring a novel glycine residue [141]. The point mutation in IDH1 is more critical as only one amino acid is exchanged.

Although wt IDH1 epitopes bound to MHC class II with the same efficiency and stability as IDH1R132H epitopes *in vitro* (see 3.1.2, Fig. 3.3), T cells that were stimulated by specific peptide vaccination *in vivo* were significantly more responsive to mutated epitopes (e.g. Fig. 3.4). This specificity was also verified when mice were immunized with IDH1R132H or wt-expressing tumor cells (Fig. 3.15), indicating that non-mutated protein regions were recognized as self and subjected to central tolerance. As opposed to overexpressed antigens, where an efficient immune response might be limited due to central tolerance [166, 167], this is not a problem when targeting IDH1R132H, which is why strong immune responses could be observed. Although reactivity against IDH1wt epitopes could be detected in some mice (Fig. 3.4, 3.6), no tumor growth suppression of IDH1wt tumors was observed after IDH1R132H-specific vaccination (Fig. 3.15), strengthening the observation that IDH1R132H-primed T cells remain mutation-specific *in vivo*. With respect to reactivity against IDH1wt in non-transformed cells, cross-reactivity is a major concern due to the important metabolic function of IDH [108, 109]. No significant reduction of IDH1 and IDH2 enzymatic activity – neither in liver nor in brain – was observed in IDH1R132H-vaccinated mice (Fig. 3.16), nor could pathological evidence for toxic side effects be found (Table 3.1). Thus, T cells that are induced by IDH1R132H-targeted vaccination are specific for the mutation, as are spontaneously occurring IDH1R132H-specific T cells in the peripheral blood of glioma patients with IDH1R132H-positive tumors (Fig. 3.12).

This specificity against histidine-containing and not arginine-containing epitopes might be explained by structural properties of these amino acids [85], with an aromatic imidazole in

the histidine residue, which might be critical for TCR binding. Moreover, the neoepitope that is generated by the mutation seems to be unique as to no cross-reactivity to other epitopes occurs. The same consideration holds true for B cell receptor specificity and antibody responses, which are also observed after vaccination and spontaneously in patients with IDH1R132H-mutated tumors and which explicitly bind to IDH1R132H, but not wt IDH1 (Fig. 3.11, 3.13).

For many antigen-specific immunotherapies especially in glioma, which are in general characterized by intra-tumoral heterogeneity [168-171], immunological escape constitutes a conceptual pitfall, which arises when not all tumor cells carry the mutation [35]. Indeed, with the preclinical vaccination approach using tumors in which not 100 % of tumor cells expressed IDH1R132H (Fig. 3.14, 3.15), evidence of immunological escape was found, which is a robust sign of biological activity in an experimental setting where not all tumor cells are transduced with the therapeutic target (Fig. 3.15). However, fortunately, this does not reflect the clinical situation, in which all tumor cells are IDH1R132H mutated [105, 107, 172] and therefore immunological escape by outgrowth of target-negative tumor cells is unlikely to occur. In a therapeutic vaccination setting *in vivo*, IDH1R132H mutated tumors were even more efficiently controlled, most probably due to homogeneous target expression in all tumor cells (Fig. 3.14, 3.16). Therefore, the ubiquitous expression of IDH1R132H in glioma cells without respective heterogeneity within one tumor as it is observed for most other potential immunotherapeutic targets in glioma [35, 171] make IDH1R132H a very effective glioma-specific antigen.

The fact that a fraction of patients with IDH1R132H-mutated tumors harbor detectable amounts of IDH1R132H-specific T cells and antibodies in their peripheral blood (Fig. 3.12, 3.13) supports the observation that the immunogenic epitope is presented on MHC molecules to T cells, be it by tumor cells themselves or antigen-presenting cells which are found in the tumor stroma (see 4.3). This essential prerequisite for an effective immune response is also proven by MHC binding studies (Fig. 3.3) and whole tumor cell vaccination in mice (Fig. 3.15). Spontaneous immune responses to relevant tumor antigens have been observed, e.g. against NY-ESO-1 in melanoma patients [40, 41], and support the suitability of IDH1R132H as an immunologically targetable molecule.

In conclusion, the IDH1R132H mutation fulfills important requirements for an immunotherapeutically relevant target neoantigen: (i) It is tumor-specifically expressed and

hence autoimmunity is unlikely to occur. Indeed, no hints for autoimmune reactions or side effects could be observed in mice (Fig. 3.16, Table 3.1). (ii) It has a high uniformity and penetrance, being present in more than 70 % of grade II and grade III gliomas and in other tumor entities, but more importantly being uniformly expressed within one tumor, making immunological escape that can occur due to selection for IDH1R132H-negative cells by targeting IDH1R132H-expressing cells unlikely. In the mouse model, IDH1R132H-positive tumor cells were lost in a slow-growing tumor after vaccination only when not all implanted tumor cells expressed the antigen (Fig. 3.14, 3.15), but no immunological escape in the clinically relevant situation was observed (Fig. 3.16). A prerequisite for an effective T cell activation is (iii) the presentation of epitopes on MHC and (iv) stability of the MHC:peptide complex. IDH1 epitopes containing the mutation were processed and presented *in vivo* (Fig. 3.15) and bound to MHC class II *in vitro* with a stability that was comparable to a positive control (Fig. 3.3). (v) Presentation of the epitope leads to highly mutation-specific T cells (Fig. 3.4-9, 3.12) that are (vi) tumor-reactive and capable of controlling the growth of IDH1R132H-expressing but not IDH1wt tumors (Fig. 3.15, 3.16). (vii) Furthermore, vaccination and induction of IDH1R132H-specific T helper cells lead to production of antibodies specifically binding mutated IDH1 (Fig. 3.11, 3.13), which are in principle also able to exhibit anti-tumor activity [173, 174]. Beyond IDH1R132H being a suitable target for immunotherapy in itself, it is principally appropriate for a patient population among glioma patients that can particularly benefit from immunotherapy.

4.2 IDH1R132H – a versatile target?

The delineated data underline that mutant IDH1 may serve as a therapeutic target not only through drug-mediated inhibition of the neomorphic enzymatic function [108, 109], but also through T cell-based targeting of the mutant epitope.

Inhibition of mutant IDH1 and IDH2 using small molecules relies on its neomorphic enzymatic production of 2-HG, and inhibitors of enzymatic function with respect to 2-HG production have been developed [108, 109]. In erythroleukemia cells, where mutant IDH2R140Q led to growth factor-independency and de-differentiation towards hematopoietic stem cells, and in primary AML cells with endogenous IDH2R140Q, inhibition of mutant IDH2 resulted in restoration of differentiation capacity and induction of

maturation to monocytes and granulocytes shown by specific marker expression, which was accompanied by decreased blast numbers, respectively [109]. Likewise, inhibiting IDH1R132H in primary oligodendroglioma cells endogenously and heterozygously expressing IDH1R132H induced differentiation into astrocytic cells evidenced by RNA expression profiling and the increase in glial fibrillary acidic protein (GFAP)-expressing astrocytes and concomitant loss of Nestin, a neuroprogenitor marker, expression [108]. In the glioma model, re-differentiation was most probably due to a decrease in repressive histone methylation of respective promoters, as would be expected by inhibition of 2-HG production [97]; however, no decrease in DNA methylation was observed. The effectiveness of the inhibitor was evident *in vivo* through specific reduction of growth of established tumors in the flank of immunodeficient mice, which was due to reduced proliferation, but not apoptosis induction. Nevertheless, most strikingly, no alteration of histone methylation was achieved by low doses of the inhibitor, whereas the same tumor growth suppression was observed, suggesting non-transcriptional mechanisms of IDH1R132H independent of epigenetic effects [108]. These might be associated with the cardiovascular system, which is altered in IDH1R132H-expressing mouse brain *in vivo* [175].

Of note and in contrast to IDH1R132H-targeted immunotherapy, enzymatic inhibition of mutant IDH did not lead to loss of target gene expression nor apoptosis-mediated tumor reduction [108, 109]. Although apoptosis in IDH1R132H-expressing tumor cells after vaccination was not addressed within this thesis, it can be assumed that these cells were lysed by cytotoxic activity of T lymphocytes or other effector cells which might have been induced by vaccination and recruited into the tumor (see 4.3). In view of this background, it is interesting to speculate about the fate of still mutant IDH-expressing cells, which have been subjected to 2-HG-decreasing inhibition and underwent re-differentiation, when treatment with the inhibitor is discontinued. It is believed – and evidence has accumulated recently by analysis of multiple biopsies of same patients at recurrence [172] – that the IDH1 mutation in glioma [67] and other tumor entities [92, 100] is an early and maybe even a driving event in tumorigenesis [82, 84, 172]. Ohgaki and Kleihues speculate that the mutation of IDH1 or IDH2 in a common glial precursor cell is the first step towards low-grade glioma and precedes TP53 mutation or 1p/19q co-deletion as driving forces towards astrocytomas and oligodendrogliomas, respectively [67]. They further conjecture that the acquirement of an IDH mutation confers a growth advantage in early stages of development

and differentiation [67], which is in contrast to later stages and the better prognosis of IDH1R132H-mutated gliomas compared to IDH1wt gliomas, probably representing a distinctive tumor entity. However, *in vivo* studies indicate that the cell of glioma origin is not necessarily a neural stem cell or a common precursor cell, but might also be a committed glial cell, i.e. an astrocyte or oligodendrocyte [59]. For these reasons, it cannot be excluded that re-differentiated IDH1R132H-expressing glial cells that are no longer treated with the inhibitor might again malignantly transform to form a low-grade glioma. Although GFAP-specific heterozygous knock in of IDH1R132H in mice does not lead to glioma development in these mice, this is most probably due to the early death of these mice [175].

As opposed to inhibitor treatment, IDH1R132H-expressing cells are not expected to persist with targeted vaccination, but to be specifically lysed. Hence, malignant transformation of these cells should not occur. Moreover, immunotherapy has the advantage of immunological memory, defined by antigen-specific memory T cells remaining and readily being expanded and activated at antigen encounter, and therefore can exhibit long-term therapeutic beneficial effects maybe even at recurrence without continuous treatment throughout life even years after final boost vaccination [176-178]. In this context, administration might also be an advantage of immunotherapy, because it is not required daily, as the inhibitor might need to be administered [108]. For glioma treatment, the administration of an inhibitor might need to take other routes than the described oral application [108]. Vaccination therapy on the other hand might require adjuvant therapies to reduce immunosuppression and to enhance recruitment of effector cells to the tumor, or immune checkpoint blockade (see 4.5). These strategies might reduce the frequency of non-responders, who do not benefit from a vaccine.

In any case, the biological activity and effectiveness of mutant IDH inhibitors in terms of tumor growth suppression [108, 109] demonstrate the suitability of the IDH1 mutation as a therapeutic target, supporting the strategy of IDH1R132H-targeted immunotherapy.

4.3 Cellular and molecular mechanisms of IDH1-targeted anti-tumor immunity

T cell-mediated immunotherapies have mainly focused on CD8+ T cells due to their high cytolytic activity against target antigen-expressing tumors [179, 180]. However, it has also

been shown that the cytotoxic anti-tumor effect of CD8+ T cells depends on CD4+ T cells in their role of T helper cells, augmenting and supporting CD8+ T cell activity [181, 182] by providing growth factors and cytokines such as IL-2 for CD8+ T cells, enabling CD8+ memory T cells to acquire effector phenotype and function [183, 184]. Without CD4+ T cell help, CD8+ T cells might fail to elicit sufficient responses [185]. Even more, it has more recently been appreciated that CD4+ T cells can in addition directly mediate specific tumor cell killing and are suitable for use in adoptive T cell transfer for cancer immunotherapy [186-189].

It has been shown that tumor cells can endogenously process MHC class II-binding epitopes by autophagy and present them on their surface [190]. Although most tumors are MHC class II deficient, IFN-γ exposure can lead to upregulation of MHC class II also in gliomas [191, 192]. The human glioma cell line LN229 even ubiquitously expresses MHC class II *in vitro* and expression can be enhanced by IFN-β, as has been found in the course of this work. The mechanisms of CD4+ T cell-mediated immune responses and tumor eradication in the context of specific tumor-associated antigens (TAA; NY-ESO-1, TYRP1) have been extensively studied using adoptive transfer (AT) of antigen-specific CD4+ T cells in preclinical models of melanoma [149, 151] and demonstrated in melanoma patients [30]. Using CD4+ TRYP1 TCR-transgenic mice as a source for CD4+ T cells for AT, Quezada and co-workers [151] showed that these T cells were sufficient to completely eliminate exclusively antigen-expressing melanoma and revealed a dependency on IFN-γ production by these cells when combined with CTLA-4 blockade and radiotherapy (RT). As evidenced by depletion experiments and knock out (KO) mice, this effect was independent of host T cells, B cells, or natural killer (NK) cells, and TNF-α secretion. The authors propose a model in which RT-induced lymphopenia allows *in vivo* differentiation and expansion of transferred CD4+ T cells and due to reduced T_{reg} functions by CTLA-4 blockade, these CD4+ T cells are able to produce sufficient amounts of IFN-γ, which in turn together with RT leads to enhanced MHC-class II expression on the tumor, making it susceptible to CD4+ T cell-mediated killing [151]. Comparable anti-tumor effects were achieved when substituting CTLA-4 blockade with engagement of OX40, a co-stimulatory molecule expressed on activated CD4+ T cells [149].

Based on and in line with these findings, it is reasonable to speculate that with IDH1R132H-specific vaccination using the HLA-DR1-binding p123-142 epitope, induced IFN-γ-secreting CD4+ T cells specific for IDH1R132H are capable of and sufficient in directly killing and controlling established IDH1R132H-mutated tumors in MHC-humanized mice. This is

supported by the notion that IDH1R132H-specific CD8+ T cells cannot be induced by vaccination (Fig. 3.18).

However, the classical mechanism of an MHC class II-restricted CD4+ T cell-mediated anti-tumor immune response is the release of antigen – in this case IDH1R132H epitopes – by apoptotic tumor cells, which is phagocytosed, processed in phagosomes, and presented on MHC class II by professional antigen-presenting cells (APC) that are recruited into the tumor. Antigen encounter and recognition of APC by T helper cells stimulates cytokine secretion by T helper cells, which in turn activate APC and induce an inflammatory tumor microenvironment, providing co-stimulation for innate and adaptive immune cells [150]. This recruits additional CD4+ and CD8+ T cells as well as NK or NKT cells, which infiltrate into the tumor, results in the upregulation of MHC class I expression by tumor cells and enhances tumor immunogenicity. These mechanisms are essential in tumors deficient in MHC class II, but which are recognized and eliminated by CD4+ T cells via indirect recognition of TAA on APC which recruit innate and adaptive immune cells [188], e.g. macrophages which are stimulated to secrete IFN-γ [186, 193], or activated NK cells [189]. Of note, Th1-polarized CD4+ T cells are probably the most effective T helper cells because of their IFN-γ secretion; however, Th17 cells might play an important role via the recruitment of innate immune cells [150, 194]. The consideration that this classical mechanism applies for the effect of IDH1R132H vaccination is reinforced by the fact that the sarcoma cells used in the therapeutic model do not express MHC class II *per se* nor after IFN-γ stimulation *in vitro* (Fig. 3.14), speaking against direct recognition and killing of tumor cells by CD4+ T cells. Whether MHC II expression in the tumor that was observed *in vivo* can be assigned to the sarcoma cells or infiltrating cells in the tumor microenvironment needs to be elucidated. Another point is the finding of antigen loss in previously IDH1R132H-expressing tumors after vaccination (Fig. 3.15), because immunologic escape is rather unlikely to be induced by exclusively CD4+ T cell-mediated immunity but has been described for CD8+ T cell responses [195].

With this rationale, it can be expected that tumor-infiltrating T cells (Fig. 3.18) in addition to IDH1R132H-specific CD4+ T cells contain CD8+ T cells, and NK or NKT cells, which might as well exhibit anti-tumor activity by antigen-spreading, which is the immune response to other TAA apart from IDH1R132H p123-142, in this case, arising from antigen release by apoptotic tumor cells and encounter of these antigens by T cells of appropriate specificity, so-called

cross-presentation and cross-priming [196]. Antigen spreading has been observed in CD4+ T cell AT for melanoma expressing several relevant TAA [30]. Antigens that are recognized by locally activated CD8+ T cells in the therapeutic vaccination model using IDH1R132H p123-142 might include other IDH1R132H epitopes or other antigens expressed by the tumor cells. APC, which might present the IDH1R132H epitope on MHC II to specific CD4+ T cells in the tumor, instead of tumor cells themselves, can include infiltrating macrophages or DC, but also B cells, which can infiltrate into and represent a considerable amount within the tumor [197]. Of note, B cells are capable to enrich small amounts of antigen and present on MHC class II [198]. This B cell function might play a role in IDH1R132H-specific anti-tumor immunity, because anti-tumor effectiveness was lost when CD19+ B cells were depleted in vaccinated mice (Fig. 3.19) and this effect was probably not completely dependent on IDH1R132H-specific antibody production evidenced by the fact that not all vaccinated and responding mice developed specific antibodies. Yet, clinical responses correlated with IDH1R132H-binding antibodies in vaccinated mice (data not shown), supporting the notion that antibody production is another B cell function that contributes to B cell-dependent anti-tumor immunity. Nevertheless, it might also be possible that MHC class II expression on tumor cells is upregulated by IFN-γ-secreting IDH1R132H-specific CD4+ T cells that infiltrate into the tumor (Fig. 3.18) as observed in the experimental AT of antigen-specific CD4+ T cells for melanoma [151]. The finding of HLA-DR expression in tumors from vaccinated mice supports all these hypotheses.

Further clarification will be achieved by analyzing tumor-infiltrating lymphocytes in more detail by staining for specific markers such as CD8, CD19, and NK-1.1 for cytotoxic T cells, B cells, and NK cells, respectively, and co-stainings with HLA-DR to delineate if tumor cells or recruited TILs present IDH1R132H epitopes to specific CD4+ T cells inside the tumor. Insights into the contribution of the different lymphocytic subpopulations to therapeutic efficacy can be gained by depletion of these cells *in vivo*. Interestingly, depletion of CD8+ T cells in the therapeutic setting dramatically diminished the vaccination effect similar to CD4+ T cell depletion (data not shown). Finally, IDH1R132H-specific CD4+ T cells – which are available – can be adoptively transferred into lymphopenic or immunodeficient mice to reveal if CD4+ T cells alone are sufficient for the anti-tumor response. This approach could be facilitated by cloning of the IDH1R132H-binding TCR and the generation of a CD4+ TCR-transgenic mouse as a source for IDH1R132H-specific CD4+ T cells.

The mechanism behind the observed vaccination-induced loss of antigen expression (Fig. 3.15) also remains unclear. As stated above, it is usually not induced by sole CD4+ T cell-mediated responses. Related to the considerations outlined above, the effects responsible for this phenomenon might be locally activated IDH1R132H-specific or bystander CD8+ T cells, or IFN-γ secretion by CD4+ T cells in the tumor, which lead to antigen loss [199, 200]. However, no reduced IDH1R132H expression within the tumor was observed in vaccinated mice compared to sham treated mice when a completely homogenous tumor with respect to IDH1R132H expression was implanted and established tumors were therapeutically treated (data not shown). This points towards a limited vaccination-driven loss of antigen expression in that the clonal tumor cells are limited in proliferation but are not able to escape the immune system by antigen loss *in vivo* after vaccination. Rather, it is likely that in the preventive vaccination with heterogeneous tumor cells, IDH1R132H-positive tumor cells were eliminated, be it due to CD4+ or CD8+ T cell activity, and IDH1R132H-negative tumor cells grew out in response to selective pressure by vaccination in addition to their growth advantage *per se* (Fig. 3.14). This scenario would be in contrast to downregulation and gene silencing of IDH1R132H in previously IDH1R132H-expressing cells, but in line with observations made in clinical studies targeting the tumor antigen EGFRvIII by peptide vaccination in glioma patients [35]. Here, the primary tumor was heterogeneous for EGFRvIII expression and vaccination led to loss of antigen expression in recurrent tumors. Although this can be interpreted as a sign of biological activity, this would be unwanted in the clinical situation. As this is after IDH1R132H vaccination only observed with a heterogeneous tumor, it is unlikely to occur in glioma patients with IDH1R132H-mutated tumors, where all cells express the antigen [105, 107, 172].

Conceptually, CD4+ T cells might indeed be more efficient in anti-tumor activity than CD8+ CTL [150, 189]. Since CD8+ T cells recognize endogenous antigens presented on MHC class I, expressed by normal and tumor cells, CD8+ T cell-mediated TAA-specific immune responses rely on the MHC class I expression and antigen presentation on tumor cells. But because of genomic instability, tumor cells are mostly defective in antigen presentation due to loss of molecules required for antigen processing and presentation, such as β2-microglobulin, TAP or MHC I chains [15, 201]. Conversely, CD4+ T cell functions are independent of autophagy-mediated antigen presentation on tumor cells. Instead, CD4+ T cells recognize antigens

commonly presented on APC. Moreover, CD4+ T cells exhibit versatile effector functions and represent a plastic cell population capable to “evolve, adapt, and self-regulate” [150].

4.4 IDH1R132H-derived 2-HG and the immune system

The IDH mutations are unique tumor-specific mutations inasmuch as they produce 2-HG, which in turn reduces histone and DNA methylation, thereby altering the entire epigenome of the tumor. The mode of autocrine action of 2-HG has been a matter of extensive research and is now largely understood [92]. 2-HG is a competitive antagonist of the natural IDH product α-KG, because it binds to α-KG-dependent dioxygenases. Among these are histone- and DNA-demethylating enzymes, which are inhibited by 2-HG [97]. The broad and constant autocrine effects of endogenous 2-HG on all solid tumors expressing mutant IDH [73, 95, 99], but also cells of the hematopoietic system in the context of leukemia [97] as well as the possibility to mimic these effects by applying exogenous 2-HG to cells not expressing the IDH mutation [95], gave rise to the hypothesis that T cells – and possibly other lymphocytes and innate immune cells – might as well be altered in function by exposure to 2-HG. Particularly, T cell functions are important in the context of T cell-mediated IDH1R132H-targeted immunotherapy.

Treatment of human peripheral blood mononuclear cells (PBMC) did not reveal any 2-HG effects on T cell proliferation, activation, nor differentiation into effector phenotypes (see 3.6, Fig. 3.20-22). Many explanations why 2-HG did not affect T cells in this experimental model are possible.

One reason might be the 2-HG concentrations used, which with 100 µM lie below the concentrations of up to 30 mM now found in IDH1R132H+ tumor tissue [92, 147]. Another reason could be the exposure time, which is not long enough to induce 2-HG-mediated changes. In tumor cells, all 2-HG-mediated alterations are induced via methylation-induced epigenetic rearrangements, which generally require time to lock in, hence occur over extended periods of time [98, 202, 203]. In fact, epigenetic changes and establishment of the hypermethylation phenotype via introduction of IDH1R132H are detectable only after prolonged culture periods and numerous passages *in vitro*, not only in primary astrocytes, but also in fibroblasts differentiating into adipocytes [95, 98]. Thus, the time factor seems to be independent of cell type. Reasoning that any 2-HG-mediated influence on T cells should

be mediated via epigenetic changes, the treatment over 10 days is most likely not sufficient for this analysis. Longer exposure times in primary T cells are difficult to achieve due to limited survival of these cells *in vitro*. Thus, it might be feasible to use T cell lines, e.g. human immortalized Jurkat T cells [204], or antigen-specific murine T cells such as CD8+ gp100-specific T cells from pmel mice [205], CD4+ ovalbumin (OVA)-specific T cells from OT-II mice [206], or CD4+ IDH1R132H-specific T cells described here (see 3.2.3). These cells have the advantage of not only prolonged culture, but also of the possibility to study effects on antigen-specific activation. Yet, the question remains if 2-HG is able to enter T cells or other cell types and thus to exhibit paracrine effects. It has been assumed that 2-HG is in general not cell-permeable, which is the reason why cell-permeable derivatives of the metabolite have been developed and used to study if mutant IDH exerts its effects via 2-HG production in an autocrine manner [100]. Nevertheless, cell-permeable 2-HG did not have any detectable impact for T cell functions in preliminary experiments (data not shown).

Still, due to the non-permeability of 2-HG, another possibility that appears more likely than direct effects is that 2-HG affects T cells indirectly via epigenetic changes in and therefore altered expression profile of tumor cells. Since IDH-mutated cells secrete 2-HG [147], it is reasonable to hypothesize that 2-HG might alter the tumor microenvironment. *In vivo* studies using a unique heterozygous conditional IDH1R132H knock in (KI) mouse model [96, 175] show that expression of IDH1R132H specifically in nestin+ neural stem cells or GFAP-expressing astrocytes induces brain hemorrhage and alters collagen maturation, leading to perturbed basement membrane (BM) formation [175]. These effects are attributed to 2-HG-mediated competitive inhibition of the prolyl hydroxylase domain-containing proteins (PHD) and collagen prolyl-hydroxylases, which both belong to α-KG-dependent prolyl hydroxylases. PHD mark hypoxia-inducible factors 1/2 α (HIF1/2α) for ubiquitination and subsequent proteasomal degradation [207]; thus, PHD inhibition leads to HIF1/2α protein stabilization and target gene expression. One important target gene in the context of glioma and other solid tumors that was upregulated in nestin-IDH1R132H KI mouse embryos is vascular endothelial growth factor (VEGF), which is an important growth factor regulating vasculogenesis and angiogenesis during development [208] and which is upregulated in glioma [209-211]. Consequently, the IDH1R132H-driven enhancement of VEGF levels does not only contribute to embryonic hemorrhage in this mouse model [175], but bears considerable implications for glioma pathology. In this regard, it might be noteworthy that

preliminary results obtained during this thesis showed that 2-HG increased the angiogenic potential of human umbilical vein endothelial cells (HUVEC) in a sprouting assay *in vitro*. Impaired collagen maturation in nestin-IDH1R132H KI mice appeared to be caused by diminished hydroxylation of collagen IV, which is a central BM component and which mediates interactions between astrocytes and endothelial cells [212]. Thus, collagen IV disruption led to BM breakdown in these mice [175]. Strikingly, in relation to IDH1R132H and 2-HG-mediated effects on the immune system, some viable GFAP-IDH1R132H KI mice demonstrated splenomegaly and an elevated white blood cell count as well as inflammatory symptoms. Although the authors report on leaky gene expression in other tissues [175], it is tempting to speculate that astrocytic IDH1R132H expression might affect the immune system *in vivo*.

Despite these findings and observed changes that are connected to tumorigenesis, GFAP-IDH1R132H KI mice did not develop brain tumors, most probably due to reduced life span [175]. While reduced hydroxymethylation, which precedes hypermethylation, was detectable, no changes in histone methylation were observed, leading to the hypothesis that epigenetic modifications are the key factor required for malignant transformation and tumorigenesis [175] and therefore also for microenvironmental alterations. Indeed, hypermethylation-mediated alterations within tumor cells that might presumably affect the microenvironment have been described in human astrocytes and primary low-grade gliomas *in vitro* [98]. These are transcriptional programs related to several cellular pathways, including TGF-β signaling, PDGF and EGFR signaling, wnt signaling, and angiogenesis, to name just a few. Given the versatile roles and paracrine impact of these pathways on cells in the tumor stroma, e.g. the suppression of T cell proliferation and NK cell activity and induction of T cell apoptosis by TGF-β [111], the connection between IDH1R132H-derived 2-HG, hypermethylation, and tumor-infiltrating lymphocytes or resident microglia is certainly worth investigating. In fact, IDH1R132H-mutated anaplastic astrocytomas (A°III) are less infiltrated by T cells than IDH1wt A°III (TCGA data analysis).

To verify this finding in an *in vivo* model, to examine the underlying mechanisms of this correlation, and to identify the compartments of the immune system involved, will be main aims of prospective studies.

4.5 Translating the IDH1R132H vaccine to the clinic – implications and considerations

Among gliomas, GBM are the most aggressive tumors with dramatically decreased survival times (14-17 months) compared to low-grade and anaplastic gliomas [63, 64]. Consequently, most clinical studies that have been conducted in the last years have focused on GBM patients. Yet, although patients with low-grade and anaplastic gliomas have a median overall survival of 7-10 or 2-5 years, respectively, these patients inevitably suffer from recurrence and ultimately malignant progression and eventually die of the disease [60-62]. Therefore, novel therapeutic strategies are required not only for GBM patients, but also for low-grade glioma patients in order to prevent progression. For many of these patients, no appropriate follow-up therapy is available after resection, while grade III glioma patients often receive radiotherapy or chemotherapy [66]. Since this patient group is generally immunocompetent, immunotherapy is a promising option for these patients. Peptide vaccinations for glioma patients using cocktails of several epitopes from glioma-associated antigens have been developed and are under investigation in clinical trials. An example for HLA-A*02 positive GBM patients are the IMA950 trials, which are phase 1/2 studies using 11 different specific peptides [134].

An IDH1R132H-targeting vaccine has the advantage of a single epitope being homogenously expressed throughout the tumor. Moreover, IDH1R132H as a target is not prone to be lost, but expression persists in recurrent tumors [172], making IDH1R132H-targeted immunotherapy an option even at recurrence. The finding that GBM of mesenchymal subtype are more susceptible to DC vaccine using autologous tumor lysates than proneural – hence mostly IDH1R132H positive – tumors [137] seems to be counteracting the suitability of IDH1R132H vaccination, but has not been verified in low-grade and anaplastic glioma.

Although the efficacy of the IDH1R132H-specific vaccine was shown in a mouse sarcoma model instead of an intracranial tumor model, the finding of spontaneous peripheral cellular and humoral immune responses in patients (see 3.3) supports the reasoning that such a vaccine can be effective in glioma patients. It has been shown for NY-ESO-1 that spontaneously occurring antigen-specific IgG increase the probability that T cell responses, including CTL and Th responses, can be generated *ex vivo* [40, 213], thus maybe also by vaccination, although antigen-binding IgG levels are not necessarily enhanced after vaccination [30]. A total of seven patients of the screened 45 patients (16 %) with

IDH1R132H-mutated gliomas exhibited detectable peripheral specific immunity, of which only one patient had both specific T cells and antibodies at the time analyzed. This discrepancy and difference to the correlation of T cell and antibody responses against NY-ESO-1 in melanoma [40] most likely arises from T helper cell and antibody biology and the therapeutic status of the patient at the time of blood withdrawal. B cells are commonly stimulated by Th2-derived IL-4 to differentiate into plasma cells to secrete IgG, particularly IgG1 and later class switch to IgE, whereas IFN-γ-producing Th1 cells can inhibit IgG production; alternatively, IFN-γ is able to induce class switching to IgG2a [214, 215]. Therefore, Th1 responses, which were screened for by detecting IFN-γ production, usually do not correlate with IgG1, which were detected. Worth mentioning in this regard is that Th2 responses were not detected, because L-4 was not analyzed; however, Th2 responses can reduce Th1 activity [216]. In addition to these considerations, T cell responses and antibodies have distinct kinetics in that IgG are more stable than T cell activities, the latter being prone to influences of therapy. T cell numbers and activities can decline dramatically when chemotherapy is applied. Since time of blood taking was not controlled with respect to current therapy, these were unknown factors influencing detectable T cell responses. Of note, when previously positive patients were repeatedly tested, at some time points, their T cell responses fell under the detection level for positivity. Apart from therapy, the screened patient cohort (see Appendix, Table 6.1) was heterogeneous with respect to numerous prognostic factors such as tumor grade and age, but also molecular markers, e.g. MGMT status (L. Bunse, data not shown), not allowing for a correlation between immune response and potentially favorable prognosis. Advantageously, a spontaneous immune response to IDH1R132H was not associated with a distinct class II HLA-DR type in patients (L. Bunse, data not shown), nor in vaccinated mice (see 3.2.4, Fig. 3.9), making a vaccination therapy applicable for IDH1R132H-positive patients irrespective of their HLA-type. This is in contrast to other peptide vaccination trials such as IMA950 [134].

In addition to the fact that gliomas are largely immunosuppressive tumors recruiting suppressive immune cells such as MDSC and T_{reg} into their microenvironment, the entire peripheral immune system is characterized by suppression, in part due to radio- and chemotherapy, including anergic and dysfunctional T cells, impaired co-stimulation and TCR signaling, diminished IgG synthesis by B cells and general lymphopenia [217]. Yet, at least lymphopenia is in fact favorable during immunotherapy, because it allows the expansion of

relevant clones [218], and for immunotherapeutic AT of tumor antigen-specific T cells, leukapheresis or other means of lymphodepletion, such as total body irradiation, are commonly applied as pre-treatments [29, 219, 220].

Several strategies are possible to increase the potential of immunotherapies during combination therapy together with standard therapy in glioma patients. Radiotherapy in itself can be beneficial for tumor antigen-directed immune responses, because it not only induces lymphodepletion and hence depletes immunosuppressive immune cells [29], but also increases MHC expression on glioma cells, thereby facilitating recognition by T cells [151]. Immunomodulatory agents such as checkpoint blockers can be applied as adjuvant therapy to overcome immunosuppression. For instance, CTLA-4 blockade using the antibody ipilimumab has proven extremely efficient for patients with melanoma [25, 26] and shown encouraging results in other cancers such as lung and prostate cancer [221, 222]. Similarly, PD1-blocking antibodies lambrolizumab and nivolumab prolong survival in melanoma patients [28, 223] and are under investigation for treatment of lung cancer [224]. Since glioma cells express elevated levels of PD1L [114, 225], which might correlate with progression [226], PD1 blockade might be a rational option for concomitant treatment. Also, CTLA-4 blockade proved to be efficient in a mouse model for glioma [227], and a clinical trial is currently under way comparing nivolumab and ipilimumab for glioma patient treatment. Inhibition of TGF-βR-I is also under clinical investigation to target TGF-β signaling in glioma, and could potentially be combined with vaccination-based immunotherapy.

The present study not only provides evidence for functional immunogenicity of IDH1R132H in tumor-bearing mice and spontaneously occurring immune responses in glioma patients, but also the tools needed for monitoring immune responses during a possible clinical vaccine trial. IFN-γ ELISpot and peptide IgG ELISA were established to monitor T cell responses and serum IgG levels, respectively. The development of the IDH1R132H-peptide ELISA is of particular importance for screening for specific IgG in multiple serum samples at a time, allowing direct comparison between pre-treatment, during treatment, and post-treatment samples of one patient. In addition, monitoring will involve general immunophenotyping, including number, activation state, and phenotype of lymphocytes and other immune cells.

With these conclusions and techniques, a clinical vaccine trial in IDH1R132H-positive glioma is currently being prepared to give answers on the therapeutic benefit of IDH1R132H-directed immunotherapy.

5 REFERENCES

1. Hajdu, S.I., *A note from history: landmarks in history of cancer, part 1.* Cancer, 2011. **117**(5): p. 1097-102.
2. Coley, W.B., *II. Injury as a Causative Factor in Cancer (Continued).* Ann Surg, 1911. **53**(5): p. 615-50.
3. Coley, W.B., *I. Injury as a Causative Factor in Cancer.* Ann Surg, 1911. **53**(4): p. 449-88.
4. Bugelski, P.J., et al., *Critical review of preclinical approaches to evaluate the potential of immunosuppressive drugs to influence human neoplasia.* Int J Toxicol, 2010. **29**(5): p. 435-66.
5. Vial, T. and J. Descotes, *Immunosuppressive drugs and cancer.* Toxicology, 2003. **185**(3): p. 229-40.
6. Dieci, M.V., et al., *Prognostic value of tumor-infiltrating lymphocytes on residual disease after primary chemotherapy for triple-negative breast cancer: a retrospective multicenter study.* Ann Oncol, 2014.
7. Dunn, G.P., I.F. Dunn, and W.T. Curry, *Focus on TILs: Prognostic significance of tumor infiltrating lymphocytes in human glioma.* Cancer Immun, 2007. **7**: p. 12.
8. Jochems, C. and J. Schlom, *Tumor-infiltrating immune cells and prognosis: the potential link between conventional cancer therapy and immunity.* Exp Biol Med (Maywood), 2011. **236**(5): p. 567-79.
9. Nosho, K., et al., *Tumour-infiltrating T-cell subsets, molecular changes in colorectal cancer, and prognosis: cohort study and literature review.* J Pathol, 2010. **222**(4): p. 350-66.
10. Oble, D.A., et al., *Focus on TILs: prognostic significance of tumor infiltrating lymphocytes in human melanoma.* Cancer Immun, 2009. **9**: p. 3.
11. Uppaluri, R., G.P. Dunn, and J.S. Lewis, Jr., *Focus on TILs: prognostic significance of tumor infiltrating lymphocytes in head and neck cancers.* Cancer Immun, 2008. **8**: p. 16.
12. Ward, M.J., et al., *Tumour-infiltrating lymphocytes predict for outcome in HPV-positive oropharyngeal cancer.* Br J Cancer, 2014. **110**(2): p. 489-500.
13. Shankaran, V., et al., *IFNgamma and lymphocytes prevent primary tumour development and shape tumour immunogenicity.* Nature, 2001. **410**(6832): p. 1107-11.
14. Dunn, G.P., et al., *Cancer immunoediting: from immunosurveillance to tumor escape.* Nat Immunol, 2002. **3**(11): p. 991-8.
15. Khong, H.T. and N.P. Restifo, *Natural selection of tumor variants in the generation of "tumor escape" phenotypes.* Nat Immunol, 2002. **3**(11): p. 999-1005.
16. Gabrilovich, D., *Mechanisms and functional significance of tumour-induced dendritic-cell defects.* Nat Rev Immunol, 2004. **4**(12): p. 941-52.
17. Smyth, M.J., et al., *New aspects of natural-killer-cell surveillance and therapy of cancer.* Nat Rev Cancer, 2002. **2**(11): p. 850-61.
18. Zou, W., *Regulatory T cells, tumour immunity and immunotherapy.* Nat Rev Immunol, 2006. **6**(4): p. 295-307.
19. Umansky, V. and A. Sevko, *Tumor microenvironment and myeloid-derived suppressor cells.* Cancer Microenviron, 2013. **6**(2): p. 169-77.
20. Rabinovich, G.A., D. Gabrilovich, and E.M. Sotomayor, *Immunosuppressive strategies that are mediated by tumor cells.* Annu Rev Immunol, 2007. **25**: p. 267-96.

21. Scott, A.M., J.D. Wolchok, and L.J. Old, *Antibody therapy of cancer.* Nat Rev Cancer, 2012. **12**(4): p. 278-87.
22. Keir, M.E., et al., *PD-1 and its ligands in tolerance and immunity.* Annu Rev Immunol, 2008. **26**: p. 677-704.
23. Peggs, K.S., et al., *Principles and use of anti-CTLA4 antibody in human cancer immunotherapy.* Curr Opin Immunol, 2006. **18**(2): p. 206-13.
24. Korman, A.J., K.S. Peggs, and J.P. Allison, *Checkpoint blockade in cancer immunotherapy.* Adv Immunol, 2006. **90**: p. 297-339.
25. Hodi, F.S., et al., *Improved survival with ipilimumab in patients with metastatic melanoma.* N Engl J Med, 2010. **363**(8): p. 711-23.
26. Robert, C., et al., *Ipilimumab plus dacarbazine for previously untreated metastatic melanoma.* N Engl J Med, 2011. **364**(26): p. 2517-26.
27. Li, B., et al., *Anti-programmed death-1 synergizes with granulocyte macrophage colony-stimulating factor--secreting tumor cell immunotherapy providing therapeutic benefit to mice with established tumors.* Clin Cancer Res, 2009. **15**(5): p. 1623-34.
28. Hamid, O., et al., *Safety and tumor responses with lambrolizumab (anti-PD-1) in melanoma.* N Engl J Med, 2013. **369**(2): p. 134-44.
29. Restifo, N.P., M.E. Dudley, and S.A. Rosenberg, *Adoptive immunotherapy for cancer: harnessing the T cell response.* Nat Rev Immunol, 2012. **12**(4): p. 269-81.
30. Hunder, N.N., et al., *Treatment of metastatic melanoma with autologous CD4+ T cells against NY-ESO-1.* N Engl J Med, 2008. **358**(25): p. 2698-703.
31. Robbins, P.F., et al., *Tumor regression in patients with metastatic synovial cell sarcoma and melanoma using genetically engineered lymphocytes reactive with NY-ESO-1.* J Clin Oncol, 2011. **29**(7): p. 917-24.
32. Johnson, L.A., et al., *Gene therapy with human and mouse T-cell receptors mediates cancer regression and targets normal tissues expressing cognate antigen.* Blood, 2009. **114**(3): p. 535-46.
33. Kawakami, Y., et al., *Cloning of the gene coding for a shared human melanoma antigen recognized by autologous T cells infiltrating into tumor.* Proc Natl Acad Sci U S A, 1994. **91**(9): p. 3515-9.
34. Kawakami, Y., et al., *Identification of a human melanoma antigen recognized by tumor-infiltrating lymphocytes associated with in vivo tumor rejection.* Proc Natl Acad Sci U S A, 1994. **91**(14): p. 6458-62.
35. Sampson, J.H., et al., *Immunologic escape after prolonged progression-free survival with epidermal growth factor receptor variant III peptide vaccination in patients with newly diagnosed glioblastoma.* J Clin Oncol, 2010. **28**(31): p. 4722-9.
36. Almeida, L.G., et al., *CTdatabase: a knowledge-base of high-throughput and curated data on cancer-testis antigens.* Nucleic Acids Res, 2009. **37**(Database issue): p. D816-9.
37. Chen, Y.T., et al., *A testicular antigen aberrantly expressed in human cancers detected by autologous antibody screening.* Proc Natl Acad Sci U S A, 1997. **94**(5): p. 1914-8.
38. Chen, J.L., et al., *Identification of NY-ESO-1 peptide analogues capable of improved stimulation of tumor-reactive CTL.* J Immunol, 2000. **165**(2): p. 948-55.
39. Gnjatic, S., et al., *Strategy for monitoring T cell responses to NY-ESO-1 in patients with any HLA class I allele.* Proc Natl Acad Sci U S A, 2000. **97**(20): p. 10917-22.
40. Jager, E., et al., *Simultaneous humoral and cellular immune response against cancer-testis antigen NY-ESO-1: definition of human histocompatibility leukocyte antigen (HLA)-A2-binding peptide epitopes.* J Exp Med, 1998. **187**(2): p. 265-70.

41. Jager, E., et al., *Monitoring CD8 T cell responses to NY-ESO-1: correlation of humoral and cellular immune responses.* Proc Natl Acad Sci U S A, 2000. **97**(9): p. 4760-5.
42. Stockert, E., et al., *A survey of the humoral immune response of cancer patients to a panel of human tumor antigens.* J Exp Med, 1998. **187**(8): p. 1349-54.
43. Sugita, Y., et al., *NY-ESO-1 expression and immunogenicity in malignant and benign breast tumors.* Cancer Res, 2004. **64**(6): p. 2199-204.
44. Karbach, J., et al., *Efficient in vivo priming by vaccination with recombinant NY-ESO-1 protein and CpG in antigen naive prostate cancer patients.* Clin Cancer Res, 2011. **17**(4): p. 861-70.
45. Sabbatini, P., et al., *Phase I trial of overlapping long peptides from a tumor self-antigen and poly-ICLC shows rapid induction of integrated immune response in ovarian cancer patients.* Clin Cancer Res, 2012. **18**(23): p. 6497-508.
46. Khazaie, K., A. Bonertz, and P. Beckhove, *Current developments with peptide-based human tumor vaccines.* Curr Opin Oncol, 2009. **21**(6): p. 524-30.
47. Feyerabend, S., et al., *Novel multi-peptide vaccination in Hla-A2+ hormone sensitive patients with biochemical relapse of prostate cancer.* Prostate, 2009. **69**(9): p. 917-27.
48. Pashenkov, M., et al., *Phase II trial of a toll-like receptor 9-activating oligonucleotide in patients with metastatic melanoma.* J Clin Oncol, 2006. **24**(36): p. 5716-24.
49. Wysocka, M., et al., *Enhancement of the host immune responses in cutaneous T-cell lymphoma by CpG oligodeoxynucleotides and IL-15.* Blood, 2004. **104**(13): p. 4142-9.
50. Kantoff, P.W., et al., *Sipuleucel-T immunotherapy for castration-resistant prostate cancer.* N Engl J Med, 2010. **363**(5): p. 411-22.
51. Clarke, S.L., et al., *CD4+CD25+FOXP3+ regulatory T cells suppress anti-tumor immune responses in patients with colorectal cancer.* PLoS One, 2006. **1**: p. e129.
52. Kim, J.M., J.P. Rasmussen, and A.Y. Rudensky, *Regulatory T cells prevent catastrophic autoimmunity throughout the lifespan of mice.* Nat Immunol, 2007. **8**(2): p. 191-7.
53. Sakaguchi, S., et al., *Immunologic self-tolerance maintained by activated T cells expressing IL-2 receptor alpha-chains (CD25). Breakdown of a single mechanism of self-tolerance causes various autoimmune diseases.* J Immunol, 1995. **155**(3): p. 1151-64.
54. Vanneman, M. and G. Dranoff, *Combining immunotherapy and targeted therapies in cancer treatment.* Nat Rev Cancer, 2012. **12**(4): p. 237-51.
55. Dolecek, T.A., et al., *CBTRUS statistical report: primary brain and central nervous system tumors diagnosed in the United States in 2005-2009.* Neuro Oncol, 2012. **14 Suppl 5**: p. v1-49.
56. Buckner, J.C., et al., *Central nervous system tumors.* Mayo Clin Proc, 2007. **82**(10): p. 1271-86.
57. Greter, M. and M. Merad, *Regulation of microglia development and homeostasis.* Glia, 2013. **61**(1): p. 121-7.
58. Saijo, K. and C.K. Glass, *Microglial cell origin and phenotypes in health and disease.* Nat Rev Immunol, 2011. **11**(11): p. 775-87.
59. Jiang, Y. and L. Uhrbom, *On the origin of glioma.* Ups J Med Sci, 2012. **117**(2): p. 113-21.
60. Louis, D.N., et al., *The 2007 WHO classification of tumours of the central nervous system.* Acta Neuropathol, 2007. **114**(2): p. 97-109.
61. Soffietti, R., et al., *Guidelines on management of low-grade gliomas: report of an EFNS-EANO Task Force.* Eur J Neurol, 2010. **17**(9): p. 1124-33.
62. Adamson, D.C., et al., *Central nervous system.* Cancer Biomark, 2010. **9**(1-6): p. 193-210.

63. Gilbert, M.R., et al., *Dose-dense temozolomide for newly diagnosed glioblastoma: a randomized phase III clinical trial.* J Clin Oncol, 2013. **31**(32): p. 4085-91.
64. Stupp, R., et al., *Radiotherapy plus concomitant and adjuvant temozolomide for glioblastoma.* N Engl J Med, 2005. **352**(10): p. 987-96.
65. Tabatabai, G., et al., *Molecular diagnostics of gliomas: the clinical perspective.* Acta Neuropathol, 2010. **120**(5): p. 585-92.
66. Wick, W. and M. Weller, *Classification and management of anaplastic gliomas.* Curr Opin Neurol, 2009. **22**(6): p. 650-6.
67. Ohgaki, H. and P. Kleihues, *The definition of primary and secondary glioblastoma.* Clin Cancer Res, 2013. **19**(4): p. 764-72.
68. Ohgaki, H. and P. Kleihues, *Genetic pathways to primary and secondary glioblastoma.* Am J Pathol, 2007. **170**(5): p. 1445-53.
69. Balss, J., et al., *Analysis of the IDH1 codon 132 mutation in brain tumors.* Acta Neuropathol, 2008. **116**(6): p. 597-602.
70. Parsons, D.W., et al., *An integrated genomic analysis of human glioblastoma multiforme.* Science, 2008. **321**(5897): p. 1807-12.
71. Yan, H., et al., *IDH1 and IDH2 mutations in gliomas.* N Engl J Med, 2009. **360**(8): p. 765-73.
72. Verhaak, R.G., et al., *Integrated genomic analysis identifies clinically relevant subtypes of glioblastoma characterized by abnormalities in PDGFRA, IDH1, EGFR, and NF1.* Cancer Cell, 2010. **17**(1): p. 98-110.
73. Noushmehr, H., et al., *Identification of a CpG island methylator phenotype that defines a distinct subgroup of glioma.* Cancer Cell, 2010. **17**(5): p. 510-22.
74. Hegi, M.E., et al., *MGMT gene silencing and benefit from temozolomide in glioblastoma.* N Engl J Med, 2005. **352**(10): p. 997-1003.
75. Sturm, D., et al., *Hotspot mutations in H3F3A and IDH1 define distinct epigenetic and biological subgroups of glioblastoma.* Cancer Cell, 2012. **22**(4): p. 425-37.
76. Xu, X., et al., *Structures of human cytosolic NADP-dependent isocitrate dehydrogenase reveal a novel self-regulatory mechanism of activity.* J Biol Chem, 2004. **279**(32): p. 33946-57.
77. Geisbrecht, B.V. and S.J. Gould, *The human PICD gene encodes a cytoplasmic and peroxisomal NADP(+)-dependent isocitrate dehydrogenase.* J Biol Chem, 1999. **274**(43): p. 30527-33.
78. Kim, S.Y., et al., *Regulation of singlet oxygen-induced apoptosis by cytosolic NADP+-dependent isocitrate dehydrogenase.* Mol Cell Biochem, 2007. **302**(1-2): p. 27-34.
79. Lee, S.M., et al., *Cytosolic NADP(+)-dependent isocitrate dehydrogenase status modulates oxidative damage to cells.* Free Radic Biol Med, 2002. **32**(11): p. 1185-96.
80. Weller, M., et al., *Personalized care in neuro-oncology coming of age: why we need MGMT and 1p/19q testing for malignant glioma patients in clinical practice.* Neuro Oncol, 2012. **14 Suppl 4**: p. iv100-8.
81. Yan, H., et al., *Mutant metabolic enzymes are at the origin of gliomas.* Cancer Res, 2009. **69**(24): p. 9157-9.
82. Kim, Y.H., et al., *Molecular classification of low-grade diffuse gliomas.* Am J Pathol, 2010. **177**(6): p. 2708-14.
83. Watanabe, T., et al., *Phenotype versus genotype correlation in oligodendrogliomas and low-grade diffuse astrocytomas.* Acta Neuropathol, 2002. **103**(3): p. 267-75.
84. Watanabe, T., et al., *IDH1 mutations are early events in the development of astrocytomas and oligodendrogliomas.* Am J Pathol, 2009. **174**(4): p. 1149-53.
85. Dang, L., et al., *Cancer-associated IDH1 mutations produce 2-hydroxyglutarate.* Nature, 2009. **462**(7274): p. 739-44.

86. Chou, W.C., et al., *Distinct clinical and biologic characteristics in adult acute myeloid leukemia bearing the isocitrate dehydrogenase 1 mutation.* Blood, 2010. **115**(14): p. 2749-54.
87. Mardis, E.R., et al., *Recurring mutations found by sequencing an acute myeloid leukemia genome.* N Engl J Med, 2009. **361**(11): p. 1058-66.
88. Ward, P.S., et al., *The common feature of leukemia-associated IDH1 and IDH2 mutations is a neomorphic enzyme activity converting alpha-ketoglutarate to 2-hydroxyglutarate.* Cancer Cell, 2010. **17**(3): p. 225-34.
89. Amary, M.F., et al., *IDH1 and IDH2 mutations are frequent events in central chondrosarcoma and central and periosteal chondromas but not in other mesenchymal tumours.* J Pathol, 2011. **224**(3): p. 334-43.
90. Arai, M., et al., *Frequent IDH1/2 mutations in intracranial chondrosarcoma: a possible diagnostic clue for its differentiation from chordoma.* Brain Tumor Pathol, 2012. **29**(4): p. 201-6.
91. Wang, P., et al., *Mutations in isocitrate dehydrogenase 1 and 2 occur frequently in intrahepatic cholangiocarcinomas and share hypermethylation targets with glioblastomas.* Oncogene, 2013. **32**(25): p. 3091-100.
92. Losman, J.A. and W.G. Kaelin, Jr., *What a difference a hydroxyl makes: mutant IDH, (R)-2-hydroxyglutarate, and cancer.* Genes Dev, 2013. **27**(8): p. 836-52.
93. Zhao, S., et al., *Glioma-derived mutations in IDH1 dominantly inhibit IDH1 catalytic activity and induce HIF-1alpha.* Science, 2009. **324**(5924): p. 261-5.
94. Gross, S., et al., *Cancer-associated metabolite 2-hydroxyglutarate accumulates in acute myelogenous leukemia with isocitrate dehydrogenase 1 and 2 mutations.* J Exp Med, 2010. **207**(2): p. 339-44.
95. Lu, C., et al., *IDH mutation impairs histone demethylation and results in a block to cell differentiation.* Nature, 2012. **483**(7390): p. 474-8.
96. Sasaki, M., et al., *IDH1(R132H) mutation increases murine haematopoietic progenitors and alters epigenetics.* Nature, 2012. **488**(7413): p. 656-9.
97. Figueroa, M.E., et al., *Leukemic IDH1 and IDH2 mutations result in a hypermethylation phenotype, disrupt TET2 function, and impair hematopoietic differentiation.* Cancer Cell, 2010. **18**(6): p. 553-67.
98. Turcan, S., et al., *IDH1 mutation is sufficient to establish the glioma hypermethylator phenotype.* Nature, 2012. **483**(7390): p. 479-83.
99. Xu, W., et al., *Oncometabolite 2-hydroxyglutarate is a competitive inhibitor of alpha-ketoglutarate-dependent dioxygenases.* Cancer Cell, 2011. **19**(1): p. 17-30.
100. Losman, J.A., et al., *(R)-2-hydroxyglutarate is sufficient to promote leukemogenesis and its effects are reversible.* Science, 2013. **339**(6127): p. 1621-5.
101. Sanson, M., et al., *Isocitrate dehydrogenase 1 codon 132 mutation is an important prognostic biomarker in gliomas.* J Clin Oncol, 2009. **27**(25): p. 4150-4.
102. Dubbink, H.J., et al., *IDH1 mutations in low-grade astrocytomas predict survival but not response to temozolomide.* Neurology, 2009. **73**(21): p. 1792-5.
103. van den Bent, M.J., et al., *MGMT promoter methylation is prognostic but not predictive for outcome to adjuvant PCV chemotherapy in anaplastic oligodendroglial tumors: a report from EORTC Brain Tumor Group Study 26951.* J Clin Oncol, 2009. **27**(35): p. 5881-6.
104. Wick, W., et al., *NOA-04 randomized phase III trial of sequential radiochemotherapy of anaplastic glioma with procarbazine, lomustine, and vincristine or temozolomide.* J Clin Oncol, 2009. **27**(35): p. 5874-80.
105. Capper, D., et al., *Characterization of R132H mutation-specific IDH1 antibody binding in brain tumors.* Brain Pathol, 2010. **20**(1): p. 245-54.

106. Capper, D., et al., *Monoclonal antibody specific for IDH1 R132H mutation.* Acta Neuropathol, 2009. **118**(5): p. 599-601.
107. Sahm, F., et al., *Addressing diffuse glioma as a systemic brain disease with single-cell analysis.* Arch Neurol, 2012. **69**(4): p. 523-6.
108. Rohle, D., et al., *An inhibitor of mutant IDH1 delays growth and promotes differentiation of glioma cells.* Science, 2013. **340**(6132): p. 626-30.
109. Wang, F., et al., *Targeted inhibition of mutant IDH2 in leukemia cells induces cellular differentiation.* Science, 2013. **340**(6132): p. 622-6.
110. Fenstermaker, R.A. and M.J. Ciesielski, *Immunotherapeutic strategies for malignant glioma.* Cancer Control, 2004. **11**(3): p. 181-91.
111. Wick, W., U. Naumann, and M. Weller, *Transforming growth factor-beta: a molecular target for the future therapy of glioblastoma.* Curr Pharm Des, 2006. **12**(3): p. 341-9.
112. Opitz, C.A., et al., *An endogenous tumour-promoting ligand of the human aryl hydrocarbon receptor.* Nature, 2011. **478**(7368): p. 197-203.
113. Bournazou, E. and J. Bromberg, *Targeting the tumor microenvironment: JAK-STAT3 signaling.* JAKSTAT, 2013. **2**(2): p. e23828.
114. Grauer, O.M., P. Wesseling, and G.J. Adema, *Immunotherapy of diffuse gliomas: biological background, current status and future developments.* Brain Pathol, 2009. **19**(4): p. 674-93.
115. Bloch, O., et al., *Gliomas promote immunosuppression through induction of B7-H1 expression in tumor-associated macrophages.* Clin Cancer Res, 2013. **19**(12): p. 3165-75.
116. Fujita, M., et al., *COX-2 blockade suppresses gliomagenesis by inhibiting myeloid-derived suppressor cells.* Cancer Res, 2011. **71**(7): p. 2664-74.
117. Kohanbash, G., et al., *GM-CSF promotes the immunosuppressive activity of glioma-infiltrating myeloid cells through interleukin-4 receptor-alpha.* Cancer Res, 2013. **73**(21): p. 6413-23.
118. Prosniak, M., et al., *Glioma grade is associated with the accumulation and activity of cells bearing M2 monocyte markers.* Clin Cancer Res, 2013. **19**(14): p. 3776-86.
119. Raychaudhuri, B., et al., *Myeloid-derived suppressor cell accumulation and function in patients with newly diagnosed glioblastoma.* Neuro Oncol, 2011. **13**(6): p. 591-9.
120. Jackson, C., et al., *Challenges in immunotherapy presented by the glioblastoma multiforme microenvironment.* Clin Dev Immunol, 2011. **2011**: p. 732413.
121. Vauleon, E., et al., *Overview of cellular immunotherapy for patients with glioblastoma.* Clin Dev Immunol, 2010. **2010**.
122. Platten, M. and L. Steinman, *Multiple sclerosis: trapped in deadly glue.* Nat Med, 2005. **11**(3): p. 252-3.
123. Smolders, J., et al., *Characteristics of differentiated CD8(+) and CD4 (+) T cells present in the human brain.* Acta Neuropathol, 2013. **126**(4): p. 525-35.
124. Mittelbronn, M., et al., *Elevated HLA-E levels in human glioblastomas but not in grade I to III astrocytomas correlate with infiltrating CD8+ cells.* J Neuroimmunol, 2007. **189**(1-2): p. 50-8.
125. Waziri, A., et al., *Preferential in situ CD4+CD56+ T cell activation and expansion within human glioblastoma.* J Immunol, 2008. **180**(11): p. 7673-80.
126. Barcia, C., Jr., et al., *Infiltrating CTLs in human glioblastoma establish immunological synapses with tumorigenic cells.* Am J Pathol, 2009. **175**(2): p. 786-98.
127. Fathallah-Shaykh, H.M., et al., *Priming in the brain, an immunologically privileged organ, elicits anti-tumor immunity.* Int J Cancer, 1998. **75**(2): p. 266-76.
128. Brooks, W.H., et al., *Relationship of lymphocyte invasion and survival of brain tumor patients.* Ann Neurol, 1978. **4**(3): p. 219-24.

129. Kim, Y.H., et al., *Tumour-infiltrating T-cell subpopulations in glioblastomas.* Br J Neurosurg, 2012. **26**(1): p. 21-7.
130. Kmiecik, J., et al., *Elevated CD3+ and CD8+ tumor-infiltrating immune cells correlate with prolonged survival in glioblastoma patients despite integrated immunosuppressive mechanisms in the tumor microenvironment and at the systemic level.* J Neuroimmunol, 2013. **264**(1-2): p. 71-83.
131. Lohr, J., et al., *Effector T-cell infiltration positively impacts survival of glioblastoma patients and is impaired by tumor-derived TGF-beta.* Clin Cancer Res, 2011. **17**(13): p. 4296-308.
132. Sawamura, Y., et al., *Antitumor activity and surface phenotypes of human glioma-infiltrating lymphocytes after in vitro expansion in the presence of interleukin 2.* Cancer Res, 1989. **49**(7): p. 1843-9.
133. Saikali, S., et al., *Expression of nine tumour antigens in a series of human glioblastoma multiforme: interest of EGFRvIII, IL-13Ralpha2, gp100 and TRP-2 for immunotherapy.* J Neurooncol, 2007. **81**(2): p. 139-48.
134. Dutoit, V., et al., *Exploiting the glioblastoma peptidome to discover novel tumour-associated antigens for immunotherapy.* Brain, 2012. **135**(Pt 4): p. 1042-54.
135. Neidert, M.C., et al., *Natural HLA class I ligands from glioblastoma: extending the options for immunotherapy.* J Neurooncol, 2013. **111**(3): p. 285-94.
136. Okada, H., *Brain tumor immunotherapy with type-1 polarizing strategies.* Ann N Y Acad Sci, 2009. **1174**: p. 18-23.
137. Prins, R.M., et al., *Gene expression profile correlates with T-cell infiltration and relative survival in glioblastoma patients vaccinated with dendritic cell immunotherapy.* Clin Cancer Res, 2011. **17**(6): p. 1603-15.
138. Batra, S.K., et al., *Epidermal growth factor ligand-independent, unregulated, cell-transforming potential of a naturally occurring human mutant EGFRvIII gene.* Cell Growth Differ, 1995. **6**(10): p. 1251-9.
139. Nishikawa, R., et al., *A mutant epidermal growth factor receptor common in human glioma confers enhanced tumorigenicity.* Proc Natl Acad Sci U S A, 1994. **91**(16): p. 7727-31.
140. Lammering, G., et al., *Radiation-induced activation of a common variant of EGFR confers enhanced radioresistance.* Radiother Oncol, 2004. **72**(3): p. 267-73.
141. Choi, B.D., et al., *EGFRvIII-targeted vaccination therapy of malignant glioma.* Brain Pathol, 2009. **19**(4): p. 713-23.
142. Pajot, A., et al., *A mouse model of human adaptive immune functions: HLA-A2.1-/HLA-DR1-transgenic H-2 class I-/class II-knockout mice.* Eur J Immunol, 2004. **34**(11): p. 3060-9.
143. Ito, K., et al., *HLA-DR4-IE chimeric class II transgenic, murine class II-deficient mice are susceptible to experimental allergic encephalomyelitis.* J Exp Med, 1996. **183**(6): p. 2635-44.
144. Lundegaard, C., O. Lund, and M. Nielsen, *Accurate approximation method for prediction of class I MHC affinities for peptides of length 8, 10 and 11 using prediction tools trained on 9mers.* Bioinformatics, 2008. **24**(11): p. 1397-8.
145. Rammensee, H., et al., *SYFPEITHI: database for MHC ligands and peptide motifs.* Immunogenetics, 1999. **50**(3-4): p. 213-9.
146. Nielsen, M. and O. Lund, *NN-align. An artificial neural network-based alignment algorithm for MHC class II peptide binding prediction.* BMC Bioinformatics, 2009. **10**: p. 296.
147. Balss, J., et al., *Enzymatic assay for quantitative analysis of (D)-2-hydroxyglutarate.* Acta Neuropathol, 2012. **124**(6): p. 883-91.

148. Gonzalez-Galarza, F.F., et al., *Allele frequency net: a database and online repository for immune gene frequencies in worldwide populations.* Nucleic Acids Res, 2011. **39**(Database issue): p. D913-9.
149. Hirschhorn-Cymerman, D., et al., *Induction of tumoricidal function in CD4+ T cells is associated with concomitant memory and terminally differentiated phenotype.* J Exp Med, 2012. **209**(11): p. 2113-26.
150. Muranski, P. and N.P. Restifo, *Adoptive immunotherapy of cancer using CD4(+) T cells.* Curr Opin Immunol, 2009. **21**(2): p. 200-8.
151. Quezada, S.A., et al., *Tumor-reactive CD4(+) T cells develop cytotoxic activity and eradicate large established melanoma after transfer into lymphopenic hosts.* J Exp Med, 2010. **207**(3): p. 637-50.
152. Billiau, A. and P. Matthys, *Modes of action of Freund's adjuvants in experimental models of autoimmune diseases.* J Leukoc Biol, 2001. **70**(6): p. 849-60.
153. Fletcher, J.M., et al., *T cells in multiple sclerosis and experimental autoimmune encephalomyelitis.* Clin Exp Immunol, 2010. **162**(1): p. 1-11.
154. Barve, M., et al., *Induction of immune responses and clinical efficacy in a phase II trial of IDM-2101, a 10-epitope cytotoxic T-lymphocyte vaccine, in metastatic non-small-cell lung cancer.* J Clin Oncol, 2008. **26**(27): p. 4418-25.
155. Fourcade, J., et al., *Immunization with analog peptide in combination with CpG and montanide expands tumor antigen-specific CD8+ T cells in melanoma patients.* J Immunother, 2008. **31**(8): p. 781-91.
156. Aranda, F., et al., *Adjuvant combination and antigen targeting as a strategy to induce polyfunctional and high-avidity T-cell responses against poorly immunogenic tumors.* Cancer Res, 2011. **71**(9): p. 3214-24.
157. Widenmeyer, M., et al., *Promiscuous survivin peptide induces robust CD4+ T-cell responses in the majority of vaccinated cancer patients.* Int J Cancer, 2012. **131**(1): p. 140-9.
158. Macian, F., et al., *Transcriptional mechanisms underlying lymphocyte tolerance.* Cell, 2002. **109**(6): p. 719-31.
159. Arstila, T.P., et al., *A direct estimate of the human alphabeta T cell receptor diversity.* Science, 1999. **286**(5441): p. 958-61.
160. Ueda, R., et al., *Spontaneous immune responses against glioma-associated antigens in a long term survivor with malignant glioma.* J Transl Med, 2007. **5**: p. 68.
161. Chen, Y.T., et al., *Genomic cloning and localization of CTAG, a gene encoding an autoimmunogenic cancer-testis antigen NY-ESO-1, to human chromosome Xq28.* Cytogenet Cell Genet, 1997. **79**(3-4): p. 237-40.
162. Zarour, H.M., et al., *NY-ESO-1 119-143 is a promiscuous major histocompatibility complex class II T-helper epitope recognized by Th1- and Th2-type tumor-reactive CD4+ T cells.* Cancer Res, 2002. **62**(1): p. 213-8.
163. Cairncross, G., et al., *Phase III trial of chemoradiotherapy for anaplastic oligodendroglioma: long-term results of RTOG 9402.* J Clin Oncol, 2013. **31**(3): p. 337-43.
164. van den Bent, M.J., et al., *Adjuvant procarbazine, lomustine, and vincristine chemotherapy in newly diagnosed anaplastic oligodendroglioma: long-term follow-up of EORTC brain tumor group study 26951.* J Clin Oncol, 2013. **31**(3): p. 344-50.
165. Jansen, M., S. Yip, and D.N. Louis, *Molecular pathology in adult gliomas: diagnostic, prognostic, and predictive markers.* Lancet Neurol, 2010. **9**(7): p. 717-26.
166. Pardoll, D., *Does the immune system see tumors as foreign or self?* Annu Rev Immunol, 2003. **21**: p. 807-39.
167. Teague, R.M., et al., *Peripheral CD8+ T cell tolerance to self-proteins is regulated proximally at the T cell receptor.* Immunity, 2008. **28**(5): p. 662-74.

168. Glas, M., et al., *Targeting the cytosolic innate immune receptors RIG-I and MDA5 effectively counteracts cancer cell heterogeneity in glioblastoma.* Stem Cells, 2013. **31**(6): p. 1064-74.
169. Kim, Y., et al., *Platelet-derived growth factor receptors differentially inform intertumoral and intratumoral heterogeneity.* Genes Dev, 2012. **26**(11): p. 1247-62.
170. Little, S.E., et al., *Receptor tyrosine kinase genes amplified in glioblastoma exhibit a mutual exclusivity in variable proportions reflective of individual tumor heterogeneity.* Cancer Res, 2012. **72**(7): p. 1614-20.
171. Szerlip, N.J., et al., *Intratumoral heterogeneity of receptor tyrosine kinases EGFR and PDGFRA amplification in glioblastoma defines subpopulations with distinct growth factor response.* Proc Natl Acad Sci U S A, 2012. **109**(8): p. 3041-6.
172. Lass, U., et al., *Clonal analysis in recurrent astrocytic, oligoastrocytic and oligodendroglial tumors implicates IDH1- mutation as common tumor initiating event.* PLoS One, 2012. **7**(7): p. e41298.
173. Park, J.M., et al., *Therapy of advanced established murine breast cancer with a recombinant adenoviral ErbB-2/neu vaccine.* Cancer Res, 2008. **68**(6): p. 1979-87.
174. Triulzi, C., et al., *Antibody-dependent natural killer cell-mediated cytotoxicity engendered by a kinase-inactive human HER2 adenovirus-based vaccination mediates resistance to breast tumors.* Cancer Res, 2010. **70**(19): p. 7431-41.
175. Sasaki, M., et al., *D-2-hydroxyglutarate produced by mutant IDH1 perturbs collagen maturation and basement membrane function.* Genes Dev, 2012. **26**(18): p. 2038-49.
176. Atanackovic, D., et al., *Booster vaccination of cancer patients with MAGE-A3 protein reveals long-term immunological memory or tolerance depending on priming.* Proc Natl Acad Sci U S A, 2008. **105**(5): p. 1650-5.
177. Butler, M.O., et al., *Establishment of antitumor memory in humans using in vitro-educated CD8+ T cells.* Sci Transl Med, 2011. **3**(80): p. 80ra34.
178. Tuettenberg, A., et al., *Induction of strong and persistent MelanA/MART-1-specific immune responses by adjuvant dendritic cell-based vaccination of stage II melanoma patients.* Int J Cancer, 2006. **118**(10): p. 2617-27.
179. Mackensen, A., et al., *Phase I study of adoptive T-cell therapy using antigen-specific CD8+ T cells for the treatment of patients with metastatic melanoma.* J Clin Oncol, 2006. **24**(31): p. 5060-9.
180. Yee, C., et al., *Adoptive T cell therapy using antigen-specific CD8+ T cell clones for the treatment of patients with metastatic melanoma: in vivo persistence, migration, and antitumor effect of transferred T cells.* Proc Natl Acad Sci U S A, 2002. **99**(25): p. 16168-73.
181. Antony, P.A., et al., *CD8+ T cell immunity against a tumor/self-antigen is augmented by CD4+ T helper cells and hindered by naturally occurring T regulatory cells.* J Immunol, 2005. **174**(5): p. 2591-601.
182. Pardoll, D.M. and S.L. Topalian, *The role of CD4+ T cell responses in antitumor immunity.* Curr Opin Immunol, 1998. **10**(5): p. 588-94.
183. Gao, F.G., et al., *Antigen-specific CD4+ T-cell help is required to activate a memory CD8+ T cell to a fully functional tumor killer cell.* Cancer Res, 2002. **62**(22): p. 6438-41.
184. Greenberg, P.D., *Adoptive T cell therapy of tumors: mechanisms operative in the recognition and elimination of tumor cells.* Adv Immunol, 1991. **49**: p. 281-355.
185. Shedlock, D.J. and H. Shen, *Requirement for CD4 T cell help in generating functional CD8 T cell memory.* Science, 2003. **300**(5617): p. 337-9.
186. Corthay, A., et al., *Primary antitumor immune response mediated by CD4+ T cells.* Immunity, 2005. **22**(3): p. 371-83.

187. Hung, K., et al., *The central role of CD4(+) T cells in the antitumor immune response.* J Exp Med, 1998. **188**(12): p. 2357-68.
188. Mumberg, D., et al., *CD4(+) T cells eliminate MHC class II-negative cancer cells in vivo by indirect effects of IFN-gamma.* Proc Natl Acad Sci U S A, 1999. **96**(15): p. 8633-8.
189. Perez-Diez, A., et al., *CD4 cells can be more efficient at tumor rejection than CD8 cells.* Blood, 2007. **109**(12): p. 5346-54.
190. Nuchtern, J.G., W.E. Biddison, and R.D. Klausner, *Class II MHC molecules can use the endogenous pathway of antigen presentation.* Nature, 1990. **343**(6253): p. 74-6.
191. Heller, K.N., C. Gurer, and C. Munz, *Virus-specific CD4+ T cells: ready for direct attack.* J Exp Med, 2006. **203**(4): p. 805-8.
192. Takamura, Y., et al., *Regulation of MHC class II expression in glioma cells by class II transactivator (CIITA).* Glia, 2004. **45**(4): p. 392-405.
193. Lauritzsen, G.F. and B. Bogen, *The role of idiotype-specific, CD4+ T cells in tumor resistance against major histocompatibility complex class II molecule negative plasmacytoma cells.* Cell Immunol, 1993. **148**(1): p. 177-88.
194. Lee, Y.K., et al., *Late developmental plasticity in the T helper 17 lineage.* Immunity, 2009. **30**(1): p. 92-107.
195. Sanchez-Perez, L., et al., *Potent selection of antigen loss variants of B16 melanoma following inflammatory killing of melanocytes in vivo.* Cancer Res, 2005. **65**(5): p. 2009-17.
196. Nowak, A.K., et al., *Induction of tumor cell apoptosis in vivo increases tumor antigen cross-presentation, cross-priming rather than cross-tolerizing host tumor-specific CD8 T cells.* J Immunol, 2003. **170**(10): p. 4905-13.
197. Ruffell, B., et al., *Leukocyte composition of human breast cancer.* Proc Natl Acad Sci U S A, 2012. **109**(8): p. 2796-801.
198. Wennhold, K., et al., *CD40-activated B cells as antigen-presenting cells: the final sprint toward clinical application.* Expert Rev Vaccines, 2013. **12**(6): p. 631-7.
199. DuPage, M., et al., *Expression of tumour-specific antigens underlies cancer immunoediting.* Nature, 2012. **482**(7385): p. 405-9.
200. Guo, Z.S., et al., *De novo induction of a cancer/testis antigen by 5-aza-2'-deoxycytidine augments adoptive immunotherapy in a murine tumor model.* Cancer Res, 2006. **66**(2): p. 1105-13.
201. Restifo, N.P., et al., *Loss of functional beta 2-microglobulin in metastatic melanomas from five patients receiving immunotherapy.* J Natl Cancer Inst, 1996. **88**(2): p. 100-8.
202. Mutskov, V. and G. Felsenfeld, *Silencing of transgene transcription precedes methylation of promoter DNA and histone H3 lysine 9.* EMBO J, 2004. **23**(1): p. 138-49.
203. Ohm, J.E., et al., *A stem cell-like chromatin pattern may predispose tumor suppressor genes to DNA hypermethylation and heritable silencing.* Nat Genet, 2007. **39**(2): p. 237-42.
204. Schneider, U., H.U. Schwenk, and G. Bornkamm, *Characterization of EBV-genome negative "null" and "T" cell lines derived from children with acute lymphoblastic leukemia and leukemic transformed non-Hodgkin lymphoma.* Int J Cancer, 1977. **19**(5): p. 621-6.
205. Overwijk, W.W., et al., *Tumor regression and autoimmunity after reversal of a functionally tolerant state of self-reactive CD8+ T cells.* J Exp Med, 2003. **198**(4): p. 569-80.
206. Barnden, M.J., et al., *Defective TCR expression in transgenic mice constructed using cDNA-based alpha- and beta-chain genes under the control of heterologous regulatory elements.* Immunol Cell Biol, 1998. **76**(1): p. 34-40.

207. Rankin, E.B. and A.J. Giaccia, *The role of hypoxia-inducible factors in tumorigenesis.* Cell Death Differ, 2008. **15**(4): p. 678-85.
208. Patan, S., *Vasculogenesis and angiogenesis as mechanisms of vascular network formation, growth and remodeling.* J Neurooncol, 2000. **50**(1-2): p. 1-15.
209. Falcon, B.L., et al., *Reduced VEGF production, angiogenesis, and vascular regrowth contribute to the antitumor properties of dual mTORC1/mTORC2 inhibitors.* Cancer Res, 2011. **71**(5): p. 1573-83.
210. Plate, K.H., et al., *Vascular endothelial growth factor is a potential tumour angiogenesis factor in human gliomas in vivo.* Nature, 1992. **359**(6398): p. 845-8.
211. Winkler, F., et al., *Kinetics of vascular normalization by VEGFR2 blockade governs brain tumor response to radiation: role of oxygenation, angiopoietin-1, and matrix metalloproteinases.* Cancer Cell, 2004. **6**(6): p. 553-63.
212. Kalluri, R., *Basement membranes: structure, assembly and role in tumour angiogenesis.* Nat Rev Cancer, 2003. **3**(6): p. 422-33.
213. Gnjatic, S., et al., *Survey of naturally occurring CD4+ T cell responses against NY-ESO-1 in cancer patients: correlation with antibody responses.* Proc Natl Acad Sci U S A, 2003. **100**(15): p. 8862-7.
214. Abbas, A.K., et al., *Heterogeneity of helper/inducer T lymphocytes. IV. Stimulation of resting and activated B cells by Th1 and Th2 clones.* J Immunol, 1990. **144**(6): p. 2031-7.
215. King, C., *New insights into the differentiation and function of T follicular helper cells.* Nat Rev Immunol, 2009. **9**(11): p. 757-66.
216. Mosmann, T.R. and S. Sad, *The expanding universe of T-cell subsets: Th1, Th2 and more.* Immunol Today, 1996. **17**(3): p. 138-46.
217. Hussain, S.F. and A.B. Heimberger, *Immunotherapy for human glioma: innovative approaches and recent results.* Expert Rev Anticancer Ther, 2005. **5**(5): p. 777-90.
218. King, C., et al., *Homeostatic expansion of T cells during immune insufficiency generates autoimmunity.* Cell, 2004. **117**(2): p. 265-77.
219. Rosenberg, S.A., et al., *Durable complete responses in heavily pretreated patients with metastatic melanoma using T-cell transfer immunotherapy.* Clin Cancer Res, 2011. **17**(13): p. 4550-7.
220. Wrzesinski, C., et al., *Increased intensity lymphodepletion enhances tumor treatment efficacy of adoptively transferred tumor-specific T cells.* J Immunother, 2010. **33**(1): p. 1-7.
221. Lynch, T.J., et al., *Ipilimumab in combination with paclitaxel and carboplatin as first-line treatment in stage IIIB/IV non-small-cell lung cancer: results from a randomized, double-blind, multicenter phase II study.* J Clin Oncol, 2012. **30**(17): p. 2046-54.
222. Slovin, S.F., et al., *Ipilimumab alone or in combination with radiotherapy in metastatic castration-resistant prostate cancer: results from an open-label, multicenter phase I/II study.* Ann Oncol, 2013. **24**(7): p. 1813-21.
223. Weber, J.S., et al., *Safety, efficacy, and biomarkers of nivolumab with vaccine in ipilimumab-refractory or -naive melanoma.* J Clin Oncol, 2013. **31**(34): p. 4311-8.
224. Creelan, B.C., *Update on immune checkpoint inhibitors in lung cancer.* Cancer Control, 2014. **21**(1): p. 80-9.
225. Jacobs, J.F., et al., *Regulatory T cells and the PD-L1/PD-1 pathway mediate immune suppression in malignant human brain tumors.* Neuro Oncol, 2009. **11**(4): p. 394-402.
226. Wei, B., et al., *The upregulation of programmed death 1 on peripheral blood T cells of glioma is correlated with disease progression.* Tumour Biol, 2013.
227. Vom Berg, J., et al., *Intratumoral IL-12 combined with CTLA-4 blockade elicits T cell-mediated glioma rejection.* J Exp Med, 2013. **210**(13): p. 2803-11.

6 APPENDIX

6.1 Abbreviations

2-HG	(R)-2-hydroxyglutarate
α-KG	α-ketoglutarate
α-MM	α-methylmannopyranoside
A	astrocytoma
ALP	alkaline phosphatase
AML	acute myeloid leukemia
APC	antigen-presenting cells
AT	adoptive transfer
AUC	area under the curve
BBB	blood-brain barrier
BM	basement membrane
CAR	chimeric antigen receptor
CD	cluster of differentiation
CFA	complete Freund's adjuvant
CLIP	class II-associated invariant chain peptide
CNS	central nervous system
cpm	counts per minute
CSF	cerebrospinal fluid
CTAG1	cancer testis antigen 1
CTL	cytotoxic T lymphocyte
CTLA-4	cytotoxic T lymphocyte-associated antigen 4
DAPI	4',6-diamidino-2-phenylindole
DC	dendritic cell
DKFZ	Deutsches Krebsforschungszentrum
DMSO	dimethylsulfoxide
EAE	experimental autoimmune encephalomyelitis
EBV	Epstein-Barr-virus

ECL	enhanced chemiluminescence
EDTA	ethylenediaminetetraacetic acid
EGFR	epidermal growth factor receptor
EGFRvIII	EGFR variant III
ELISA	enzyme-linked immunoadsorbent assay
ELISpot	enzyme-linked immunoadsorbent spot assay
ER	endoplasmatic reticulum
FasL	Fas ligand
FBS	fetal bovine serum
FDA	U.S. Food and Drug Administration
FoxP3	forkhead box P3
GABA	gamma-aminobutyric acid
GABRA1	gamma-aminobutyric acid (GABA) A receptor, alpha 1
G-CIMP	glioma CpG island methylator phenotype
GBM	glioblastoma multiforme
G-CIMP	glioma CpG island methylation phenotype
GFAP	glial fibrillary acidic protein
GM-CSF	granulocyte-macrophage colony-stimulating factor
HIF	hypoxia-inducible factor
HIV	human immunodeficiency virus
HLA	human leukocyte antigen
HPV	human papillomavirus
HRP	horseradish peroxidase
HTLV	human T lymphotropic virus
HUVEC	human umbilical vein endothelial cells
IHC	immunohistochemistry
IDH	isocitrate dehydrogenase
IDO	indoleamine 2,3-dioxygenase
IF	immunofluorescence
IFN	interferon
IgG	immunoglobulin G
IL	interleukin

KI	knock in
KO	knock out
LN	lymph node
LOH	loss of heterozygosity
LPS	lipopolysaccharides
MACS	magnetic cell sorting
MAPK	mitogen-activated protein kinase
MART1	melanoma antigen recognized by T cells 1
MCA	3-methylcholantrene
MDSC	myeloid-derived suppressor cell
MERTK	c-mer proto-oncogene tyrosine kinase
MFI	mean fluorescence intensity
MGMT	O6-methylguanine-DNA methyl-transferase
MHC	major histocompatibility complex
MLR	mixed leukocyte reaction
MOG	myelin oligodendrocyte glycoprotein
MRI	magnetic resonance imaging
MS	multiple sclerosis
NADPH	nicotinamide adenine dinucleotide phosphate
NEFL	*neurofilament light polypeptide*
NF	neurofibromin
NIH	National Institute of Health
NK	natural killer
NOS	nitric oxide synthase
NY-ESO-1	New York esophageal squamous cell carcinoma 1
O	oligodendroglioma
OA	oligoastrocytoma
OVA	ovalbumin
PAP	prostatic acid phosphatase
PBMC	peripheral blood mononuclear cells
PBS	phosphate-buffered saline
PCR	polymerase chain reaction

PCV	procarbazine, lomustine, and vincristine
PD1	programmed cell death protein 1
PDGFRA	platelet-derived growth factor receptor alpha
PFA	paraformaldehyde
PHD	prolyl hydroxylase domain-containing protein
PI	propidium iodide
PMA	phorbol-12-myristate-13-acetate
PMSF	phenylmethylsulphonyl fluoride
PNS	peripheral nervous system
PTEN	phosphatase and tensin homologue
RB	retinoblastoma
RT	radiotherapy / room temperature
s. c.	subcutaneous(ly)
SEB	staphylococcus-derived enterotoxin B
secGBM	secondary glioblastoma multiforme
TAA	tumor-associated antigen
TAP	transporter associated with antigen processing
TBS	Tris-based saline
TCR	T cell receptor
TDO	tryptophan-2,3-dioxygenase
T_{eff}	effector T cell
TGF-β	transforming growth factor β
Th	T helper cell
TIL	tumor-infiltrating lymphocyte
TLR	Toll-like receptor
TMZ	temozolomide
TNF-α	tumor necrosis factor α
T_{reg}	regulatory T cell
TYRP1	tyrosinase-related protein 1
VEGF	vascular endothelial growth factor
WHO	World Health Organization
WRS	Wilcoxon rank-sum

wt	wildtype

6.2 cDNA sequences

6.2.1 human IDH1 cDNA

```
atgtccaaaaaaatcagtggcggttctgtggtagagatgcaaggagatgaaatgacacgaatcatttgggaattg
attaaagagaaactcatttttccctacgtggaattggatctacatagctatgatttaggcatagagaatcgtgat
gccaccaacgaccaagtcaccaaggatgctgcagaagctataaagaagcataatgttggcgtcaaatgtgccact
atcactcctgatgagaagagggttgaggagttcaagttgaaacaaatgtggaaatcaccaaatggcaccatacga
aatattctgggtggcacggtcttcagagaagccattatctgcaaaaatatcccccggcttgtgagtggatgggta
aaacctatcatcataggtcgtcatgcttatggggatcaatacagagcaactgattttgttgttcctgggcctgga
aaagtagagataacctacacaccaagtgacggaacccaaaaggtgacatacctggtacataactttgaagaaggt
ggtggtgttgccatggggatgtataatcaagataagtcaattgaagattttgcacacagttccttccaaatggct
ctgtctaagggttggcctttgtatctgagcaccaaaaacactattctgaagaaatatgatgggcgttttaaagac
atctttcaggagatatatgacaagcagtacaagtcccagtttgaagctcaaaagatctggtatgagcataggctc
atcgacgacatggtggcccaagctatgaaatcagagggaggcttcatctgggcctgtaaaaactatgatggtgac
gtgcagtcggactctgtggcccaagggtatggctctctcggcatgatgaccagcgtgctggtttgtccagatggc
aagacagtagaagcagaggctgcccacgggactgtaacccgtcactaccgcatgtaccagaaaggacaggagacg
tccaccaatcccattgcttccatttttgcctggaccagagggttagcccacagagcaaagcttgataacaataaa
gagcttgccttctttgcaaatgctttggaagaagtctctattgagacaattgaggctggcttcatgaccaaggac
ttggctgcttgcattaaaggtttacccaatgtgcaacgttctgactacttgaatacatttgagttcatggataaa
cttggagaaaacttgaagatcaaactagctcaggccaaactttaagttcatacctgagctaagaaggataattgt
cttttggtaactaggtctacaggtttacatttttctgtgttacactcaaggataaaggcaaaatcaattttgtaa
tttgtttagaagccagagtttatcttttctataagtttacagccttttcttatatatacagttattgccaccttt
tgtgaacatggcaagggacttttttacaatttttatttttatttctagtaccagcctaggaattcggttagtact
catttgtattcactgtcacttttctcatgttctaattataaatgaccaaaatcaagattgctcaaaagggtaaa
tgatagccacagtattgctccctaaaatatgcataaagtagaaattcactgccttcccctcctgtccatgacctt
gggcacagggaagttctggtgtcatagatatcccgttttgtgaggtagagctgtgcattaaacttgcacatgact
ggaacgaagtatgagtgcaactcaaatgtgttgaagatactgcagtcatttttgtaaagaccttgctgaatgttt
ccaatagactaaatactgtttaggccgcaggagagtttggaatccggaataaatactacctggaggtttgtcctc
tccatttttctctttctcctcctggcctggcctgaatattatactactctaaatagcatatttcatccaagtgca
ataatgtaagctgaatctttttttggacttctgctggcctgttttatttcttttatataaatgtgatttctcagaa
attgatattaaacactatcttatcttctcctgaactgttgattttaattaaaattaagtgctaattaccattaaa
aaaaaaa
```

Sequence is shown from start codon to polyA.

6.2.2 mouse IDH1 cDNA

```
atgtccagaaaaatccaaggaggttctgtggtggagatgcaaggagatgaaatgacacgaatcatttgggaattg
attaaggaaaaacttattcttccctatgtggaactggatctgcatagctatgatttaggcatagagaatcgtgat
gccaccaatgaccaggtcaccaaagatgctgcagaggctataaagaaatacaacgtgggcgtcaagtgtgctacc
atcacccccgatgagaagagggttgaagaattcaagttgaaacaaatgtggaaatccccaaatggcaccatccga
aacattctgggtggcactgtcttcagggaagctattatctgcaaaaatatcccccggctagtgacaggctgggta
aaacccatcatcattggccgacatgcatatggggaccaatacagagcaactgattttgttgttcctgggcctgga
aaagtagagataacctacacaccaaaagatggaactcagaaggtgacatacatggtacatgactttgaagaaggt
ggtggtgttgccatgggcatgtacaaccaggataagtcaattgaagactttgcacacagttccttccaaatggct
ctgtccaagggctggcctttgtatctcagcaccaagaacactattctgaagaagtatgatgggcgtttcaaagac
atcttccaggagatctatgacaagaaatacaagtcccagtttgaagctcagaagatctgctatgaacacaggctc
atagatgacatggtggcccaagctatgaagtccgagggaggcttcatctgggcctgtaagaattacgatggggat
gtgcagtcagactcagtcgcccaaggttatggctcccttggcatgatgaccagtgtgctgatttgtccagatggt
aagacggtagaagcagaggctgcccatggcactgtcacacgtcactaccgcatgtaccagaaagggcaagagacg
tccaccaaccccattgcttccatttttgcctggtcccgagggttagcccacagagcaaagcttgataacaatact
gagctcagcttcttcgcaaaggctttggaagacgtctgcattgagaccattgaggctggctttatgactaaggac
ttggctgcttgcattaaaggcttacccaatgtacaacgttctgactacttgaatacatttgagtttatggacaaa
cttggagaaaacttgaaggccaaattagctcaggccaaactttaaggtcaaacctgggcttagaatgagtctttg
```

cggtaactaggtccacaggtttacgtatttttttttttttttagtaacactcaagattaaaaacaaaaatcatt
ttgtaatttgtttagaagacaaagttgaacttttatatatgtttacagtctttttctttttcatacagttattg
ccaccttaatgaatgtggtggggaaatttttttaattgtattttattgtgtagtagcagtgtaggaattatgtta
gtacctgttcacaattaactgtcatgttttctcatgctctaatgtaaatgaccaaaatcagaagtgctccaaggg
tgaacaatagctacagtatggttccccataaggggaaaagagaaactcacttcccctgttgtccatgagtgtgaa
cactggggcctttgtacgcaaatgttgtactgtgtgtgggagagctatacagtaagctcacataagactggaaca
gataggatgtgtgtagctaaaatgcatggcagacgtgtttataaagagcatgtatgtgtccaatatactagttat
attttaagaccactggagaattccaagtctagaataaatgcagactggaggattctgctctttgatttctcttct
cctgtgacccagcctaagtattatcctaccccaagcagtacatttcacccatgggcaataatgggagctgtaccg
tttggatttctgctgacctgctgcatttcttttatataaatgtgacttttttttcccagaagttgatattaaaca
ctattccagtctagtccttctaaactgttaattttaattaaaatgaagtactaatgactcttctttgaaaaaaaa
a

Sequence is shown from start codon to polyA.

6.2.3 human CTAG1B cDNA

atgcaggccgaaggccggggcacaggggttcgacgggcgatgctgatggcccaggaggccctggcattcctgat
ggcccaggggcaatgctggcggcccaggagaggcgggtgccacgggcggcagaggtccccggggcgcaggggca
gcaagggcctcggggccgggaggaggcgccccgcggggtccgcatggcggcgcggcttcagggctgaatggatgc
tgcagatgcggggccaggggccggagagccgcctgcttgagttctacctcgccatgcctttcgcgacacccatg
gaagcagagctggcccgcaggagcctggcccaggatgccccaccgcttcccgtgccaggggtgcttctgaaggag
ttcactgtgtccggcaacatactgactatccgactgactgctgcagaccaccgccaactgcagctctccatcagc
tcctgtctccagcagctttccctgttgatgtggatcacgcagtgctttctgcccgtgtttttggctcagcctccc
tcagggcagaggcgctaagcccagcctggcgccccttcctaggtcatgcctcctcccctagggaatggtcccagc
acgtcattgtgggggcctgattgtttgtcgctgg

Sequence is shown from start codon.

6.3 Amino acid sequences

6.3.1 human IDH1 protein

MSKKISGGSVVEMQGDEMTRIIWELIKEKLIFPYVELDLHSYDLGIENRDATNDQVTKDAAEAIKKHNVGVKCAT
ITPDEKRVEEFKLKQMWKSPNGTIRNILGGTVFREAIICKNIPRLVSGWVKPIIIGRHAYGDQYRATDFVVPGPG
KVEITYTPSDGTQKVTYLVHNFEEGGGVAMGMYNQDKSIEDFAHSSFQMALSKGWPLYLSTKNTILKKYDGRFKD
IFQEIYDKQYKSQFEAQKIWYEHRLIDDMVAQAMKSEGGFIWACKNYDGDVQSDSVAQGYGSLGMMTSVLVCPDG
KTVEAEAAHGTVTRHYRMYQKGQETSTNPIASIFAWTRGLAHRAKLDNNKELAFFANALEEVSIETIEAGFMTKD
LAACIKGLPNVQRSDYLNTFEFMDKLGENLKIKLAQAKL

pink, R132

6.3.2 mouse IDH1 protein

MSRKIQGGSVVEMQGDEMTRIIWELIKEKLILPYVELDLHSYDLGIENRDATNDQVTKDAAEAIKKYNVGVKCAT
ITPDEKRVEEFKLKQMWKSPNGTIRNILGGTVFREAIICKNIPRLVTGWVKPIIIGRHAYGDQYRATDFVVPGPG
KVE*I*TYTP*K*DGTQKVTY*M*VH*D*FEEGGGVAMGMYNQDKSIEDFAHSSFQMALSKGWPLYLSTKNTILKKYDGRFKD
IFQEIYDKKYKSQFEAQKICYEHRLIDDMVAQAMKSEGGFIWACKNYDGDVQSDSVAQGYGSLGMMTSVLICPDG
KTVEAEAAHGTVTRHYRMYQKGQETSTNPIASIFAWSRGLAHRAKLDNNTELSFFAKALEDVCIETIEAGFMTKD
LAACIKGLPNVQRSDYLNTFEFMDKLGENLKAKLAQAKL

6.3.3 Alignment of human and mouse IDH1 proteins

Score	Expect	Method	Identities	Positives	Gaps
835 bits(2156)	0.0	Compositional matrix adjust.	395/414(95%)	406/414(98%)	0/414(0%)

```
Query  1    MSKKISGGSVVEMQGDEMTRIIWELIKEKLIFPYVELDLHSYDLGIENRDATNDQVTKDA  60
            MS+KI GGSVVEMQGDEMTRIIWELIKEKLI PYVELDLHSYDLGIENRDATNDQVTKDA
Sbjct  1    MSRKIQGGSVVEMQGDEMTRIIWELIKEKLILPYVELDLHSYDLGIENRDATNDQVTKDA  60

Query  61   AEAIKKHNVGVKCATITPDEKRVEEFKLKQMWKSPNGTIRNILGGTVFREAIICKNIPRL  120
            AEA+KK+NVGVKCATITPDEKRVEEFKLKQMWKSPNGTIRNILGGTVFREAIICKNIPRL
Sbjct  61   AEALKKYNVGVKCATITPDEKRVEEFKLKQMWKSPNGTIRNILGGTVFREAIICKNIPRL  120

Query  121  VSGWVKPIIIGRHAYGDQYRATDFVVPGPGKVEITYTPSDGTQKVTYLVHNFEEGGGVAM  180
            V+GWVKPIIIGRHAYGDQYRATDFVVPGPGKVEITYTP DGTQKVTY+VH+FEEGGGVAM
Sbjct  121  VTGWVKPIIIGRHAYGDQYRATDFVVPGPGKVEITYTPKDGTQKVTYMVHDFEEGGGVAM  180

Query  181  GMYNQDKSIEDFAHSSFQMALSKGWPLYLSTKNTILKKYDGRFKDIFQEIYDKQYKSQFE  240
            GMYNQDKSIEDFAHSSFQMALSKGWPLYLSTKNTILKKYDGRFKDIFQEIYDK+YKSQFE
Sbjct  181  GMYNQDKSIEDFAHSSFQMALSKGWPLYLSTKNTILKKYDGRFKDIFQEIYDKKYKSQFE  240

Query  241  AQKIWYEHRLIDDMVAQAMKSEGGFIWACKNYDGDVQSDSVAQGYGSLGMMTSVLVCPDG  300
            AQKI YEHRLIDDMVAQAMKSEGGFIWACKNYDGDVQSDSVAQGYGSLGMMTSVL+CPDG
Sbjct  241  AQKICYEHRLIDDMVAQAMKSEGGFIWACKNYDGDVQSDSVAQGYGSLGMMTSVLICPDG  300

Query  301  KTVEAEAAHGTVTRHYRMYQKGQETSTNPIASIFAWTRGLAHRAKLDNNKELAFFANALE  360
            KTVEAEAAHGTVTRHYRMYQKGQETSTNPIASIFAW+RGLAHRAKLDNN EL+FFA ALE
Sbjct  301  KTVEAEAAHGTVTRHYRMYQKGQETSTNPIASIFAWSRGLAHRAKLDNNTELSFFAKALE  360

Query  361  EVSIETIEAGFMTKDLAACIKGLPNVQRSDYLNTFEFMDKLGENLKIKLAQAKL  414
            +V IETIEAGFMTKDLAACIKGLPNVQRSDYLNTFEFMDKLGENLK KLAQAKL
Sbjct  361  DVCIETIEAGFMTKDLAACIKGLPNVQRSDYLNTFEFMDKLGENLKAKLAQAKL  414
```

query, human IDH1; sbjct, subject, mouse IDH1; red box, IDH1 p123-142

6.3.4 human CTAG1B (NY-ESO-1) protein

```
MQAEGRGTGGSTGDADGPGGPGIPDGPGGNAGGPGEAGATGGRGPRGAGAARASGPGGGAPRGPHGGAASGLNGC
CRCGARGPESRLLEFYLAMPFATPMEAELARRSLAQDAPPLPVPGVLLKEFTVSGNILTIRLTAADHRQLQLSIS
SCLQQLSLLMWITQCFLPVFLAQPPSGQRR
```

6.4 Quantification of immunohistochemistry

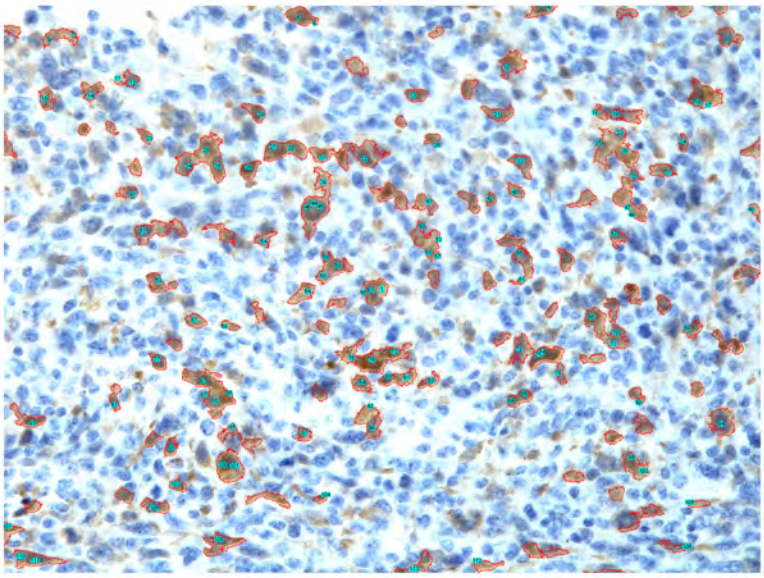

Fig. 6.1. Gating strategy and quantification of IDH1R132H+ cells in syngeneic tumor slices. IDH1R132H detection in tumor slices from IDH1R132H-expressing and IDH1wt-expressing tumors of sham-treated and vaccinated mice by DAB staining. IDH1R132H+ A2.DR1 tumor cells were counted by ImageJ with an algorithm using background subtraction and colour deconvolution plugin. Red line-framed cells are recognized by established threshold. In addition cells marked with blue numbers indicate IDH1R132H+ cells gated positive based on defined cell morphology. An IDH1R132H-expressing tumor from a sham-treated mouse is shown. Performed by L. Bunse.

6.5 Patient cohort

patients	gender	age	diagnosis	IDHstatus	ELISA	sELISA	ELISpot	SA
p001	m	50	GBM	IDH1R132H	x	x	x	x
p002	f	80	GBM	IDH1wt	x			
p003	m	68	GBM	IDH1wt	x			
p004	f	51	A°II	IDH1wt	x			
p005	m	71	GBM	IDH1wt	x			
p006	m	50	GBM	IDH1wt	x			
p007	m	48	O°II	IDH1R132H	x		x	
p008	m	79	GBM	IDH1wt	x			
p009	m	42	GBM	IDH1R132H	x	x		
p010	m	41	GBM	IDH1wt	x			
p011	f	59	GBM	IDH1wt	x			
p012	m	28	GBM	IDH1R132H	x			
p013	m	73	GBM	IDH1wt	x			
p014	f	51	GBM	IDH1wt	x			
p015	f	60	GBM	IDH1wt	x			
p016	m	54	GBM	IDH1wt	x			
p017	m	56	A°III	IDH1wt	x			
p018	m	61	O°III	IDH1R132H	x			
p019	m	44	O°III	IDH1R132H	x		x	
p020	m	52	O°III	IDH1R132H	x	x		
p021	f	71	GBM	IDH1wt	x			
p022	n.i.	n.i.	h.d.	n.d.	x			
p023	m	41	GBM	IDH1R132H	x	x		
p024	m	48	O°II	IDH1R132H	x	x		

p025	m	47	O°III	IDH1R132H	**x**	**x**		
p026	m	50	O°II	IDH1R132H	**x**			
p027	m	33	A°III	IDH1R132H	**x**	**x**		
p028	m	59	GBM	IDH1wt	**x**			
p029	f	54	O°II	IDH1R132H	**x**			
p030	m	45	O°III	IDH1R132H	**x**			
p031	f	68	GBM	IDH1wt	**x**			
p032	f	78	GBM	IDH1wt	**x**			
p033	f	66	O°III	IDH1R132H	**x**			
p034	m	40	A°II	IDH1R132H	**x**		**x**	
p035	f	51	A°III	IDH1R132H	**x**			
p036	m	37	GBM	IDH1R132H	**x**	**x**		
p037	m	27	A°III	IDH1R132H	**x**	**x**	**x**	**x**
p038	m	41	O°III	IDH1R132H	**x**			
p039	n.i.	n.i.	h.d.	n.d.	**x**			
p040	n.i.	n.i.	h.d.	n.d.	**x**			
p041	m	37	A°II	IDH1R132H	**x**	**x**		
p042	m	56	A°III	IDHR132C‡	**x**			
p043	m	34	GBM	IDH1R132H	**x**		**x**	
p044	f	63	GBM	IDH1wt	**x**			
p045	m	24	A°III	IDH1R132H	**x**		**x**	
p046	f	68	GBM	IDH1wt	**x**		**x**	
p047	m	46	OA°III	IDH1R132H	**x**		**x**	
p048	m	50	A°III	IDH1R132H	**x**		**x**	
p049	f	40	OA°III	IDH1R132H	**x**		**x**	
p050	f	31	A°III	IDH1R132H	**x**		**x**	
p051	f	57	A°II	IDH1R132H	**x**		**x**	
p052	m	39	OA°III	IDH1R132H	**x**		**x**	
p053	m	45	A°III	IDH1R132H	**x**		**x**	
p054	f	50	secGBM	IDH1R132H	**x**		**x**	
p055	f	60	GBM	IDH1wt	**x**		**x**	
p056	m	34	O°II	IDH1R132H	**x**		**x**	
p057	m	45	A°III	IDH1R132H	**x**		**x**	
p058	f	47	GBM	IDH1R132H	**x**		**x**	
p059	m	36	O°III	IDH1R132H	**x**		**x**	
p060	f	46	secGBM	IDH1R132H	**x**		**x**	
p061	f	44	O°III	IDH1wt			**x**	
p062	m	65	A°III	IDH1R132H	**x**			
p063	m	34	A°II	IDH1R132H	**x**			
p064	m	43	A°III	IDH1R132H	**x**			
p065	m	53	O°III	IDH1R132H	**x**		**x**	
p066	f	51	A°III	IDH1R132H	**x**		**x**	
p067	m	66	GBM	IDH1wt	**x**		**x**	
p068	m	71	GBM	IDH1wt	**x**		**x**	
p069	f	47	A°II	IDH1wt	**x**		**x**	
p070	f	35	A°III	IDH1wt	**x**			
p071	m	67	GBM	IDH1wt	**x**		**x**	
p072	m	27	A°II	IDH1wt	**x**		**x**	
p073	f	54	GBM	IDH1wt	**x**		**x**	
p074	m	55	OA°III	IDH1R132H			**x**	
p075	f	34	OA°II	IDH1R132H			**x**	
p076	m	35	OA°II	IDH1R132H			**x**	
p077	n.i.	n.i.	h.d.	n.d.	**x**			
p078	f	53	A°III	IDH1R132H	**x**			
p079	m	59	GBM	IDH1wt	**x**		**x**	
p080	m	56	GBM	IDH1wt	**x**		**x**	
p081	f	57	Gliosarcoma	IDH1wt	**x**		**x**	
p082	m	73	GBM	IDH1wt	**x**		**x**	
p083	m	58	GBM	IDH1wt	**x**		**x**	
p084	m	65	GBM	IDH1wt	**x**		**x**	
p085	m	34	GBM	IDH1wt	**x**		**x**	
p086	m	62	GBM	IDH1wt	**x**		**x**	
p087	m	70	GBM	IDH1wt	**x**		**x**	
p088	m	50	GBM	IDH1wt	**x**		**x**	
p089	m	47	GBM	IDH1wt	**x**		**x**	

p090	f	62	A°II	IDH1wt	**x**	**x**
p091	m	55	GBM	IDH1wt	**x**	**x**
p092	f	54	A°III	IDH1wt	**x**	**x**
p093	m	68	GBM	IDH1wt	**x**	**x**
p094	m	54	GBM	IDH1wt	**x**	**x**
p095	m	68	GBM	IDH1wt	**x**	**x**
p096	m	64	Gliosarcoma	IDH1wt	**x**	**x**
p097	m	70	GBM	IDH1wt	**x**	**x**

Table 6.1. Patient characteristics and analysis. GBM, glioblastoma multiforme; secGBM, secondary GBM; A, astrocytoma; O, oligodendroglioma; OA, oligoastrocytoma; °II, WHO grade II; °III, WHO grade III; ELISA, enzyme-linked immuonadsorbent assay; sELISA, subtype ELISA; ELISpot, enzyme-linked immunoadsorbent spot assay; SA, secretion assay; n.i., no information; h.d., healthy donor; n.d., not determined; ‡, categorized as IDH1wt. Data collected and categorized by L. Bunse.